



## Polysaccharide-based antibacterial coating technologies

Downloaded from: <https://research.chalmers.se>, 2025-12-08 23:23 UTC

Citation for the original published paper (version of record):

Ruan, H., Aulova, A., Ghai, V. et al (2023). Polysaccharide-based antibacterial coating technologies. *Acta Biomaterialia*, 168: 42-77. <http://dx.doi.org/10.1016/j.actbio.2023.07.023>

N.B. When citing this work, cite the original published paper.



Contents lists available at ScienceDirect

Acta Biomaterialia

journal homepage: [www.elsevier.com/locate/actbio](http://www.elsevier.com/locate/actbio)

## Review article

## Polysaccharide-based antibacterial coating technologies

Hengzhi Ruan<sup>a</sup>, Alexandra Aulova<sup>a</sup>, Viney Ghai<sup>a</sup>, Santosh Pandit<sup>b</sup>, Martin Lovmar<sup>b,c</sup>,  
Ivan Mijakovic<sup>b,d,\*</sup>, Roland Kádár<sup>a,e,\*</sup>

<sup>a</sup> Department of Industrial and Materials Science, Chalmers University of Technology, 412 96 Göteborg, Sweden<sup>b</sup> Department of Biology and Biological Engineering, Chalmers University of Technology, 412 96 Göteborg, Sweden<sup>c</sup> Wellspect Healthcare AB, 431 21 Mölndal, Sweden<sup>d</sup> The Novo Nordisk Foundation Center for Biosustainability, Technical University of Denmark, 2800 Kongens Lyngby, Denmark<sup>e</sup> Wallenberg Wood Science Centre (WWSC), Chalmers University of Technology, 412 96 Göteborg, Sweden

## ARTICLE INFO

## Article history:

Received 28 March 2023

Revised 16 June 2023

Accepted 17 July 2023

Available online xxx

## Keywords:

Antibacterial coatings

Polysaccharides

Coating technology

Antibacterial testing

## ABSTRACT

To tackle antimicrobial resistance, a global threat identified by the United Nations, is a common cause of healthcare-associated infections (HAI) and is responsible for significant costs on healthcare systems, a substantial amount of research has been devoted to developing polysaccharide-based strategies that prevent bacterial attachment and biofilm formation on surfaces. Polysaccharides are essential building blocks for life and an abundant renewable resource that have attracted much attention due to their intrinsic remarkable biological potential antibacterial activities. If converted into efficient antibacterial coatings that could be applied to a broad range of surfaces and applications, polysaccharide-based coatings could have a significant potential global impact. However, the ultimate success of polysaccharide-based antibacterial materials will be determined by their potential for use in manufacturing processes that are scalable, versatile, and affordable. Therefore, in this review we focus on recent advances in polysaccharide-based antibacterial coatings from the perspective of fabrication methods. We first provide an overview of strategies for designing polysaccharide-based antimicrobial formulations and methods to assess the antibacterial properties of coatings. Recent advances on manufacturing polysaccharide-based coatings using some of the most common polysaccharides and fabrication methods are then detailed, followed by a critical comparative overview of associated challenges and opportunities for future developments.

## Statement of significance

Our review presents a timely perspective by being **the first review** in the field to focus on advances on polysaccharide-based antibacterial coatings from the perspective of fabrication methods along with an overview of strategies for designing polysaccharide-based antimicrobial formulations, methods to assess the antibacterial properties of coatings as well as a critical comparative overview of associated challenges and opportunities for future developments.

Meanwhile this work is specifically targeted at an audience focused on featuring critical information and **guidelines** for developing polysaccharide-based coatings. Including such a complementary work in the journal could lead to further developments on polysaccharide antibacterial applications.

© 2023 The Authors. Published by Elsevier Ltd on behalf of Acta Materialia Inc.

This is an open access article under the CC BY license (<http://creativecommons.org/licenses/by/4.0/>)

## 1. Introduction

Healthcare-associated infections (HAI) are the infections acquired during the process of receiving or giving healthcare, thus

affecting both patients and healthcare professionals [1]. HAI can be found in hospitals, long-term and elderly care facilities, outpatient settings, and even after discharge, especially for patients who rely on medical devices such as implants, catheters, hernia meshes, wound dressings, and vascular grafts [2]. HAI is one of the most common adverse events including surgical site infections, pneumonia, gastrointestinal infections, and bloodstream infections [3], threatening the safety of patients. It is a significant cause for

\* Corresponding authors.

E-mail addresses: [ivan.mijakovic@chalmers.se](mailto:ivan.mijakovic@chalmers.se) (I. Mijakovic), [roland.kadar@chalmers.se](mailto:roland.kadar@chalmers.se) (R. Kádár).

## Nomenclature

ALG	alginate
AMP	antimicrobial peptide
CA	cellulose acetate
CFU	counting colony forming units
CMC	carboxymethylcellulose
CNC	cellulose nanocrystals
CNF	cellulose nanofibers
CS	chitosan
CSCT	catechol functionalized chitosan
DVLO	Derjaguin-Landau-Verwey-Overbeek
EPS	exopolysaccharides
ES	electrospinning, electrospun
MIC	minimum inhibitory concentration
MBC	minimum bactericidal concentration
NIPAM	N-Isopropyl acrylamide
NMy	nylon monofilaments
HA	hyaluronic acid
HAI	healthcare-associated infections
HAp	hydroxyapatite
HNT	halloysite nanotubes
OD	optical density
PAA	polyacrylic acid
PEI	polyethyleneimine
PEO	polyethylene oxide
PFU	plaque forming unit
PLA	polylactic acid
PSAN	polystyrene-co-acrylonitrile
PVA	polyvinyl alcohol
PVAm	polyvinylamine
PVF	polyvinyl fluoride
QAC	quaternary ammonium compound
SEM	scanning electron microscopy
TEM	transmission electron microscopy
$\kappa$ -C	kappa carrageenan
$\iota$ -C	iota carrageenan

increased morbidity, mortality and economic burdens on patients, families, and healthcare systems worldwide.

An additional complication of HAI is that the misuse and overuse of antibiotics has been one the main drivers for the spread of antimicrobial resistance i.e., causing bacteria to become resistant to most common antibiotics, making HAI very difficult to treat. Consequently, antimicrobial resistance has been called a global threat by the United Nations [4]. Device-related infections begin with bacteria adhering to the surface of a medical device. Once bound, the bacteria proliferate on the surface and many bacterial species can form a biofilm which becomes a haven where the bacteria are well protected from both anti-biodegradable-biotics and the immune system [5,6]. Therefore, the most effective and straightforward way to reduce HAI and fight against the spread of antimicrobial resistance is to interfere with bacterial colonization at the initial stage. Hence, intensive efforts have been put into development and fabrication of biomaterials with antibacterial properties.

Polysaccharides are a group of biomacromolecules composed of different kinds of glycosidic-bonded monosaccharides, and because they are essential building blocks for life they are commonly found in nature from renewable sources [7]. Polysaccharides have attracted much attention due to their intrinsic remarkable biological activities, including hypoglycemic, hypolipidemic, anticancer, antioxidant, immune enhancing, antibacterial activities, etc. [8] Further, it has been suggested that polysaccharide-based antibacterial

formulation can have significant impact on bacterial biofilms by interfering with quorum sensing [9], adhesion activity [10], formation process [11] and efflux pumps [12]. In addition, it has been proposed that polysaccharides can damage the cell wall and cell membrane of bacteria via different mechanisms, such as altering the permeability of the bacterial cell walls and cell membrane [13], undermining enzyme system integrity in bacterial membrane [14], impeding cell membrane function [15], as well as exert antibacterial activities via affecting the nucleic acid and even changing the intracellular metabolic pathways of bacteria [16]. At the same time, polysaccharides are attractive for their potential to facilitate the end-of-use disposal of coatings without harming the environment [62].

However, to transform antibacterial polysaccharides into commercially useful materials it is important that they are compatible with manufacturing processes that are scalable, versatile and affordable. In particular, polysaccharide-based antibacterial formulations that could be applied as coatings on the surface of a wide variety of substrate materials with any kind of shape while at the same time being mechanically and environmentally stable will be decisive factors for their applicability. In this review we therefore compare the potential use of polysaccharide-based formulations as coatings from the perspective of fabrication methods. We focus on recent advances using several of the most widely applied techniques for the fabrication of polysaccharide-based antibacterial coatings: dip coating, spin coating, spray coating, 3D printing, electrospinning, and layer-by-layer assembly, Fig. 1. Complementary recent reviews have been mostly focused on polysaccharide-based antibiofilm surfaces that mainly involve chitosan and its derivatives [17]. However, here we provide a unique and timely perspective by focusing on recent advances and challenges of polysaccharide-based antibiofilm surfaces in terms of coating technology. This assessment could be crucial for new antibacterial formulations when it comes to choosing the most promising methods for their evaluation and commercialization assessment.

Polysaccharides have various chemical components and are widely used for different applications [18,19]. Chitosan (CS), in particular, plays an important role in the antibacterial field [20], see Table 1. A deacetylated biopolymer derived from chitin, chitosan (CS) is a natural polysaccharide with a relatively high molecular weight that is made up of copolymers of d-glucosamine and N-acetyl-d-glucosamine [21]. Chitosan has been used as an antibacterial agent to combat bacteria, algae, yeast, and fungi. Several internal and extrinsic parameters, including the degree of deacetylation, molecular weight, concentration, pH, and target microorganism, affect the antibacterial effect of the substance [22]. A current hypothesis is that the antibacterial effect of chitosan is due to an electrostatic interaction between the positively charged amino groups of CS and the negatively charged microbial cell membrane. This interaction alters the permeability of the cell membrane, which leads to the leakage of cell contents and microbial death [23].

Hyaluronic acid (HA) is a non-sulphated glycosaminoglycan (GAG) that contains alternating repeat units of 1,4-D-glucuronic acid and 1,3-N-acetyl-D-glucosamine and is a crucial part of the extracellular and pericellular matrixes of all bodily tissues. It has been suggested that HA can be used as antimicrobial polymers for a variety of biomedical and pharmaceutical applications [24]. According to several studies, the soluble HA's in vitro bacteriostatic activity may be due to the medium's excess HA saturating the bacterial hyaluronidase [25]. Consequently, bacterial proliferation profile is slowed. Furthermore, HA shows antifouling effectiveness against bio pollutants enhanced by HA's negative net charge, which can cause steric repulsion of the negatively charged bacterium cell wall [26].

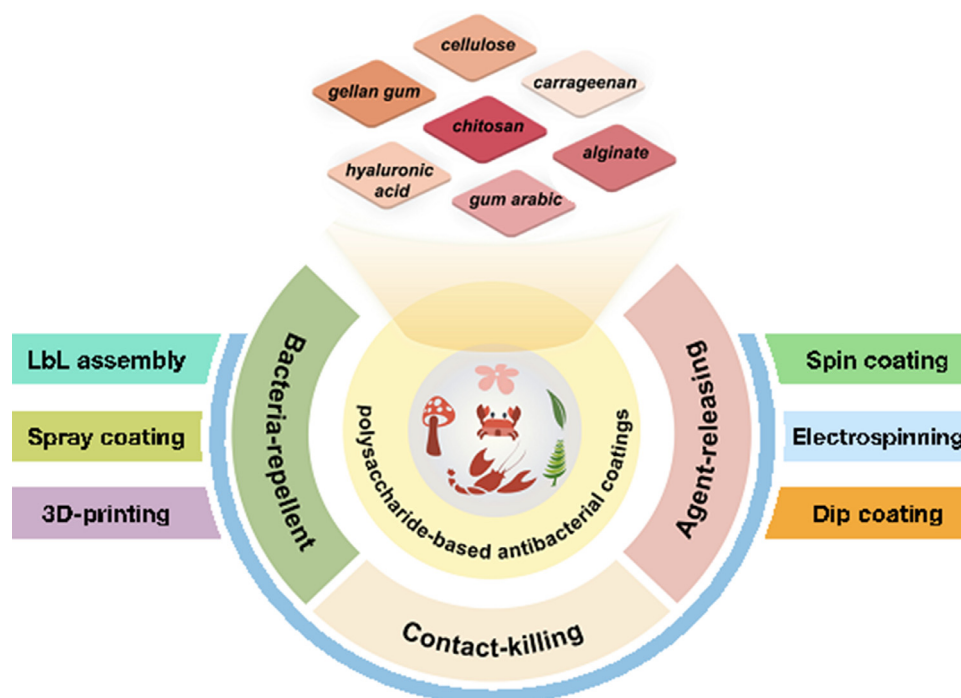


**Fig. 1.** Illustration of polysaccharide-based antibacterial coating technologies: main types of polysaccharides, strategies for killing bacteria and typical fabrication methods.

As the result of the development of drug-resistant bacteria and fungi, pectin has received a growing interest with respect to its natural antibacterial properties caused by the undissociated acid form. With the emergence of several new uses, current research assigns the anti-inflammatory activities of pectin, which are primarily attributed to the galacturonan chain [27].

In addition, some polysaccharides without antibacterial activities still play an important role for potential antibacterial coatings. An anionic polysaccharide widely used for biomedical applications, alginate (ALG), is recognized as a family of linear copolymers made up of blocks of (1, 4)-linked  $\alpha$ -D-mannuronate (M) and  $\alpha$ -L-guluronate (G) residues that are commonly derived from brown algae (*Phaeophyceae*).

Carrageenan is a sulfated galactan isolated primarily from marine red algae and is composed of 1,3-linked  $\beta$ -D-galactose and 1,4-linked  $\alpha$ -D-galactose. Due to the different numbers and positions of the ester sulfate groups on the repeating galactose units, carrageenan can be divided into  $\kappa$ -type (Kappa),  $\iota$ -type (iota),  $\lambda$ -type (lambda). The gel strength and solubility of carrageenan are also affected by the levels of ester sulfate groups. For example,  $\kappa$ -C can form strong and rigid gel crosslinked with potassium ions while  $\iota$ -C gel is softer in the presence of calcium ions and  $\lambda$ -C does not have gelation behavior. Due to its inherent physical properties and antioxidant activity, carrageenan plays an important role as functional additive or thickening agent in the industry for the application of food and bioengineering [28,29].

Cellulose is the most widely distributed and most abundant polysaccharide in nature, consisting of linear glucan chains linked by  $\beta$ -1,4-glycosidic bonds. Cellulose nanofibrils or nanocrystals, which are bundles of cellulose molecules in crystalline-amorphous and crystalline forms, known as generically nanocellulose, are also regarded as potential polysaccharides for antibacterial coatings due to their high specific surface area, biodegradability and high mechanical properties [30].

Gellan gum, produced by the bacterium *Sphingomonas* (*Pseudomonas*) *elodea*, is an anionic polysaccharide with a repeating

tetrasaccharide unit, including two glucose residues, one glucuronic acid and one rhamnose residue [31]. Due to its biocompatibility and processing versatility through chemical modifications, gellan gum has been widely used for drug delivery and tissue engineering [32].

Polyanion gum arabic is an edible tree gum exudate used mainly in food, cosmetic and pharmaceutical industries [259].

Further details regarding the structure and properties of polysaccharides can be found in the works of Heinze (Ed.) [33], Tiwari [34], Dumitriu [35], among many others.

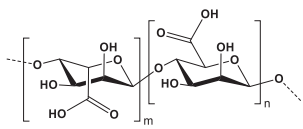
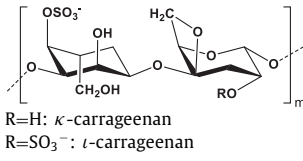
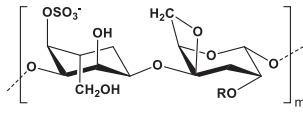
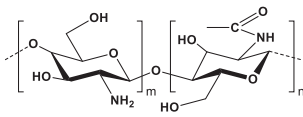
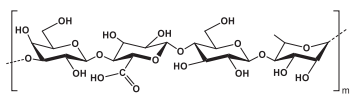
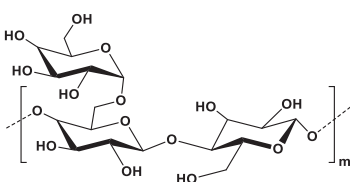
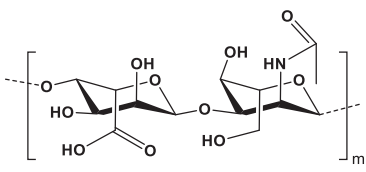
At first, we provide a summary of antibacterial strategies for polysaccharide-based formulations followed by an overview of methods and good practices for assessing the antibacterial properties of coatings. Thereafter we discuss recent advances in polysaccharide-based coating, followed by a critical discussion on the potential for manufacturing polysaccharide-based antibiofilm surfaces and future related opportunities and challenges.

## 2. Strategies for designing polysaccharide-based antibacterial materials

Here we summarize specific strategies that can be employed for designing polysaccharide-based systems with potential for use as antibacterial coatings. Several comprehensive reviews on the topic can be found elsewhere [36,37]. Driven by reproductive fitness, bacteria have evolved their biofilms to resist physical forces such as shear forces generated by blood flow and washing effect of saliva. This is achieved through extracellular polymeric secretions primarily consisting of exopolysaccharides (EPS), proteins, and nucleic acids [38]. In addition, the formation of biofilms helps bacteria to survive in various assaults in environments of animal or human hosts [39]. Similarly, the initial cause of HAI, such as medical device related infections, is bacterial adhesion to the surface of biomaterials and adjacent tissues [40]. The adhesion process of bacteria is complex and is usually separated in two stages [41], as illustrated in Fig. 2. In the first stage, the interaction between bacterial cells and material surface is rapid and reversible. Generally, this

**Table 1**

Main polysaccharides considered for antibacterial coatings: structure, properties and origins.

Polysaccharide	Structure	Properties	Origins
Alginate ( <i>anionic</i> ) 1,4- $\beta$ -D-mannuronate, $\alpha$ -L-guluronate residues		Film-forming ability, gelling, non-toxicity, pH responsiveness, hydrophilicity, biocompatibility, biodegradability, processability and ionic crosslinking	Derived from brown algae ( <i>Phaeophyceae</i> ), such as <i>Laminaria hyperborea</i> , <i>Laminaria digitata</i> , <i>Laminaria japonica</i> , <i>Ascophyllum nodosum</i> and <i>Macrocystis pyrifera</i> . Bacterial alginate can be produced from <i>Azotobacter</i> and <i>Pseudomonas</i> .
Carrageenan ( <i>anionic</i> ) 1,3- $\beta$ -D-galactose, 1,4- $\beta$ -D-galactose	 R=H: $\kappa$ -carrageenan R=SO <sub>3</sub> <sup>-</sup> : $\iota$ -carrageenan	Thickening, gelling, stabilizing, antitumor, immunomodulatory, antihyperlipidemic and anticoagulant activities	Derived from red algae ( <i>Rhodophyta</i> ), including <i>Chondrus</i> , <i>Eucheuma</i> , <i>Gigartina</i> and <i>Kappaphycus</i> species.
Cellulose ( <i>neutral</i> ) 1,4- $\beta$ -D-glucose		Biocompatibility, biodegradability, non-toxicity, low-cost, flexibility, high thermal stability, good mechanical properties	Derived from green plants such as cotton, wood and hemp. Also, cellulose can be produced from bacteria including <i>Acetobacter xylinum</i> , <i>Gluconacetobacter xylinus</i> and others.
Chitosan ( <i>cationic</i> ) 1,4- $\beta$ -D-glucosamine		High antibacterial activity, biocompatibility, biodegradability, non-toxicity, hemostatic effect, rigidity and brittleness	Derived from the chitin of crustaceans, such as lobsters, crabs, and shrimps, as well as from fish scales and many other types of organisms including insects and fungi.
Gellan gum ( <i>anionic</i> ) 1,3- $\beta$ -D-glucose, 1,4- $\beta$ -D-glucuronic acid, 1,4- $\beta$ -D-glucose, 1,4- $\alpha$ -L-rhamnose		Gelling, flexibility, biocompatibility, biodegradability, non-toxicity, heat and acid resistance	Produced by aerobic submerged fermentation of <i>Sphingomonas elodea</i> .
Gum arabic ( <i>anionic</i> ) 1,3- $\beta$ -D-galactopyranosyl		Film-forming ability, gelling, emulsifying, thickening, non-toxicity, biocompatibility, biodegradability and antibacterial activity	Derived from the stems and branches of the Acacia Senegal tree.
Hyaluronic acid ( <i>anionic</i> ) D-glucuronic acid, N-acetyl-D-glucosamine, linked via alternating $\beta$ -(1 $\rightarrow$ 4) and $\beta$ -(1 $\rightarrow$ 3) glycosidic bonds		Gelling, biocompatibility, biodegradability, non-toxicity and significant bioactivities	Derived from rooster comb. Produced from <i>streptococci</i> for industrial purposes.
Pectin ( <i>anionic</i> ) 6-methylated and 2- and/or 3-acetylated poly- $\alpha$ -(1-4)-D-galacturonic acid residues, alternating with branched $\alpha$ -(1-2)-L-rhamnosyl- $\alpha$ -(1-4)-D-galacturonosyl chains substituted with side chains of mainly $\alpha$ -L-arabinofuranose and $\alpha$ -D-galactopyranose.	Pectin structure remains uncertain based on current studies.	Gelling, thickening, antibacterial activity, biocompatibility, biodegradability	Large levels of pectin can be found in pears, apples, guavas, quince, plums, gooseberries, oranges, and other citrus fruits, while smaller amounts can be found in soft fruits like cherries, grapes, and strawberries.

interaction is nonspecific and can be easily destroyed through phagocytosis, a cellular process for ingesting and eliminating microorganisms, foreign substances etc. Then in the second stage, bacteria start to excrete adhesion proteins which mediate the interaction with molecules of the material surface. This step is irreversible (or only slowly reversible) due to the presence of adhesins on the microbial cell surfaces [41]. Once the bacterial cells are firmly adhered to the surfaces, they start to proliferate and some bacterial species can produce biofilm, i.e. a glue-like matrix consisting of excreted polysaccharides, proteins and DNA. These

components can either be a biproduct from bacterial metabolism or from the growth and autolysis of bacterial communities. The mature biofilm protects the bacterial community and provides support for a three-dimensional architecture shown in the final stage of Fig 2.

Accordingly, the main approach for designing antibacterial surfaces is to prevent bacteria from adhering to the surface of the material or kill the attached bacteria. Therefore, three strategies to design antibacterial coatings have been proposed: bacteria-repelling, contact-killing, and antibacterial agent release [42].



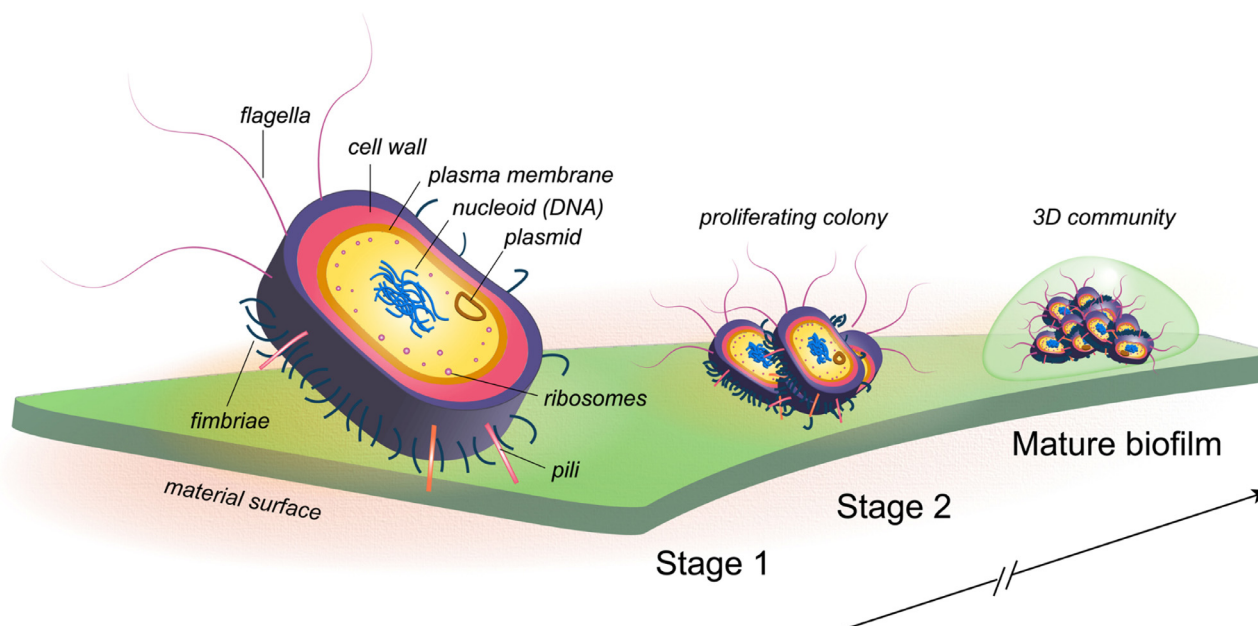


**Fig. 2.** Illustration of the stages of bacterial adhesion. First, the free-floating planktonic bacteria attach reversible to the material surface, where it in the next stage attempts to anchor itself by adhesion structures such as pili and fimbriae. Once bound to the surface it starts to proliferate and produce biofilm and with time the mature biofilm gives strong support and protection for the bacteria growing in it.

Bacteria-repelling surfaces can prevent the initial attachment of bacteria in Stage 1. Through contact-killing the cell wall of bacteria is destroyed when in touch with an antibacterial surface (Stage 1). Surfaces embedded with releasable antibacterial agents could kill both adherent and planktonic bacteria efficiently.

## 2.1. Bacteria-repellent surfaces

Reduced adhesion of bacteria to a surface/substrate potentially leads to prevent the biofilm formation. Since bacteria growing in biofilms are difficult to remove, creating a surface that prevents the initial adhesion of bacteria can reduce the risk of e.g. device-associated infections [43]. Several strategies for bacteria-repellent surfaces are summarized below together with examples of their use.

### 2.1.1. Superhydrophilic surfaces

In recent years, there has been increasing interest in controlling the superhydrophilicity of specific surfaces (reducing their water contact angle,  $\theta$ , below  $5^\circ$ ) via modifying the chemical composition and morphology of the surface [44]. Hydrophilic molecules can induce hydration and form a layer of water on the surface that has been demonstrated to effectively limit or prevent the attachment of nonspecific biomolecules and microorganisms [45]. In addition, this mobile water layer could take away the pollutants from the surface and therefore lead to self-cleaning ability [46]. Based on these characteristics and potential, superhydrophilic surfaces can be an essential building block to prevent the biofilm formation. For example, Park et al. [47] developed antibacterial multi-layer coatings for oral environments composed of carboxymethyl-cellulose (CMC) and chitosan (CS). The coatings were made porous and rough through a two-step cross-linking process. This resulted in a superhydrophilic surface that prevented bacterial adhesion and exhibited activity against *Streptococcus mutans* additionally through the release of an antibacterial agent. Surfaces coated with superhydrophilic CMC/CS multilayer coatings showed a contact angle of approximately  $2.75^\circ$  and the test of antibiofilm effects exhibited around 80% reduction of *Staphylococcus aureus* and *Pseudomonas aeruginosa* biofilms at 24 h without antibacterial agents [48].

### 2.1.2. Superhydrophobic surfaces

Inspired by lotus leaves [49] and striders [50] in nature, superhydrophobic surfaces are usually obtained by hierarchical micro / nano structures [51] and materials with low surface energy [52]. The water contact angle of superhydrophobic surface is  $>150^\circ$  and its sliding angle is  $<10^\circ$ . It has been demonstrated that when superhydrophobic surfaces are exposed to external environment, an air layer will form and fill in the micro / nano structure of the superhydrophobic surface, which can reduce adhesion of bacterial cells on the surface of the material [53]. Therefore, superhydrophobic surfaces have also been proposed for antibacterial applications. As example, Zeng et al. [54] presented a biomimetic superhydrophobic coating for anti-blood adhesion based on a novel flower-like micro-nanoparticle deposited together with CS (positively charged) via electrophoretic deposition. The results indicated that the superhydrophobic coating with high contact angle of  $157.89 \pm 2.18^\circ$  can repel *Escherichia coli* adhesion.

### 2.1.3. Electrostatic repulsion

Since the net electrostatic charge of most bacterial cell walls is negative at neutral pH, by applying the Derjaguin-Landau-Verwey-Overbeek (DLVO) [55], originally developed for colloidal interactions, it has been pointed out that the adhesion of bacteria to surfaces may be affected by electrostatic repulsion at physiological pH [56]. In addition, bacterial cell surfaces also acquire charges through specific adsorption especially from multivalent cations [57] and the specific adsorption is influenced by the ability of multivalent cations to form chemical bonds with negatively charged groups on the surface [58]. Via combining anionic HA with poly-L-lysine by lay-by-layer (LbL) assembly, Alkekha et al. [59] obtained coatings which could reduce the adhesion of *S. aureus*, likely attributed to significant film hydration and electrostatic repulsion.

## 2.2. Contact-killing surfaces

Since some coated surfaces with certain bactericidal components or groups can cause physical damage to bacterial cells [60], or exert non-specific oxidative stress on bacteria rather than attacking specific targets such as ribosomes [61], they can act as

contact-killing surfaces without leading to antibiotic resistance of bacteria. Besides that, compared to biocides, such as silver or triclosan, which could contribute to the environmental pollution and increase of toxicity if they are leached out at too high speed, polysaccharide-based contact-killing coatings, such as CS and its derivatives, could be a more sustainable alternative [62]. The antibacterial effect of polysaccharides depends on many factors, such as cell surface structure, surface adhesives, polysaccharide adsorption, proteins involved in the adhesion process, cell hydrophobicity, and electrostatic interactions between cells and host surfaces [63]. All the constitutes multiple opportunities for developing polysaccharides into antibacterial materials for coatings.

### 2.2.1. Polysaccharides with inherent antibacterial properties

Some polysaccharides have unique characteristics that can play an antibacterial role through various mechanisms. For example, EPS extracts from *Pleurotus flabellatus* strain and *Mynuk mycelium* can inhibit the adhesion activity of bacteria [10]; CS [11], xanthan-oligosaccharide [64] and sulphated polysaccharides extracted from *Chlamydomonas reinhardtii* [16] can inhibit the formation of cell membranes. Therefore, these polysaccharides could have direct potential as ingredients to fabricate antibacterial coating formulations. In order to cope with catheter-associated infections, for example, Bračič et al. [65] used colloidal polysaccharide complexes to functionalize the surface of silicone catheter tubes. The results showed that the coatings improve the antimicrobial activity both against Gram-positive and Gram-negative bacteria.

### 2.2.2. Functionalized polysaccharides

Through surface modification, some polysaccharides can be endowed with new functions, while the original biocompatibility can be preserved [66]. For example, cellulose and nanocellulose cannot exert antibacterial activity alone but with surface functionalization, especially the chemistry of the hydroxyl function, they can be endowed with bacteriostatic properties [67]. In some cases, benefited by their high specific surface area and stiffness, cellulose could be also used as additives to overcome the disadvantages of polysaccharides coatings, such as poor mechanical strength and chemical stability [68]. Naturally, even polysaccharides with inherent antibacterial properties can show stronger bactericidal effects after the introduction of new components such as antimicrobial peptides (AMPs) [69], or functional groups such as quaternary ammonium compounds (QACs) [70]. Therefore, modified polysaccharides can be used as matrices or additives as part of antibacterial coating formulations. This approach could open new doors for the healthcare and food industries. As examples, aiming for long-term antibacterial activity on catheters, versatile antibacterial surfaces with amphiphilic quaternized chitin-based derivatives were presented by Xie et al [71]. In addition, Paris et al. [72] investigated two strategies for immobilization of AMPs and fabricated antibacterial coatings based on hyaluronic acid (HA).

### 2.3. Antimicrobial agent releasing surfaces

Repelling bacteria or killing them on contact is clearly the best strategy for antibacterial coatings, because it is less likely that they lead to resistance development [73]. However, in some cases there is a need for a polysaccharide coating that can release an antimicrobial agent. For example, in many environments, polysaccharide surfaces become covered through nonspecific binding, and eventually they will completely lose their antibacterial activity. Similarly, a high concentration of bacteria will leave dead cells on the coating surface [74], which may also significantly affect the long-term antibacterial properties of the coating. Impregnated biocides used in polysaccharide coatings, such as silver [75], copper [76], selenium

[77], zinc oxide [78], titanium dioxide [79] etc., can be simply released killing surrounding bacteria. Antibiotics and some functionalized polysaccharides are also used as releasing agents in surfaces made for medical applications [80].

To achieve good controlled-releasing properties, gellan gum could be a desired option to load with antimicrobial agent [81]. For example, recently, Hua et al. fabricated gellan gum-based coatings on 3D printed scaffolds, crosslinked with both isoniazid and rifampicin as drugs, on porous tantalum for the application of medical scaffolds and the obtained coatings showed significant bactericidal effects against *S. aureus* [82]. The simultaneous release of different biocides from coatings is more efficient than the release of one biocide alone [83]. Shadpour and Nasim [84] proposed a new strategy for preparing sodium alginate-pectin composite and nanocomposite films which showed biocompatibility, bioactivity, and antibacterial properties. Previously, Zhengxin et al. [85] reported a facile method for producing silver nanoparticles using soluble soybean polysaccharide and further investigated the application for food packaging [86].

To summarize, a broad range of strategies for the design of antibacterial polysaccharides are available through antifouling, contact-killing and agent-releasing means (see Table 2). We distinguish here between antibacterial formulations – compositions that have antibacterial properties – and antibacterial coatings – material formulations that have been deposited onto a surface/substrate using a coating technology. In the latter case, the manufacturing method in-itself can be an enabler of antibacterial activity, and the manufacturing parameters used in the coating process are critical for the performance thereof. In addition, converting a material formulation into a viable antibacterial coating depends on other intrinsic physical properties of the formulations, such as rheological, electrical, interfacial, that are emphasized in this review. In addition, for antibacterial strategies that rely on material surface topography, such as hydrophobic, the key challenge is developing scalable coating technologies for their large-scale fabrication. Additional factors that could influence the antibacterial performance of polysaccharide-based coatings and that are not emphasized in this review are related to the mechanical properties of the coating that can affect bacterial adhesion, effect considered to be a combination of material properties, bacterial shape and motility and experimental conditions [36].

## 3. Methods for assessing antibacterial properties of coatings: good microbiology practices and comparability of results

Before considering any factors influencing the performance of antibacterial coatings, we need to first consider the diverse methods for assessing antibacterial properties and what they entail when attempting to comparatively evaluate the coatings' antibacterial performance.

### 3.1. Methods to examine the antibacterial activity against bacterial in planktonic state

Currently, there is no clear standard for antibacterial testing in the field, which leads to difficulties with reproducibility and comparison of results from different studies. Many published articles in this field mainly use disk diffusion and measurement of optical density to monitor the bacterial growth or inhibition thereof to examine the antimicrobial effect of polysaccharide-based systems. In disk diffusion, test agents, e.g., coating materials, are placed on agar plate, where they diffuse and inhibit the bacterial growth around the deposition site, resulting in a clearance zone [88,89]. Although disk diffusion testing is used in many clinical microbiology laboratories for routine antimicrobial susceptibility testing, it

**Table 2**

Overview of findings regarding the antibacterial mechanisms of polysaccharides.

Antibacterial mechanism	Composition	Bacteria tested	Findings
Bacteria-repellent, Contact-killing [47]	CS, CMC	<i>S. mutans</i>	prevent bacterial adherence and showed a 75% reduction in bacteria
Bacteria-repellent Agent-releasing [48]	CS, CMC	<i>S. aureus</i> , <i>P. aeruginosa</i>	anti-adhesion and drug-delivery capabilities
Bacteria-repellent Contact-killing [54]	CS, Titanium phosphate particles	<i>E. coli</i>	mechanical durability, anti-bacteria adhesion and significantly anti-blood adhesion properties
Bacteria-repellent Contact-killing [59]	HA, poly(l-lysine)	<i>S. aureus</i> , <i>P. aeruginosa</i>	reduced bacterial attachment and inhibited planktonic bacterial growth
Contact-killing [65]	CS, HA	<i>E. coli</i> , <i>Candida glabrata</i> , <i>Streptococcus agalactiae</i> and <i>S. aureus</i>	Enhanced antimicrobial activity against pathogen bacteria and the antifungal activity
Contact-killing [87]	Pectin, orange oil	<i>S. aureus</i>	Enhanced antibacterial efficacy
Bacteria-repellent Contact-killing [71]	Quaternized chitin and chitosan	<i>S. aureus</i> , <i>E. coli</i>	Biocompatibility, antibacterial properties, and resistance to bacterial adhesion
Bacteria-repellent Contact-killing [72]	HA, nisin	<i>Staphylococcus epidermidis</i>	Enhanced antibacterial efficacy
Agent-releasing [82]	Gellan gum, dopamine, isoniazid, rifampicin	<i>S. aureus</i>	Biocompatibility, good antibacterial properties
Agent-releasing [84]	ALG, pectin, TiO <sub>2</sub> nanoparticles	<i>S. aureus</i> , <i>E. coli</i>	Bioactivity and antibacterial characteristics with no cytotoxicity

only provides qualitative results by categorizing bacteria as susceptible, intermediate, or resistant to tested materials [90–92]. In this sense, if a certain antimicrobial polysaccharide formulation has the ability to inhibit bacterial growth, clearance can be readily visible as an antimicrobial activity. However, bacterial growth inhibition does not always mean that the test agent is killing the bacterial cells. Therefore, this method cannot distinguish bactericidal and bacteriostatic effects. While the method can confirm the growth inhibitory effect of tested agents, it does not provide any clue for the minimum inhibitory concentration (MIC) that completely inhibits the bacterial growth and minimum bactericidal concentration (MBC) that completely deactivates the bacterial cells. In addition, high molecular weight polymeric systems may impede the diffusion of antibiotics or small molecules, which may lead to false negative results.

Another measurement commonly used is optical density (OD), which measures bacterial growth generally based on the increase in turbidity. The size of bacteria (e.g., increase in cell volume versus dividing bacterial cells), released pigments, extracellular matrix produced by bacterial cells, dilution of bacterial culture and the polysaccharides as well as any additives, e.g., nanomaterials/hybrids, in the test agent itself may influence the OD readings [93–95]. The method cannot distinguish between bacteriostatic and bactericidal effects. Even a complete inhibition in bacterial growth does not always mean the test material is bactericidal and cannot distinguish the density of live/dead bacteria [94,95]. The use of these methods should be restricted only to screening, to test antimicrobial efficiency of polymeric or composite materials does not give complete picture of antimicrobial efficiency instead sometimes may underestimate the antimicrobial potential. Thus, these methods should be avoided to examine the antimicrobial properties of polymer-based coatings. Instead, traditional but quantitative methods should be used.

If the developed coating formulation is soluble or dispersible in water, which is the case of most polysaccharides, MIC and MBC can be examined by simple and broth microdilution assay [96]. Here the test agent is serially diluted (2-fold dilution) in culture medium and the bacterial inoculum containing same number of colony forming units is loaded. After 18–24 h of incubation at the

required temperature the MIC concentration can be determined either by visual observation of bacteria or by measuring OD at 600 nm (spectrophotometry). To avoid the possible interference caused by the test material, OD of serially diluted test agent in same medium without bacteria (incubated in same condition) can be used as a background signal. Thus, the background OD can be subtracted from sample OD to calculate the MIC. From the same set of prepared samples, a fraction thereof can be spotted in agar plates to determine the MBC. The minimum concentrations that show no growth of bacteria in agar plates after 24 h of incubation can be considered as MBC. The reproducibility, quantitative analysis and requirement of small amount of test agents are key advantages of broth microdilution assay.

Counting colony forming units (CFU) is the best method for accurate counting of viable bacterial cells. This method provides the total number of live bacterial cells in the sample, thus making it easier to compare the antimicrobial efficiency of completely different tested agents quantitatively, with respect to their control counterparts [5,6]. Studies aiming to demonstrate the antimicrobial effect against bacteria in suspensions, time kill assay based on CFU method could be used to gain the better insight on antimicrobial potential [97,98].

The time kill assay can be complementary to MIC and MBC determination since these values are key for the selection of concentrations for time kill assay. In general, twice or four times the MIC is considered as starting concentrations for time kill assay [99,100]. The method provides the dynamic interaction between test agents and used microbial strains revealing the time and concentration dependent antimicrobial activity. The result from time kill assay can also be used to further clarify the bacteriostatic and bactericidal activity of test agents. If the agent/material found is to be bactericidal, scanning electron microscopy (SEM) or transmission electron microscopy (TEM) can be used to demonstrate the morphological alteration of bacterial cells.

### 3.2. Methods to examine anti-biofilm activity

The effect of polymeric systems (test agents) against biofilms can be tested either in terms of prevention of biofilm



formation or disrupting the already formed bacterial biofilms. If the test agent is expected to be used for treatment, its efficiency to disrupt preformed biofilms is more relevant. If such test agents are used as coatings on other substrates, the efficiency of such coatings to prevent the bacterial colonization or biofilm formation can be examined. To test the effect against the preformed biofilms, different concentrations and treatment times can be used. After the treatment, antibiofilm activity can be tested by means of viability determination (CFU method), quantification of biomass and 3-dimensional imaging of biofilm matrix using confocal laser scanning microscopy [101,102]. In addition, scanning electron microscopy (SEM) can be used to demonstrate the morphological alteration in bacterial cells and biofilm matrix after exposure to antibacterial coatings, providing mechanistic insights. To examine the potential of test agent coated surfaces to prevent the biofilm formation, bacterial cells can be grown on surfaces for a desired time period to evaluate bacterial adhesion and growth on the surface. The viability of bacterial cells can be determined by means of CFU. The decrease in number of CFU on coated surfaces can be either due to the bactericidal activity of coated materials or due to prevention of bacterial colonization [103]. To differentiate these possible phenomena, live/dead viability staining should be used and examined using fluorescence or confocal laser scanning microscopy. The live/dead staining can be used not only to differentiate between the density of live and dead cells but also to enable the distinction between the bactericidal effects and with anti-adhesion potential of the tested materials [104,105].

To summarize, several methods are available to assess antibacterial activity against free-living bacteria (planktonic state) and anti-biofilm activity. Critical for enabling a quantitative comparison across polysaccharide-based formulations and coatings are methods that are not susceptible to other types of interference, e.g., unknown processes affecting turbidity measurements, and distinguish between bacteriostatic and bactericidal effects and the determination of established quantitative parameters such as the minimum inhibitory concentration, minimum bactericidal concentration, counting colony forming units (CFU) and live/dead staining. We strongly encourage authors of future studies to use CFU method, combined with live-dead staining and SEM, as the new standard in the field [106,107]. However, for coatings that rely on structural effects induced through the fabrication method, further challenges may be encountered for antibacterial activity evaluation.

#### 4. Polysaccharide-based antibacterial coating technologies

Since the photographic films emerged in 19<sup>th</sup> century, the solution casting has started to be shown in the fabrication of polymer films and coatings [108]. In the process of solution casting, the polymer phase is dissolved in water or another non-aqueous volatile solvent and then cast on a flat surface followed by the evaporation process to remove the solvent phase. Due to its simplicity, the method of solution casting has been sometimes adopted to produce antibacterial coatings, combined with various polysaccharides including pectin [109–111], chitosan [112,113] etc. The design of solution casting is mainly aimed at laboratory scale, however, while other lab-scale coating methods have higher potential for large-scale production. In the following, we analyze polysaccharide-based coatings obtained using some of the most common coating technologies with industrial potential. In addition, for each technique, we also outline the operating principle, main processing parameters and advantages and disadvantages of the techniques. The key findings are summarized in tables that can be found at the end of each section.

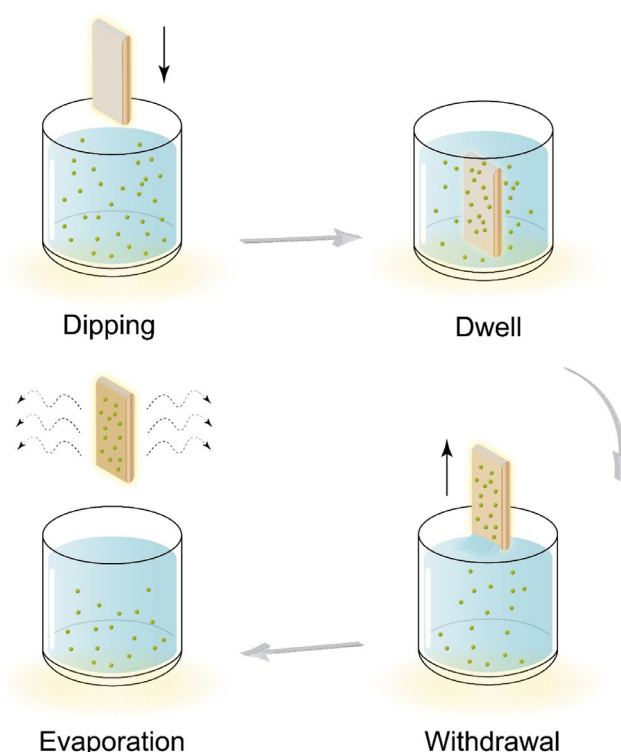


**Fig. 3.** Schematic showing the main steps of dip-coating: dipping the substrate to solution followed by dwell time and withdrawal of the substrate and the final step of drying/evaporation to make the coating rigid.

##### 4.1. Dip coating

Dip coating is arguably the most simple and one of the most popular industrial techniques for developing coatings with thicknesses ranging from 20 nm to 50  $\mu\text{m}$  [114,115]. The dip-coating method can be separated into four steps, as shown in Fig. 3. The first step is dipping, whereby the substrate is immersed into a tank containing a precursor solution. Following dipping, the substrate is kept in the solution for a fixed time. The time for which the substrate is held inside the precursor solution is called dwell time, which is the second stage of the process. The substrate is kept in the solution until the coating material fully covers it. In the third step, the substrate covered by the coating solution is withdrawn at a constant speed while avoiding any judders.

The thickness of the coating depends upon the speed of withdrawal and viscosity of the solution under controlled temperature and atmospheric conditions [115]. The last step in a dip-coating process is evaporation or drying of coating solution to make a rigid coating that is well adhered to the substrate and can be used for the desired applications [116].

The dip-coating method is cost-effective for large-scale production, along with the advantage of setup being easy to install and operate with less maintenance [116,117]. The method is also easy to implement in laboratory environments; therefore, it has been explored by many researchers to develop antibacterial coatings. Moreover, the antibacterial capability of dip coating process has been used in several significant areas such as textiles, medical devices, packing material, implants, membranes, paper coating, and wound healing [118–122]. The abundant hydroxyl groups on polysaccharides allow them to easily disperse or dissolve in the coating precursor solution due to their strong water-binding ability. In addition, film-forming properties during evaporation / drying enable polysaccharides to maximize the benefits of dip coating

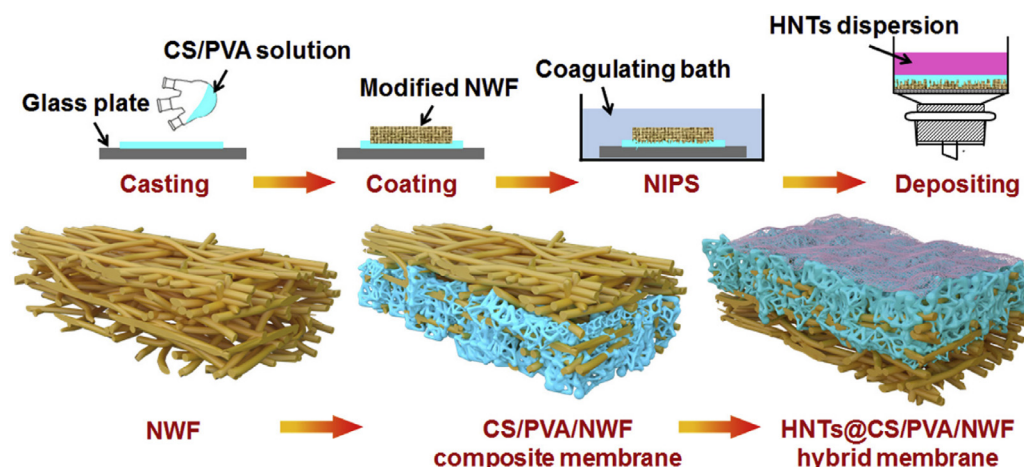


**Fig. 4.** Schematic showing membrane fabrication process having CS, PVA, and halloysite nanotubes deposition using dip coating process [125]. Reprinted from Journal of Membrane Science, 594, Wang, Z. et al., Environmentally-Friendly Halloysite Nanotubes@ Chitosan/Polyvinyl Alcohol/Non-Woven Fabric Hybrid Membranes with a Uniform Hierarchical Porous Structure for Air Filtration, 117445, Copyright (2020), with permission from Elsevier.

for industry and provide researchers plenty of possibilities to innovate [123].

#### 4.1.1. Dip-coated polysaccharide coatings for fabric and paper industry

In developing antibacterial coatings, Nawaz et al. [124] demonstrated the use of dip-coating method for fabricating a modified nonwoven cotton fabric which showed significant antibacterial efficacy against four different bacterial species. For coating development, KOH-treated cotton fabric was coated with silver nanoparticles followed by dip coating in 2% CS solution for 2 minutes. After the prepared layer was dried at 60 °C for 60 min, the Ag and CS-coated cotton fabric surface was further chlorinated as a final step in developing an antibacterial coating. It was observed that the developed coating showed a significant increase in bactericidal activity. Analysis showed that the inactivation of bacterial growth was achieved due to the release of halogen ( $\text{Cl}^+$ ) from the coating to the growth medium. Dip-coating of CS/polyvinyl alcohol (CS/PVA) blend on non-woven fabric for air filtration membranes was developed by Wang et al. [125], see Fig. 4. The developed structure (pore size of 2.88  $\mu\text{m}$  and porosity of 67.5%) showed significant enhancement in air filtration efficiency (96.8%), tensile strength (25.5 MPa) and higher bacterial efficacy, determined using OD and CFU method. Thus, the coatings showed a percentage reduction in CFU of up to 99.1% against *S. aureus* and 96.6% against *E. coli*. Apart from using dip coating for textiles, Jung et al. [126] developed a silver-CS-based coating to enhance the properties of Korean traditional paper, Hanji. A coating solution was prepared by mixing 1.5 wt.% CS in  $\text{AgNO}_3$  solution. The developed coating was further diluted in different ratios of 1/10, 1/100 and 1/1000. Using the dip-coating process, Hanji was coated by dipping for 30 s in the solution followed by drying at 90 °C for 10 min. The paper showed enhanced tensile strength (1/10), burst strength (1/100) and oil resistance (1/10) at the indicated diluted solutions. However, the developed coating exhibited higher antibacterial properties on all the diluted solutions against *E. coli*, i.e. inhibition zones > 1 mm and percentage reduction in CFU (JIS Z 2801 standard for hard and smooth plastic surfaces) relative to the control of up to 99.9%, for the highest Ag nanoparticle content, as expected. Importantly, the coating formulation significantly influenced the surface morphology of the coating, with the highest performing antibacterial coating being also the smoothest.

#### 4.1.2. Dip-coated antibacterial polysaccharide coatings for food preservation and packaging

Specific work on developing materials for food packing has been performed by Hongsriphan & Sanga [127]. They developed a CS-based coating on corona-treated polylactic acid (PLA)/polybutylene succinate (PBS) blends. A corona discharge energy of 4 A was applied to the blend of 90% PLA and 10% PBS to develop the coating. Further, the substrate was dip-coated in a CS solution for 30 min and dried at room temperature for 24 h. The developed coating showed enhanced mechanical and antibacterial properties and reduced water vapor transmission. It was observed that microorganisms reduced considerably with an increase in the CS concentration, with up to 99% percentage change in CFU method against *E. coli* (Gram-negative) and 88% against *S. aureus* (Gram-positive bacteria). This reduction was attributed to the amino group ( $\text{NH}_3^+$ ) present in CS, which caused severe damage to the cell membrane of bacteria by changing permeability. In another study, Yuan et al. fabricated a multi-component coating using sodium alginate/gum arabic/glycerol and natamycin [128]. The developed coating enhanced the shelf life of sweet potatoes to 120 days. The coating also demonstrated substantial antibacterial activity against *Penicillium*, *Aspergillus*, *Rhizopus*, and yeast, with an increased inhibition zone of 118%, 97%, 166%, and 133%, respectively. In addition, it was observed that coatings exhibit an antibacterial activity with a minimum 40  $\mu\text{g/mL}$  concentration of natamycin in the film solution. However, with an increase in the concentration of fillers, the transparency of the coating is reduced, but the mechanical, barrier properties and thermal stability are enhanced. Sanchis et al. [129] used pectin-based coating to further enhance the shelf life of food products. It has been shown that the peeled and cut pieces of persimmons when dip-coated for 3 min using apple pectin coating, obtain an enhanced antimicrobial efficacy against *E. coli*, *S. enteritidis*, and *L. monocytogenes*. Moreover, with the addition of citric acid and calcium chloride in the present coating solution, the coatings not only extend the shelf life of persimmons up to 9 days but also acts as an anti-browning and firming agent.

#### 4.1.3. Dip-coated antibacterial polysaccharide coatings for medical applications

The dip-coating process has been extensively used in the medical area to fabricate various devices. Yang et al. [130] developed hydrogel coatings using a dip-coating process for urethral

catheters. The coated formulations included HA and CS. The developed coatings had low friction (an application requirement) and showed a reduction in percentage of live cells from LIVE/DEAD BacLight Viability assay, down to  $4.70 \pm 0.95\%$  against *E. coli* for polyurethane-substrates with catechol-conjugated-CS coatings containing Ag nanoparticles and down to  $59.12 \pm 5.16\%$  for the same substrate/coating combination. Interestingly, because of particulate agglomerates present in the formulation, the coatings, when deposited on the polymers, increased the surface roughness. This decreased the friction coefficients, which further had a synergic effect in tailoring the surface energy and making it hydrophilic, which can be beneficial for certain applications.

One of the significant applications of polysaccharide-based antibacterial coatings is in medical implants. However, achieving the optimal thickness required for coatings to have an antibacterial effect and bioactivity is the main challenge from manufacturing point of view. Li et al. worked towards shedding light on this by developing a hydroxyapatite-CS-based coating using a dip-coating process [131] on a micro- nanostructured substrate. Hydroxyapatite deposited on the Ti surface using the micro-arc oxidation technique showed enhanced cell adhesion, spreading and proliferation along with enhanced antibacterial efficacy, i.e., inhibition percentage increase (inhibition rate) proportional to the CS content of up to 65% by bacterial counting method, inhibition zone test and OD measurement. In addition to using the dip-coating process for Ti implants, the method has potential for developing antibacterial coatings for wound dressing applications. Liu et al. [132] developed a similar CS-based superhydrophobic coating on cotton gauze for skin wound dressing. The coating formed was retained on the cotton even after three washing cycles which shows the stability of the layers. During antibacterial testing, it was found that the developed PFDT/GA@AgNPs/CS coating showed no live bacteria attachment even after using a high concentration of bacterial suspension, offering enhanced antibacterial properties against *E. coli* (99.99%) and *S. aureus* (99.97%). The quantification refers to a bacterial anti-adhesion rate defined as a percentage reduction in CFU relative to the control. In another study, Brindhadevi et al. [133] demonstrated a process to develop an antibacterial fabric for fast wound healing using silver nanoparticles with labdanum and sodium alginate. The developed fabric showed enhanced antimicrobial activity with 45 mm and 42 mm inhibition zones against gram-positive (*S. aureus*) and gram-negative bacteria (*Klebsiella pneumonia*).

Despite many applications of dip coating, it also suffers from several limitations, such as unbalanced surface coverage and the presence of defects due to instabilities in equipment or during withdrawal speeds. Dip coating defects may also occur due to the atmospheric conditions during the coating or due to the viscoelastic and chemical properties of the solution to be coated on the sample. One of the common issues during the dip-coating process is wettability. However, with several preventive steps, these defects can be minimized but cannot be fully eliminated from the process. A summary of the main findings of the section is presented in Table 3.

## 4.2. Spin coating

Spin coating is used to produce highly uniform coatings on flat surfaces using centrifugal forces. Spin coating (as shown in Fig. 5) is broadly described in four steps: deposition, spin-up, spin-off, and evaporation [134]. Thus, the substrate is placed on the spin coater equipment. The solution to be deposited on the substrate is dispensed at the center of the substrate, which is then spin-up followed by spin-off at high velocities of 500 to 10000 rpm [135,136]. The rotation of the coater continues to achieve spin-off of the excess material, which leads to the desired coating thickness [137]. The achieved coating is then bound to the substrate by

evaporation of solvents in the solution or UV curing, depending upon the coating solution [138,139]. In this process, the coater's rotational speed and the solution viscosity are the two significant parameters influencing coating thickness [139]. Other factors considered during the spin coating process are solvent evaporation rate, spin time, and surface wettability [140].

Many researchers have used the spin coating for various antibacterial coatings due to the ease of deposition of multiple types of materials in solution form [120,141,142]. The most common solutions used for the spin coating process are polymers, biomaterials, and different kinds of nanomaterials (suspensions). Moreover, industrial demand for spin coating has increased rapidly in the last few years due to its capability to quickly produce uniform coatings ranging from nm to a few micrometers, relatively inexpensively [134].

### 4.2.1. Spin-coated polysaccharide coatings for biomedical implants

One of the vast applications of spin coating is for biomedical implants and the major challenge is the poor adhesion of the coating to the substrate surface and the uniformity of the coating on a curvature surface. However, these challenges could be addressed by the addition of cationic and anionic polysaccharides via electrostatic effects [143]. Vakili and Asefnejad [143] have fabricated CS and alginate (ALG) coated titanium implants. During the spin coating process, a solution of CS and ALG was dispensed on the Ti implant at an optimum speed of 8000 rpm to obtain a uniform coating that showed an adhesion strength as high as 8 MPa. The Ti-coated sample was further analyzed for antibacterial behavior for *E. coli*. The CS and ALG coating showed a percentage reduction in CFU method of up to 36% (attributed to CS) and facilitated implant bone regeneration. Interestingly, while cellular viability via *in vitro* cytotoxicity tests was improved with increasing rotational speed during spin coating, this was not reported for bacterial growth inhibition. Similar to this, CS/oxacillin-melittin and CS/vancomycin-melittin coatings on Ti implants were developed for better antibacterial capability and the elimination of biofilm formation [144]. Using the spin coating process, both CS/oxacillin and CS/vancomycin coatings were deposited on the different Ti implants. The coating solutions were deposited on the Ti substrate at 600 rpm and rotated for 1 h to obtain a 15  $\mu\text{m}$  thick coating. Further, a thin layer of melittin was cast on top of the coating to obtain the final multilayer Ti-coated implant. Due to the presence of melittin on top of CS, Ti implants behaved as a bactericidal surface. Moreover, when the melittin is combined with CS/oxacillin, it deactivated all the methicillin-resistant *S. aureus* in less than 6 h. When the melittin is combined with CS/vancomycin, the vancomycin-resistant *S. aureus* bacteria was killed in less than 3 h, confirming a unique synergism in both melittin chitosan-based coatings. To further develop a polysaccharide-based antibacterial coating on Ti, Yu et al. developed a hybrid coating consisting of lysozyme, CS, silver (Ag), and hydroxyapatite (HAp) [145]. To achieve an antibacterial effect, a CS/Ag/HAp coating was first deposited by electrochemical deposition on the Ti implant, followed by spin coating (5000 rpm for 30 s) of Lys with a total thickness of 14  $\mu\text{m}$ . The developed coating showed a porous hierarchical nanostructure which helps in enhancing the antibacterial effect against both *S. aureus* and *E. coli*. We note that the porous surface structure was induced in a pre-processing state by alkali-heat treatment of the Ti surface. It is, therefore, not entirely clear to what extent spin coating is relevant for the application as opposed to dip-coating. It has been observed that the antibacterial efficiency, determined as percentage change relative to control based on optical density (OD) measurements through spectrophotometry, the coatings could reach up to 95.42% and 97.46% against *E. coli* and *S. aureus*. This was combined with very low toxicity compared to the non-toxic pure Ti samples. Following a similar procedure,



**Table 3**

Summary of target products, compositions, antibacterial efficiency, and process parameters for dip-coatings.

Products	Compositions	Antibacterial Efficiencies	Process Parameters
Cotton fabric for wound dressing [124]	Nonwoven cotton fiber was first coated with Ag nanoparticles (0.04 M silver nitrate) and dried at 65 °C for 90 min. A second layer of chitosan (2%) was deposited using dip coating process. To further form N-halamines, chitosan coated substrate was dipped in a 10 mL sodium hydrochloride solution for 30 min followed by 24 h drying.	Colony forming units count, <i>M. luteus</i> , <i>S. aureus</i> , <i>E. aerogenes</i> and <i>E. coli</i> after 24 h in incubation at 37 °C The developed coating showed a significant increase in the inhibition zone for all the four types of bacteria. However, the coating showed lower bacterial activity for Gram-negative bacteria than Gram-positive bacteria.	Chitosan was deposited using a dip coating process. Ag modified fibers were dipped for 2 min followed by drying at 60 °C for 60 min.
Antibacterial coating for food preservation [128]	Sodium alginate (2.5%), gum arabic (1%), and glycerol (2%) were mixed with deionized water (94.5%). Further, the above prepared solution was added to different concentration of natamycin solutions to prepare various coatings solutions.	Kirby-Bauer method, <i>Penicillium</i> , <i>Aspergillus</i> , <i>Rhizopus</i> , and yeast after 24 h in incubation at 37 °C Developed coating exhibits antibacterial properties with a minimum 40 µg/mL concentration of natamycin in the film solution.	Sweet potatoes are dip coated for 1 min in the prepared solutions and air-dried at room temperature.
Antimicrobial Pectin based coating [129]	Apple pectin along with citric acid, calcium chloride and nisin were added to develop the coating solution.	Colony forming units count, <i>E. coli</i> , <i>S. enteritidis</i> , and <i>L. monocytogenes</i> after 48 h in incubation at 37 °C Pectin based coating significantly reduced the antimicrobial growth. ~It was shown that <i>S. enteritidis</i> showed highest reduction in the microbial growth.	Persimmon slices were dip coated in the pectin-based solution for 3 min and dried at 5 °C.
Enhancing Hanji paper properties [126]	Hanji papers were dip coated using a solution containing chitosan (1.5 wt.%) and AgNO <sub>3</sub> (30 mmol).	Disk diffusion method, <i>E. coli</i> after 24 h in incubation at 38 °C Over 1 mm of inhibition zone was observed for the coated samples compared to the zero-inhibition zone with neat Hanji paper demonstrated higher antibacterial activity for the coated paper.	Individual Hanji papers were dipped in the solution for 30 s, followed by drying at 90 °C for 10 min.
Chitosan composite for air filtration [125]	Nonwoven fabric was coated with TiO <sub>2</sub> /H <sub>2</sub> O <sub>2</sub> hydrosol. Further a solution of CS (2.1 g) and PVA (4.9 g) in a 0.2 mol L <sup>-1</sup> adipic acid was coated on fabric. A top layer of halloysite nanotubes were deposited via vacuum filtration to fabricate composite membrane.	Colony count method, <i>S. aureus</i> and <i>E. coli</i> after 24 h in incubation at 37 °C The developed porous membrane demonstrated significant enhancement in air filtration efficiency (96.8%) and higher antibacterial rate reaching 99.1% for <i>S. aureus</i> and 99.6% for <i>E. coli</i>	Not reported
Food packing coating [127]	Chitosan (various concentrations) solution was coated on corona-treated or untreated polylactic acid (90%) and polybutylene succinate (10%) extruded sheets using dip coating process	Shake-flask culture method, <i>S. aureus</i> and <i>E. coli</i> after 24 h in incubation at 37 °C With a higher chitosan concentration larger reduction of microorganisms was observed for both <i>S. aureus</i> and <i>E. coli</i> bacteria.	5.0 cm x 15.2 cm substrates were dip coated by immersed in chitosan solution for 30 min, and dried at room temperature for 24 h
Antibacterial coating for urethral catheters [130]	Chitosan hydrogel coating was deposited on PU and PVC using catechol-conjugated solutions in a dip coating method. Catechol-conjugated HA (3mg/mL), HSA (5 mg/mL) and CS (5mg/mL) were prepared. Silver nanoparticles were added to the hydrogel coating to enhance antibacterial properties	BacLight bacterial viability kit and Spectro fluorophotometer, <i>S. aureus</i> and <i>E. coli</i> after 8 h in incubation at 37 °C For a silver doped catechol-conjugated chitosan coating cells reduces drastically to 4.70% and 59.12% for <i>E. coli</i> and <i>S. aureus</i> , respectively.	Polydopamine coated substrates were immersed in appropriate solutions for 4 h and dried in nitrogen after washing.
Chitosan coating for biomedical implants [131]	Hydroxyapatite was deposited on Ti using micro-arc oxidation process. Further chitosan solution in 2% AA was deposited by dip coating on hydroxyapatite coated Ti samples	Bacteria count method and ZOI test, <i>E. coli</i> after 24 h in incubation at 37 °C It was demonstrated that bacteria reduce drastically with an increase in chitosan concentration in the composite	Chitosan was deposited using a dip coating process. Samples were dipped for 3 min, followed by rinsing in water and drying at 55 °C for 24 h
Chitosan based Superhydrophobic wound dressing [132]	Cotton fabric was coated with chitosan solution (5 mg/mL) further a second layer of gallic acid treated silver nanoparticles (0.2 mg/mL) was deposited. A final layer of PFDT (3 µL/mL) was deposited to fabricate the superhydrophobic coating	Colony forming units count, <i>S. aureus</i> and <i>E. coli</i> after 24 h in incubation at 37 °C Developed multilayer coating demonstrated higher killing efficiency against <i>E. coli</i> (99.99%) and <i>S. aureus</i> (99.97%)	Dip coating process was used to sequential deposition of multilayers such as chitosan, gallic acid treated silver nanoparticles and PFDT for 30 min each
Alginate based Superhydrophobic wound dressing [133]	Silver nitrate was used to prepare silver nanoparticles of size 200 nm. Fabric was coated with silver nanoparticles followed by deposition of (500 µL) labdanum and (1g) alginate.	Disk diffusion method, <i>E. coli</i> , <i>K. pneumoniae</i> , <i>S. aureus</i> , <i>B. subtilis</i> , <i>fungus</i> and <i>Aspergillus niger</i> after 24 h in incubation at 37 °C The developed fabric showed enhanced antimicrobial activity with an 45 mm and 42 mm inhibition zones against <i>S. aureus</i> and <i>K. pneumoniae</i> .	Silver nanoparticles, alginate and labdanum solution were dip coated on fabric for min followed by drying in ambient conditions.



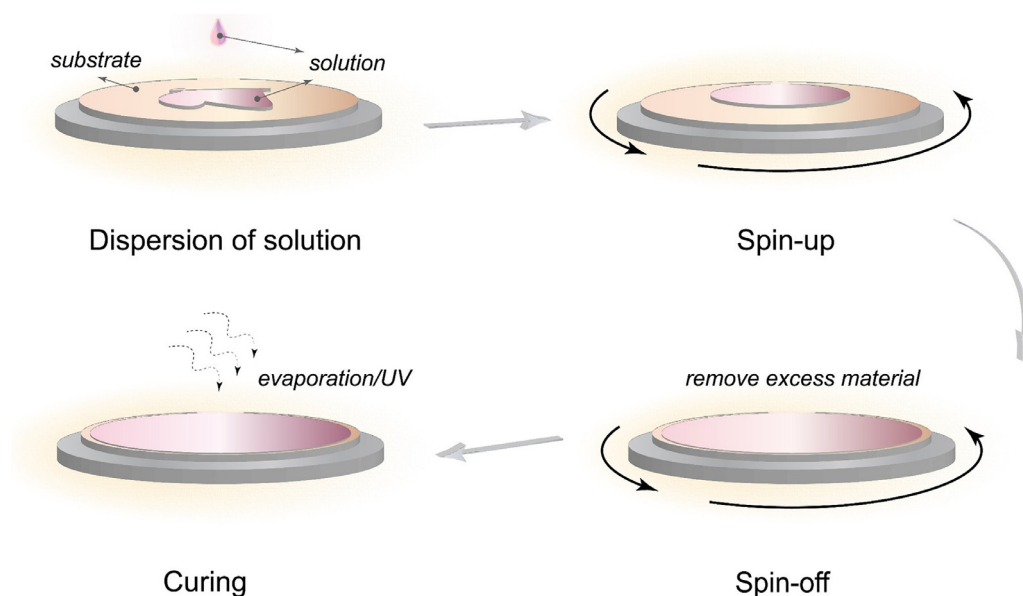


**Fig. 5.** Schematic of the spin coating process showing various steps involved, from solution dispersion followed by spin-up and spin-off to the final curing of solution on the desired substrate.

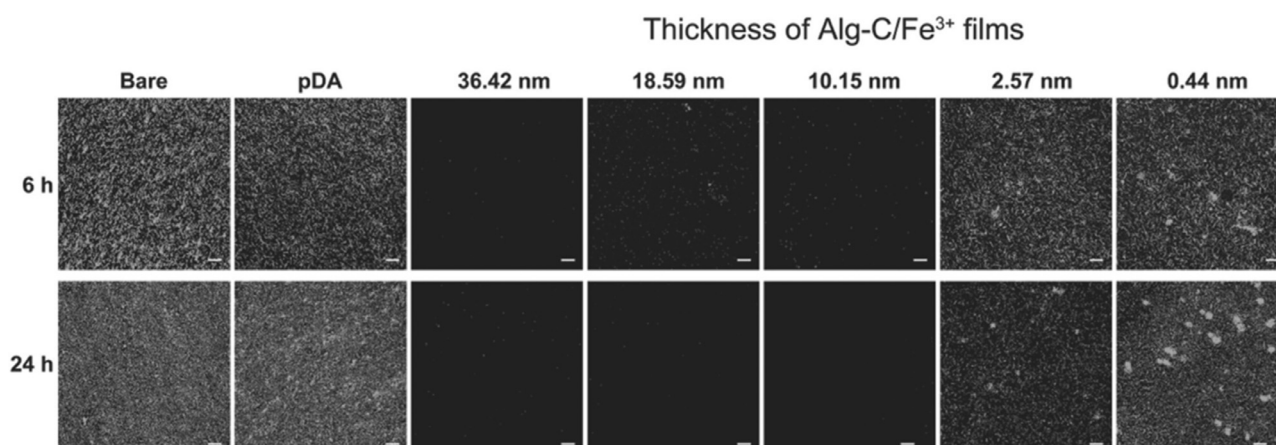


**Fig. 6.** Fluorescence microscopy image obtained using propidium iodide showing antibacterial reduction of Gram-negative bacteria on ALG film having different thicknesses for 6 and 24 h [147]. Reproduced with permission, © 2016 WILEY-VCH Verlag GmbH & Co. KGaA, Weinheim.

Ren et al. developed a catechol functionalized chitosan (CSCT)-Ag coating on Ti implants [146]. A two-step procedure was used to create the coating: first, the CSCT was electrodeposited on the Ti substrate; second, the CSCT-Ag solution was spin-coated with a speed of 4000 rpm for 40 s on the already deposited CSCT layer. The 23  $\mu\text{m}$  thick two-layer coating showed inhibition ratios of 96% and 99% against *S. aureus* and *E. coli*, respectively, see Fig. 6. Moreover, the corrosion resistance, hydrophilicity, and adhesion strength were improved significantly compared to the Ti substrate.

#### 4.2.2. Spin-coated antibacterial polysaccharide coatings for wound dressing

Ashok et al. [148] developed CS and gelatine based coatings on polystyrene-co-acrylonitrile (PSAN) microfibers for antimicrobial wound dressing. Both CS and gelatine coatings have been deposited on PSAN using a spin coating process to achieve a thickness of 4.5  $\mu\text{m}$  and 6.22  $\mu\text{m}$ , respectively. It has been observed that due to the low surface roughness, both these coatings are ideal for wound dressings. Moreover, it was shown that the gelatine coating had a maximum inhibition zone of 14 mm for *E. coli* compared to that of CS coating, having 8 mm. Korica et al.,

developed CS-based multilayer films using a spin coating process as a wound dressing material [149]. The films have been fabricated using various combinations of regenerated cellulose and 2,2,6,6-Tetramethylpiperidine-1-oxyl radical oxidized cellulose nanofibril (TOCN) with CS. All the fabricated films use a similar spin coating protocol (4000 rpm for 60 s and acceleration of 2500 rpm  $\text{s}^{-1}$ ). It was observed that the CS adsorbed sheet provides a maximum antibacterial reduction of 99.9% compared to the RC-TOCN-CN layer (99.8% and 99.6%) for *E. coli* and *S. aureus*, respectively (CFU method). Moreover, when RC films were coated with the mixture of TOCN and CS, there was no antibacterial activity due to the insufficient presence of amino groups in the film. Apart from CS, a multilayer coating using ALG film has been developed by Kim et al. [147] Alginate catechols were spin-coated (4500 rpm for 30 s) on the desired substrate, followed by crosslinking using catechol- $\text{Fe}^{3+}$ -catechol interactions. In addition to being antibacterial, the developed coating also had high resistance to protein adsorption (Fibrinogen). It was observed that coatings of 10 nm thickness showed no protein adsorption and had an antibacterial reduction of 99.80% against *E. coli* (staining, confocal microscopy and image analysis). However, the antibacterial effect of the coating could be enhanced

**Table 4**

Summary of target products, compositions, antibacterial efficiency, and process parameters for spin-coating.

Products	Compositions	Antibacterial Efficiencies	Process Parameters
Antibacterial and bioactive coating for Ti implants [143]	0.5% (w/v) CS mixed with 0.5% ALG solution was spin coated on Ti sheets followed by crosslinking using 1% calcium chloride.	Colony forming units count, <i>E. coli</i> after 48h in incubation at 37 °C For CS/ALG coated Ti substrate antibacterial activity increased to 36.31% compared to pure Ti having 4.1%. The best results were obtained at the spin speed of 8000 rpm.	Various spin speeds were used: 1000, 4000 and 8000 rpm separately for three cycles and 30 s each.
Multilayer coating on Ti implants [144]	AA (0.25 vol.%) solution were poured into CS (6 wt.%) powder. 50 µL of obtained solution is spin coated on Ti substrate. To achieve a CS/Oxacillin or CS/Vancomycin coatings; each materials was added separately to CS solution and spin coated on Ti as a first layer. Second layer of Melittin was casted (various concentration) on top of first layer.	Colony forming units count, methicillin-resistant <i>S. aureus</i> and vancomycin-resistant <i>S. aureus</i> after 24h in incubation at 37 °C. Melittin coating when applied on chitosan kills the bacteria more efficiently and prevents biofilm formation. Melittin when combined with vancomycin showed extraordinary ability of killing vancomycin-resistant <i>S. aureus</i> bacteria in less than 3 h.	Layers were spin coated on Ti substrate; samples were rotated for 1h at 600 rpm
Multicomponent hybrid coating for Ti implants [145]	Solution contains 2 mg/mL HAp, 2mg/mL CS, 2mM AgNO <sub>3</sub> and 1% (v/v) AA was deposited on Ti using electrochemical deposition process. Second layer of Lys (10 mg/mL) is deposited using spin coating process to achieve a final coating of Lys/CS/Ag/HAp-Ti.	Colony forming units count, <i>S. aureus</i> and <i>E. coli</i> after 12h in incubation at 37 °C The developed Lys/CS/Ag/Hap coating on Ti showed enhanced antibacterial efficiency of 95.48% and 97.46% against <i>E. coli</i> and <i>S. aureus</i> in 5h.	Lys is coated at 5000 rpm for 30 s to achieve a total coating thickness of 14 µm on Ti.
CSCT/Ag coating for Ti implants [146]	Two coatings were deposited on Ti. In First coating 1% CSCT was deposited on Ti using electrodeposition process. After first layer, CSCT-Ag solution (0.1 mg/mL), CSCT (5 mg/mL) and gelatin (5 mg/mL) were mixed together and spin coated to fabricate a second layer.	Disk diffusion method, <i>S. aureus</i> and <i>E. coli</i> after 24h in incubation at 37 °C Antibacterial rates for the developed two layer coatings reached 99% and 96% for <i>E.coli</i> and <i>S. aureus</i> bacteria, respectively.	Solution was spin coated as a second layer at 4000 rpm for 40 s
CS/GA coating for wound dressing [148]	PSAN microfibers were spin coated using CS and GE separately. To prepare CS solution 100 mg of CS was added to 10 mL of AA and to prepare GE solution 0.1 g of GE was added to 5 mL of AA.	Disk diffusion method, 16S rDNA identified human pathogenic bacteria strains after 24-48h in incubation at 37 °C Maximum inhibition zone of 14 mm by GE coating and of 8 mm by CS coating was obtained against <i>E. coli</i>	Both the solution were spin coated on PSAN separately at 200 rpm
Protein-repellent multilayer coating [149]	100 µL TMSC was spin coated on sensor and converted to pure cellulose using HCL vapors. Further a coating of TOCN (50 µL) was deposited on top of cellulose coating. The developed coating was named as RC/TOCN film was coated again with CS (0.5%) by casting approach.	Colony forming units count, <i>S. aureus</i> and <i>E. coli</i> The developed RC/TOCN film with CS absorbed coating as a top layer provides a maximum antibacterial reduction of 99.8% and 99.6% for <i>E. coli</i> and <i>S. aureus</i> , respectively.	Layers were spin coated using a similar procedure: all layers were spin coated at 4000 rpm for 60 s with an acceleration of 2500 rpm s <sup>-1</sup>
Alginate antibacterial coating [147]	Alginate was conjugated with catechol (15 mg/mL) and deposited on polydopamine-coated Si/SiO <sub>2</sub> substrate using spin coating process followed by crosslinking using catechol-Fe <sup>3+</sup> -catechol interactions. Coating with a thickness of 10 nm was found to be most suitable for antibacterial properties.	Disk diffusion method, <i>E. coli</i> after 14h in incubation at 37 °C The developed coating showed high resistance to protein adsorption along with 99.92% reduction in bacterial cell adhesion after 24 h at a thickness of 36.42 nm.	Coating was spin coated at 4000 rpm for 30 s
Cellulose/PLA for food packing [150]	LA (7 g) solution was added to CNC solution (1 to 5 wt.%) and spin-coated to fabricate antimicrobial coating with a thickness of 0.2 mm.	Drug release test; <i>E. coli</i> , <i>S. enteritidis</i> and <i>L. monocytogenes</i> at 37 °C PLA/CNC films showed enhanced antimicrobial efficacy.	PLA and CNC mixture was spun coated for 180 s at 150 rpm followed by drying for 4 h at room temperature.

(99.92%) and retained even after 24 h if the thickness was increased to 36.42 nm via processing conditions.

In another work, Shojaeiarani et al. demonstrated a PLA/cellulose coating leading to hydrophobicity with low water vapor permeability [150]. Further, tested against various pathogens such as *E. coli*, *S. enterica* and *L. monocytogenes*, the coating showed a 0.5–0.6 lg CFU/ml reduction against Gram-positive bacteria (*L. monocytogenes*) under 24 h of incubation. Interestingly, the disk diffusion method also used in the study, showed no bacterial growth inhibition.

A summary of the main spin-coated antibacterial coatings reviewed can be found in Table 4. One of the major limitations of the spin coating process is the limited size of the substrate [151]. This is due to the restriction in the rotational speed, which leads to achieving desired films thickness. Apart from this, there is a significant material loss during the deposition process as only 2 to 3% of material is deposited on the substrate. The remaining 98 to 97% of material is flung off, causing a very low material efficiency [139,152]. Moreover, it is extremely difficult to deposit a homogeneous thin film with a thickness of less than 10 nm using the spin

coating process. In the spin coating process, even achieving a multilayer (more than 2 layers) is challenging due to controlling the thickness and homogeneity of multilayer films [153]. As described above, the material's viscosity plays a vital role in the film thickness. Therefore, solvents are often added to the material to be deposited to reduce the viscosity, solvents which evaporate after the deposition process. However, traces of solvent have been found in most films, causing reduced efficiency and further film contamination during application [153].

#### 4.3. Spray coating

Spray coating is widely used in industry as a finishing process for painting virtually any type of product [154,155]. The coating material is directly sprayed on the substrate, as shown in Fig. 7. For this, compressed air is used to change the coating fluid into a fine mist under high pressure, which is then sprayed onto the substrate. Since droplet velocity, surface tension and fluid viscosity play an important role during the whole process including droplet formation (atomization) and droplet

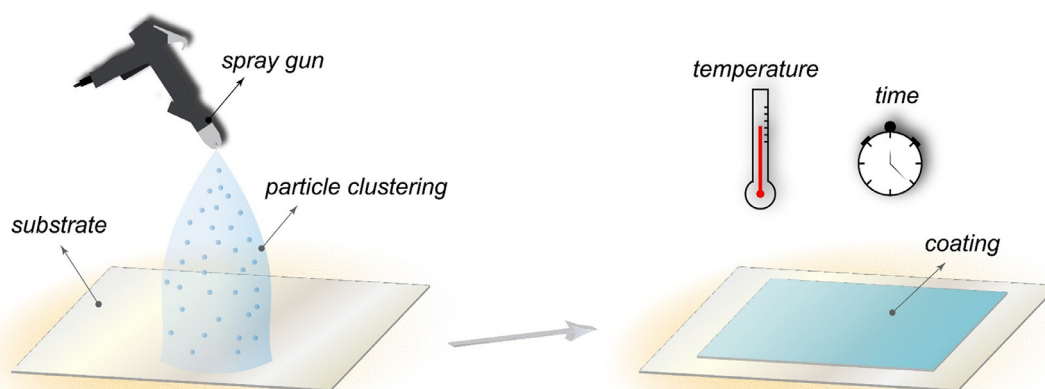


**Fig. 7.** Schematic showing spray coating process where coating fluid mist is sprayed on the substrate to achieve desired coating thickness. The coating is further dried for several minutes to achieve better adhesion to the substrate.

wetting and drying, the properties of the feed dispersion such as solubility and emulsifying properties, are key factors determining the quality of the final coatings. Therefore, due to their solubility versatility and the possibility of tuning their molecular weight, resulting in a wide range of physicochemical properties and applications, polysaccharides are suitable for spray coating [156]. Spray coating of polysaccharides finds several applications in the field of antibacterial and anti-fouling surfaces [157]. The process was used to deposit various polysaccharides to enhance the antibacterial effect and protein resistance on the substrate surface [158–161].

#### 4.3.1. Spray-coated antibacterial polysaccharide coatings for food packaging

Therefore, Gedarawatte et al. [162] used spray coating for enhancing the shelf life of vacuum-packed beef by depositing an edible coating of gelatin and CS. Both gelatin (10%) and CS (1%) coatings were spray-coated vertically on the steak samples from a distance of about 45 cm for 2 min with a flow rate of  $0.18 \text{ L min}^{-1}$ . Compared to uncoated and gelatine-coated samples, the CS-coated beef showed some antimicrobial effects (up to 21 days) with no change in the meat pH, color, and tenderness. The antimicrobial effect of the coating was determined against lactic acid bacteria and *Brochothrix thermosphacta*, while also testing for the presence of *E. coli*, via agar plate CFU method. In another study, Jovanović et al. [163] developed various coatings by combining both biopolymers (chitosan-gelatin, pectin-gelatin) with lemongrass essential oil and ZnO, as active components. The developed coating was spray-coated on cardboard boxes containing fresh raspberries. The chitosan-gelatin coating with any of the active component showed highest antibacterial efficacy against *E. coli*, *B. subtilis* and *S. aureus* along with enhanced mechanical properties such as tensile strength and elastic modulus. In addition, the coating enhanced the shelf life of raspberries from 4 to 8 days in refrigerator.

#### 4.3.2. Spray-coated antibacterial polysaccharide coatings for paper and polymer sheets

Using CS, an antibacterial coating for both polymers and metals has been developed by Mitra et al. [164]. The micrometer thick coating of tripolyphosphate (TTP, 0.6 wt.%) and quaternized chitosan (QCS, 5 wt.%) solutions have been sprayed onto plasma-treated polyvinyl fluoride (PVF) films at a nozzle moving speed of 50 mm/sec and air pressures of 0.25 and 1 bar, respectively. The developed transparent coating (PVP-QCS-50-0.6) demonstrated a 90% (CFU method followed by live/dead bacteria staining) bacterial reduction against both Gram-positive (*S. aureus*) and Gram-negative bacteria (*P. aeruginosa*) compared to pristine PVF surfaces,

as shown in Fig. 8. After wiping the contaminated surface with 70% ethanol, the coating could be reused several times. In another study using CS and cellulose, Tyagi et al. [165] have developed a high-strength antibacterial composite tissue paper using a spray coating process. CS was mixed with cellulose nanocrystals (CNC) 80:20 by weight and spray-coated to create a lightweight composite coating (CS/CNC) on tissue paper. The CS/CNC coating was further treated with plasma (P-CS/CNC) to enhance its antibacterial and water retention properties. The developed coating was hydrophilic with a contact angle of  $40^\circ$ , which leads to a high-water absorption capacity; therefore, the tissue paper with composite coating could be used after the restroom. In addition to this, the P-CS/CNC coating showed a reduction in bacterial growth (99%) for Gram-negative bacteria (*E. coli*) compared to the non-coated tissue paper, as determined using the ASTM 2149 method. Fig. 9 shows the bacterial growth on the agar plate after treating the culture with different coatings in the petri dish.

#### 4.3.3. Spray-coated antibacterial polysaccharide coatings for biomedical implants

A specific study on plasma spray coating to enhance the antibacterial effect has been performed by Banerjee & Bose [166] with depositing an aloe vera gel extract (acemannan) + CS in doped (silver oxide and silica) hydroxyapatite on Ti implants. The developed coating showed antibacterial effects against Gram-positive (*S. epidermidis*) bacteria as determined from the inhibition zone of disk diffusion tests. Moreover, silver, silicon, and acemannan in the coating prevented secondary infections, increased angiogenic effects, and accelerated healing in load-bearing bone, respectively. In another study, Jia et al. [167] demonstrated enhanced antibacterial efficacy of water-soluble and nontoxic cellulose-based photosensitizer (CPS) under 2 min sunlight. To fabricate CPS, protoporphyrin IX and quaternary ammonium salt groups have been chemically attached to cellulose. The fabricated CPS solution was sprayed on various substrates and antibacterial efficacy (percentage change in CFU method) against *E. coli* (93%) and *S. aureus* (100%) at 2 min irradiation was found [167].

Spray coating process parameters of importance for the coating quality are spray nozzle diameter, spray time, substrate distance, coating fluid velocity, and air pressure, as summarized in Table 5. Nozzle diameter and distance from the substrate must be optimum for obtaining the desired thickness and uniformity. Using the spray coating process, getting a thin film of less than 50 nm is very difficult. Moreover, compressed air is always required to achieve a precision coating. In the spray coating process, a high amount of coating solution (with volatile organic compounds) is wasted,



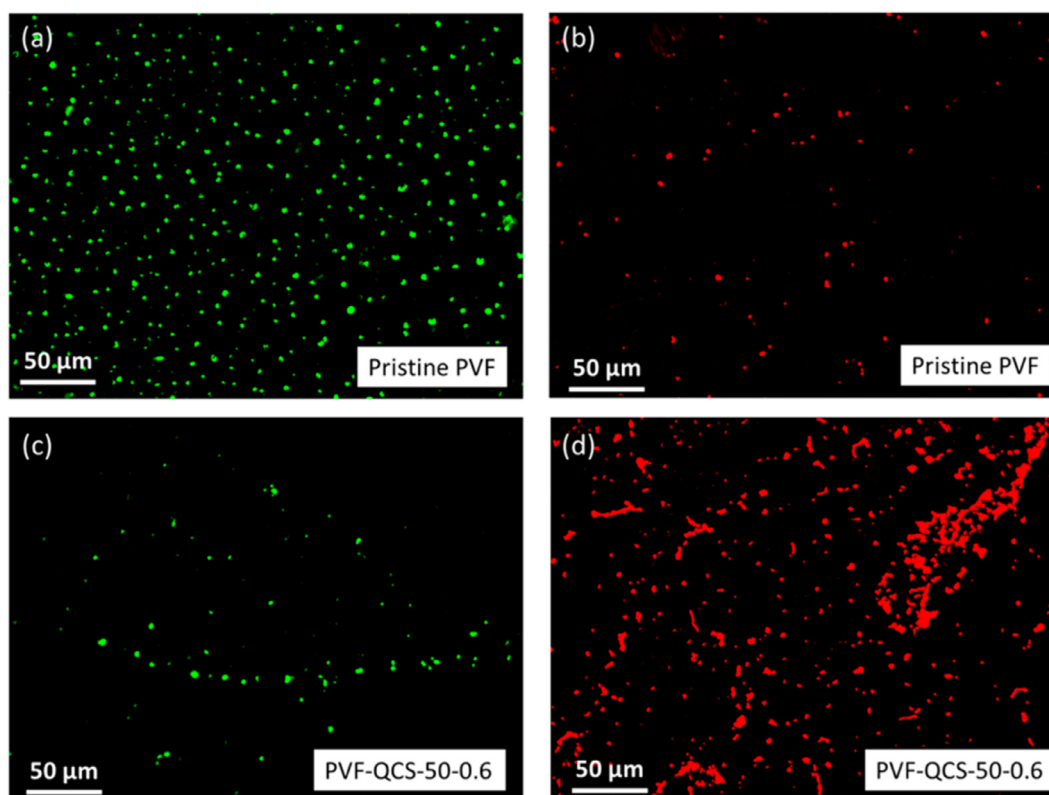


**Fig. 8.** Fluorescence microscopy images showing live (green colour) and dead (red colour) Gram-positive bacteria strained using dye solution (a,b) on pristine PVF and (c,d) on PVF-QCS-50-0.6 film [164]. Reprinted with permission from Ref. [164]. Copyright 2016 American Chemical Society.

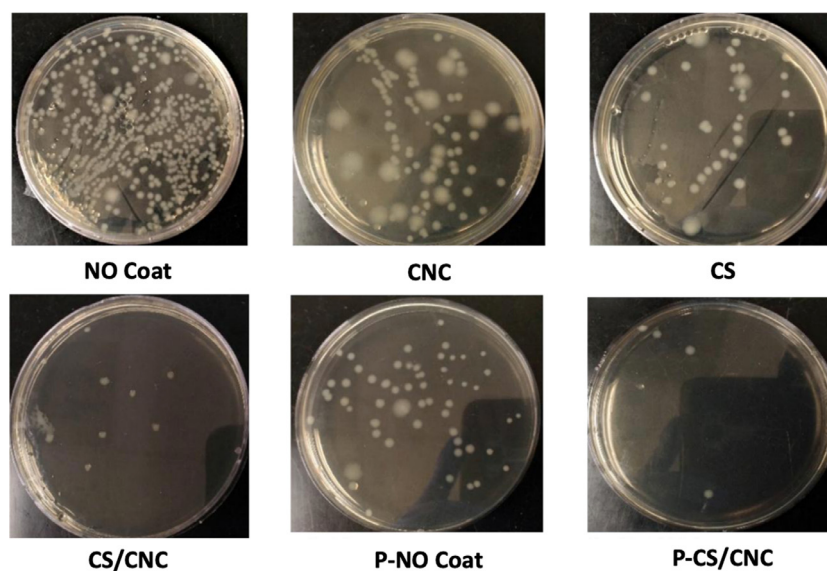


**Fig. 9.** Gram-negative bacteria (*E. coli*) growing on the agar plate having different combinations of cellulose nanocrystals (CNC) and CS coatings with and without plasma treatment in a Petri dish [165]. Reprinted with permission from Ref [165]. Copyright 2018 American Chemical Society.

which further produces hazardous waste. In addition to this, a significant challenge during the spray coating is the requirement for good ventilation. Depending on the spray-coated material, it can be highly toxic.

#### 4.4. 3D printing

3D printing was initially patented in 1971 and is nowadays intensively studied and industrially utilized for manufacturing metal,

ceramic and polymer parts of precise, complex and highly customized geometries. Bioprinting is one of the 3D printing techniques that aims at the creation of three-dimensional tissues and organs, ultimately from living cells. While printing of inks that contain live cells is an extremely challenging yet rapidly developing branch of 3D printing, some bioprinting methods can be successfully utilized for polysaccharide coating applications. There are multiple methodologies of bioprinting as reviewed by Blaaser et al. [168], see Fig. 10, among which, for example, the layer method,



**Table 5**

Summary of target products, compositions, antibacterial efficiency, and process parameters for sprayed coatings.

Products	Compositions	Antibacterial Efficiencies	Process Parameters
CS and GE coatings for food packing [162]	Two type of coatings were developed. In the first 1% CS solution was prepared and in the second 10% GE solution was prepared. Both the solutions were spray coated on steaks separately followed by vacuum packing.	Colony forming units count, lactic acid bacteria, <i>B. thermosphacta</i> and <i>E. coli</i> after 120 h in incubation at 30 °C The CS coating shows an enhanced antimicrobial and antioxidant effect (up to 21 days) with no change in the meat pH, color, and tenderness compared to GE and uncoated beef samples.	Both solutions were spray coated at a flow rate of 0.18 L min <sup>-1</sup> , from about 45 cm distance for 2 min for a complete coverage of steaks
Chitosan and pectin-based antimicrobial food packaging [163]	Various combinations of chitosan-gelatin and pectin-gelatin with lemongrass essential oil (25%, w/w) or ZnO (3%, w/w) were prepared.	Disk diffusion method, <i>S. aureus</i> , <i>B. subtilis</i> and <i>E. coli</i> after 24 h in incubation at 28 °C The chitosan-gelatin coating showed highest antibacterial efficacy. Pectin-gelatin coating with Zinc extended the shelf life of raspberries from four to eight days	Coatings were spray coated on cardboard boxes containing raspberries. Coatings were further dried under ambient conditions for 1 h.
Quaternized chitosan based antibacterial coating [164]	The micrometer thick coating of tripolyphosphate (0.6 wt.%) and quaternized chitosan (5 wt.%) solutions were sprayed onto plasma-treated polyvinyl fluoride.	Colony forming units count, <i>S. aureus</i> and <i>P. aeruginosa</i> , after 2 h in incubation at 25 °C Developed coating demonstrates a 90% reduction in bacterial count compared to uncoated surface against both <i>S. aureus</i> and <i>P. aeruginosa</i>	Tripolyphosphate and quaternized chitosan solutions were coated with a nozzle moving speed of 50 mm/sec and air pressure of 0.25 bar and 1 bar, respectively. In addition, while spraying a distance of 45 mm was maintained between nozzle and the substrate. Coatings were sprayed using RF plasma spray system
Plasma spray coating for Ti implants [166]	Hydroxyapatite powder doped 0.5 wt.% silica and 2 wt.% silver was sprayed on Ti. Acemannan (1 mg) extracted from aloe vera and (0.5 wt.%) chitosan was further casted on top of the coating.	Disk diffusion method, <i>S. epidermidis</i> after 48 h in incubation at 37 °C Combination of acemannan and chitosan demonstrated a large inhibition zone by the inoculation of <i>S. epidermidis</i> for 18 h.	
Antibacterial tissue paper [165]	Chitosan (CS) is mixed with cellulose nano crystals (CNC) 80:20 by weight and spray-coated to create the lightweight composite coating (CS/CNC) on tissue paper. The developed CS/CNC coating is further treated with plasma (P-CS/CNC).	Disk diffusion method, <i>E. coli</i> after 48 h in incubation The developed coating showed high-water absorption capacity along with a reduction in the growth <i>E. coli</i> by 99%	Not reported
Cellulose based antibacterial coating [167]	Protoporphyrin IX and quaternary ammonium salt was immobilized on cellulose chain using ionic liquid. Furthermore, CPS with glutaraldehyde was sprayed on glass, metal and fabric.	Colony forming unit count; <i>E. coli</i> and <i>S. aureus</i> after 12–16 h in incubation at 37 °C CPS coated substrates showed 93% and 100% efficiencies against <i>E. coli</i> and <i>S. aureus</i> under 2 min of sunlight	Not reported

that controls the deposition of the complete layer at once, can be used for coating applications.

Since polysaccharides are widely used in bioprinting due to their exquisite biocompatibility, a large number of publications have reviewed polysaccharide-based bioinks, but mostly for tissue reconstruction applications. Even though surface coating is not the primary application of 3D printing, coatings produced by this method have advantages of controllable porosity and surface structure, which affects cell proliferation and active surface for release of antibacterial agent. Within this review we are focused only on applications that produce coatings or can potentially be used as coatings. This includes wound dressings, scaffolds with pronounced antibacterial properties, and food packaging applications.

#### 4.4.1. 3D-printed antibacterial polysaccharide coatings for medical scaffolds

A chitosan-gelatin hydrogel coating [170] was used to improve an interface fixation for titanium alloy prosthesis, see Fig. 11. Its antibacterial properties are meant to reduce the risk of periprosthetic infection that is very difficult to treat (surgical interference or antibiotic treatments). The precision of 3D (extrusion) printing procedure allowed creating a porous CS-gelatin hydrogel coating on the surface of titanium alloy specimens. Prior to coating the surface was ground, polished, treated with laser and washed in silane and then dried. The natural antibacterial properties of CS were enhanced by immersion (dip-coating) in a 50 µg·mL<sup>-1</sup> nano-silver solution. Increase of CS content resulted in increased tensile strength and compression modulus, improved creep performance of printed structures and their bonding with the substrate (silane

coupling with hydroxyl groups of CS [171]). Antibacterial tests were done by zone inhibition method and OD measurements, in which results supported each other. Although it was claimed that antibacterial effects are intrinsic to the CS, inhibition zones for *E. coli* and *S. aureus* were well distinguished only for the nano-silver treated samples. These also resulted in 70% and 67% inhibitory efficiency (calculated via OD measurement) against *E. coli* and *S. aureus* respectively. Due to large surface, the 3D printed coatings have potential for being loaded with nano-silver particles. It is also essential for the mentioned application to study how antibacterial properties change with time, which was not addressed in this work.

#### 4.4.2. 3D-printed antibacterial polysaccharide coatings for wound dressing

Water soluble N,O-carboxymethyl CS in combination with starch was introduced as a biodegradable drug Mupirocin releasing wound dressing [172], that does not require organic solvents. The addition of starch also reduced the drug release magnitude, which was assessed by disk diffusion test. Drug release tests correspond to the corrected antibacterial inhibition zone tests, where the material with 75% of CS reached 36.28±0.69 mm inhibition zone diameter after 72 h for *S. aureus*. The best results after 72 h were obtained by 100% CS samples (38.61±0.48 mm), while higher amount of added starch decreased printability and antibacterial properties.

Another bioink for biomedical application was reported by Hidaka et al. [173]. Visible light (425 nm) curable ink based on CS derivative with phenolic hydroxy moieties is applicable for extrusion based bioprinting as well as for Vat polymerization-based bioprinting. The mechanism of visible light polymerization is based

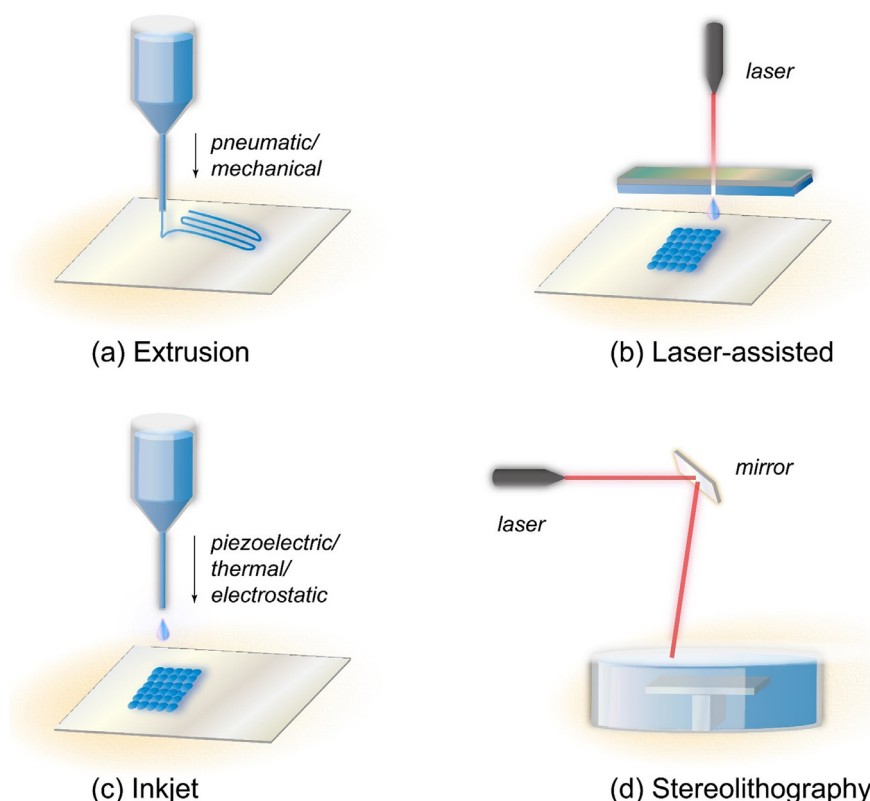


**Fig. 10.** Schematics of 3D printing methods for bioprinting applications. (a) Extrusion-based printing methods deposit the ink line-by-line. (b) Inkjet method from drop-on demand group of methods prints in droplets that can be produced using different physical principles. (c) In laser-assisted 3D printing a laser beam generates the droplet by heating the substrate with ink on it. (d) Stereolithographic methods use photosensitive inks and solidify them using precisely directed light source. A comparison of different 3D printing methods for polysaccharides can be found in McCarthy et al. [169].

on cross-linking in presence of sodium persulfate and Tris(2,2'-bipyridyl) dichlororuthenium (II) ( $\text{Ru}(\text{bpy})_3$ ). The antibacterial properties of the ink were assessed using the inhibition zone method. Unfortunately, the results were not quantified but only compared to control samples made of similarly modified ALG hydrogels, where the CS-based inks showed inhibition zones that are more pronounced against *S. aureus* compared to *E. coli*.

An unusual antibacterial component for wound dressing was introduced by Shen et al. [174]. Bacteriophages are a kind of viruses with the potential to infect and kill bacteria without affecting human cells. ALG hydrogels with *E. coli* bacteriophages were for the first time prepared as an ink for 3D-printing, that is capable of slow phage release for control of bacterial population in the wounds. This is not a trivial task, since (i) the bacteriophage nanoparticles have to be oriented into the ALG in such a way that their tails are free to be able to interact with bacteria, (ii) the required concentration of phages that is needed for the desired effect, and (iii) they have to stay lytic after 3D printing process. Additionally, calcium carbonate used for ALG cross-linking causes agglomeration of bacteriophage nanoparticles. Encapsulation lessened the lytic effect of bacteriophages and reduced the antibacterial efficiency from 99.8% to 68.5%. Antibacterial effect remained between 40 and 50% during a 24-hour period. Bacteriophage resistance to temperature and different pH values was tested and it was found that they will be effective for all possible wound healing applications. Successful encapsulation and antibacterial efficiency are encouraging for future development, however certain adjustments have to be made, as bacteria are affected only by a particular type of bacteriophage, they can develop resistivity to it and bacteriophages will never completely eliminate bacteria completely in order to sustain their own population.

Among polysaccharides, alginate (ALG) is extensively utilized for the scaffold and wound dressing production, but inadequate mechanical properties of the printed structures require reinforcement of the pure ALG inks. For this, cellulose, another polysaccharide material, is widely used as reinforcement and rheology modifier for 3D printing inks. Different forms and sources of cellulose are utilized for it, e.g. cellulose nanocrystals (CNC), cellulose nanofibers (CNF), bacterial cellulose [175] carboxymethyl cellulose, or methylcellulose [176]. Using the latter, antibacterial properties were achieved by addition of bioactive components, such as manuka honey, aloe vera gel as well as eucalyptus essential oil and were further assessed by inhibition zone method and medium pouring method (CFU). Based on inhibition zone sizes, all samples inhibited bacterial growth in a similar manner, while antibiofilm performance was more pronounced against *S. aureus* for the sample containing manuka honey. The medium pouring method showed that sample with etheric oil has the highest efficiency (>80%) and manuka honey samples were found to be more efficient than aloe vera samples. Bacterial cellulose in combination with ALG has also been reported to prevent shrinkage after cross-linking and metal ions from leaking into surroundings reducing toxicity issues of the printed structures [175]. The combination of CNC and CNF [177] allowed such modification of antibacterial N-Isopropyl acrylamide (NIPAM) based hydrogels, whereby self-sustained structures printed by direct ink writing could reach 45° inclination. While CNCs in high concentrations (up to 35 wt%) assure reinforcement of the hydrogel, CNFs added in small concentrations (1 wt%) improved shape retention and adjusted rheological properties. CNF orientation under shear and extensional forces in the nozzle during printing results in anisotropic behavior affecting swelling. Thus, such printed complex structures

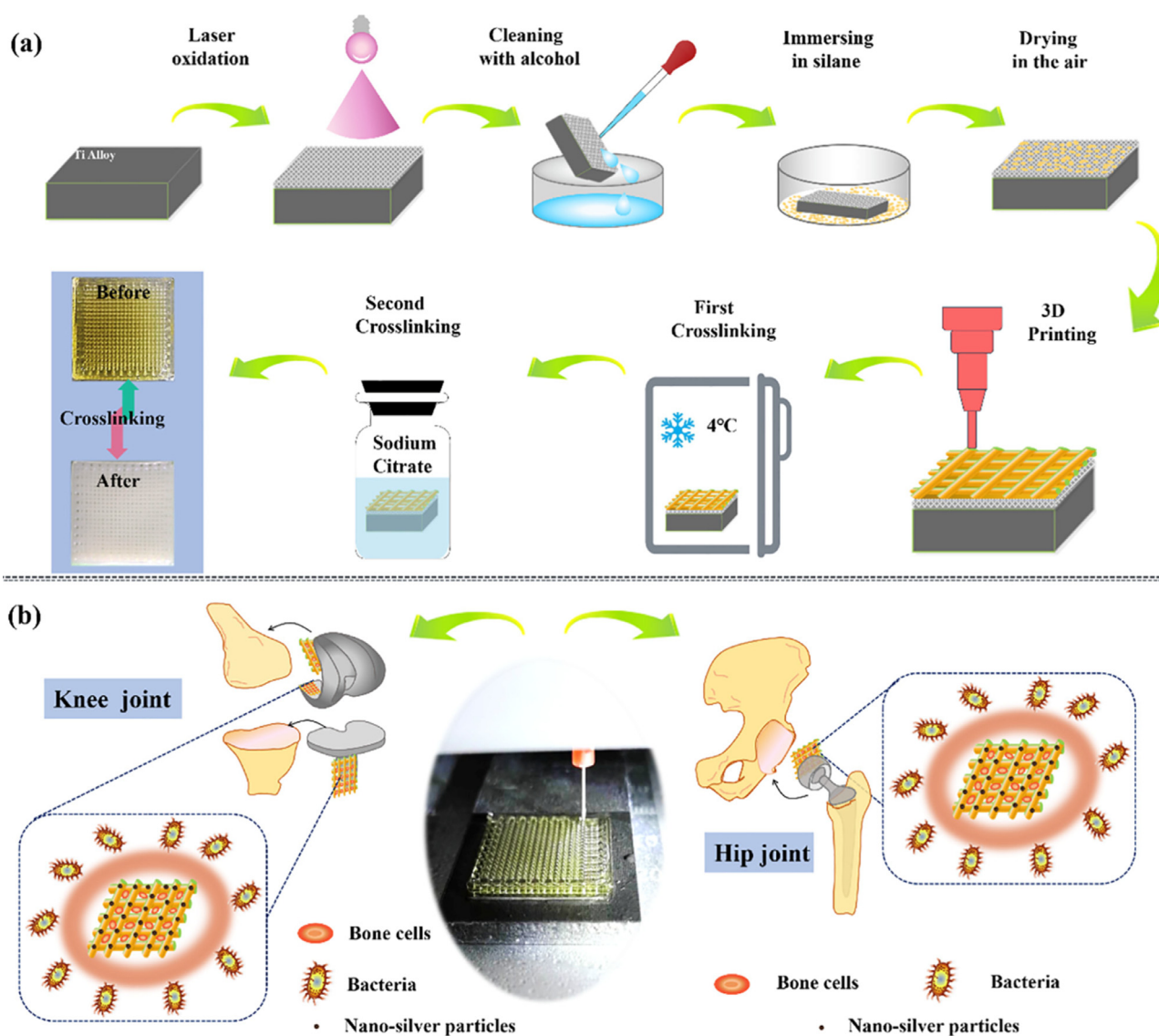


**Fig. 11.** Schematic diagram of preparation process and antimicrobial application of 3D printed CS-gelatin antimicrobial hydrogel coatings. (a) Preparation process of CS-gelatin hydrogel coating including surface preparation, 3D printing and post-processing (crosslinking). (b) 3D printed CS-gelatin-nAg antimicrobial hydrogel coating as a biological fixation interface for hip and knee prosthesis. Reprinted from Ref. [170], Copyright (2021), with permission from Elsevier.

possess programmable self-actuation properties. Their antibacterial properties were achieved by functionalization of hydrogels with modified AMP  $\epsilon$ -polylysine. Carrageenan is also extensively used in 3D bioprinting, however, mostly for tissue engineering [178].

All of the mentioned above research works utilize various strategies of boosting antibacterial properties of the used polysaccharide (if it has any) for wound dressing: modification as drug encapsulation [172] and even living bacteriophages embedding [174]. Other strategies include the addition of nanoparticles (usually silver or Zn derivatives), antimicrobial peptides, carbon-based nanomaterials, metal-organic frameworks etc. [179,180].

#### 4.4.3. 3D-printed antibacterial polysaccharide coatings for food preservation and packaging

Currently, the food packaging industry is in need of biocompatible coatings from renewable materials, and polysaccharides play important role there [181]. Edible inks [182], package films and intelligent labels that can indicate meat freshness [183] can be produced by 3D printing or other printing methods. CS-based ink modified by mulberry anthocyanin was utilized for detection of alkaline gases, lemongrass essential oil to enhance the antibacterial

effect and cassava starch for encapsulation [183]. The 3D printed labels demonstrated an extension of pork shelf life by more than 15 days at 4 °C and more than 7 days at room conditions, see Fig. 12. Mulberry anthocyanin not only provided color change indicating rotting of the pork meat but also improved thermal and antioxidant activity. Etheric oil addition improved further antioxidant and bacteriostatic properties. They were assessed using a CFU method after 24 h of incubation of *E. coli* and *S. aureus*, while more appropriate might have been strains of *Salmonella* or *L. monocytogenes* often found on rotten meat.

Other printing methods were utilized for application of edible inks, such as flexographic [184], screen printing [182,184] or even thermal inkjet [185]. Water soluble carboxymethyl CS produced using freeze thawing in alkali solution was mixed with monascus, which is a non-toxic natural colorant with antibacterial properties [184]. The “one-pot” method of CS preparation, possibility to print on curved surfaces and utilization of natural colorant with antibacterial properties, makes the proposed ink environmentally friendly. The inks not only demonstrated good printing quality for screen and flexographic printing but also showed up to 8 mm diameter of inhibition zones for *E. coli* and *S. aureus*. Wang et al. [182]



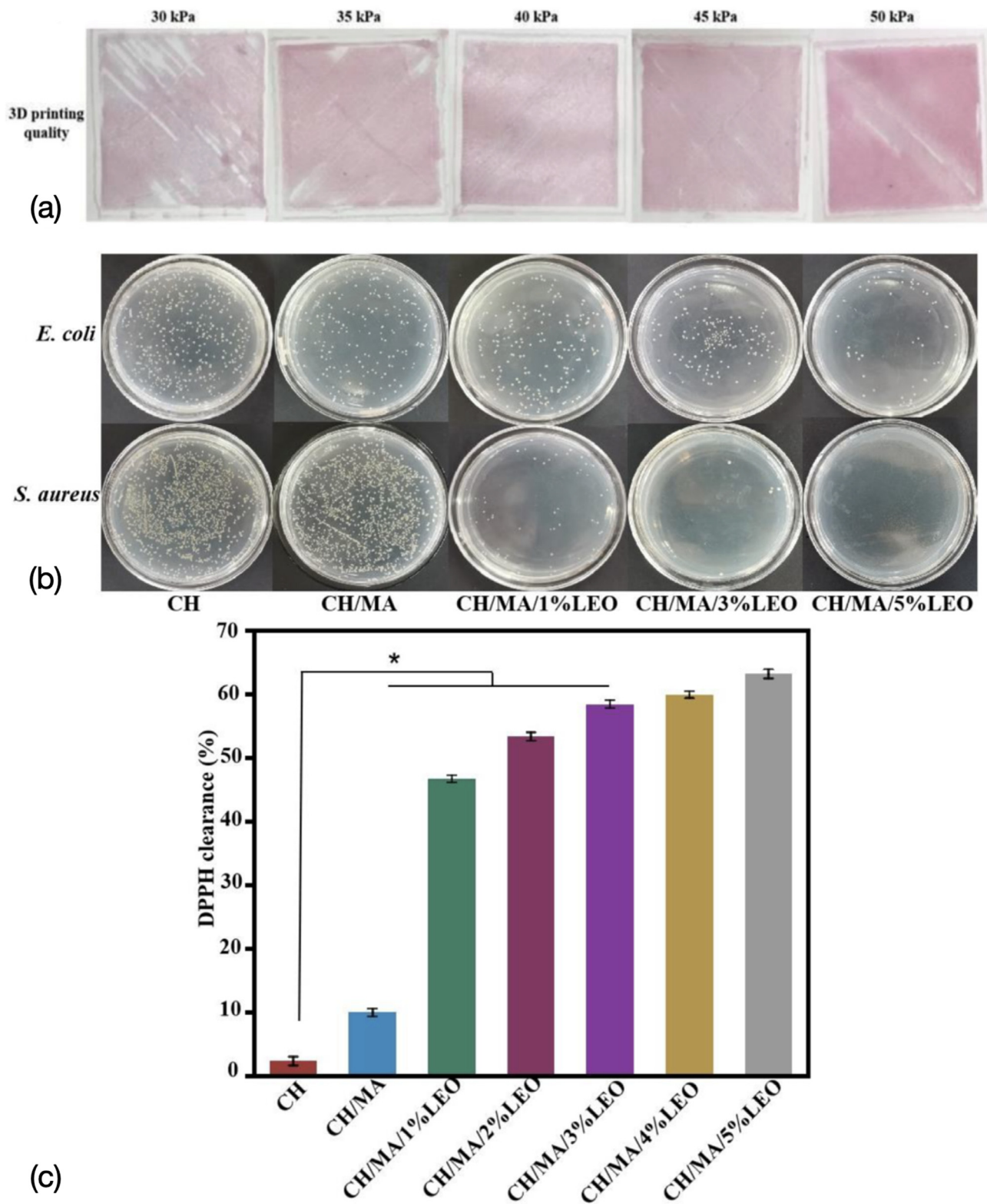


**Fig. 12.** (a) Printing suitability of indicator films under different extrusion pressures; (b) Growth of *E. coli* and *S. aureus* in different indicator film solutions; (c) DPPH (2,2-diphenyl-1-picrylhydrazyl) clearance values show the ratio of removed radicals and thus demonstrate antioxidant activities of the indicator films. \*represent significant differences ( $p < 0.05$ ). Notations: CH – chitosan, MA – mulberry anthocyanin, LEO – lemongrass etheric oil. Reprinted from Ref. [183], Copyright (2022), with permission from Elsevier.



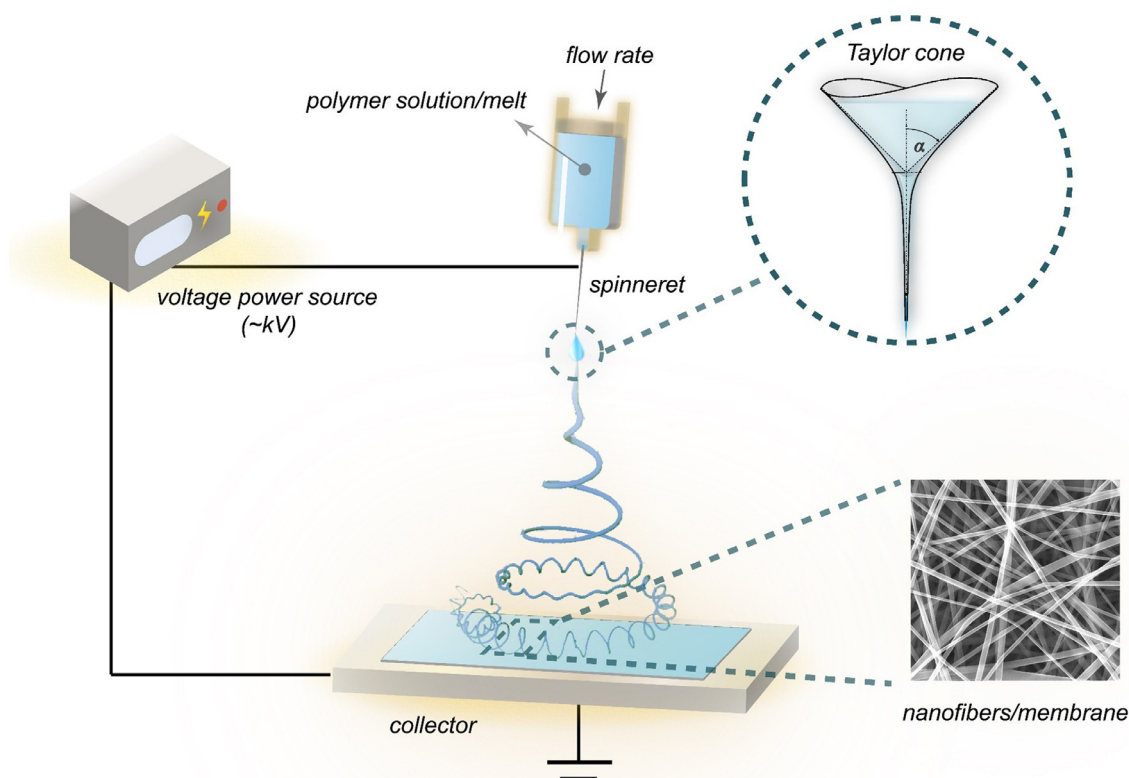


**Fig. 13.** Schematic representation of electrospinning process. Under high voltage between the spinneret and collector, Taylor cone is formed on the surface of polymer solution/melt; at critical charge concentration, the jet of the solution starts travelling to the collector drying on the way. Image of the electrospun fibers is taken from Aulova et al. [198] (used with permission).

utilized a more conventional CS dissolution method with the addition of a pigment ( $\text{FeO}(\text{OH}) \cdot x\text{H}_2\text{O}$ ). Low molecular weight CS compared with high molecular weight CS in the same concentration showed inhibition zones of  $10.2 \pm 0.2$  mm and  $11.9 \pm 0.3$  mm vs.  $12.0 \pm 0.3$  and  $10.9 \pm 0.7$  mm against *S. aureus* and *E. coli*, respectively. Surprisingly, this would indicate that low molecular weight CS is more effective against Gram-negative species. No control samples were however presented.

Originally prepared for the solution casting method of food packaging film preparation, CS with halloysite nanotubes and tea polyphenol was also tested for possible 3D printing applications [186]. Halloysite improved the mechanical properties and tea polyphenol played the role of antibacterial agent. Antibacterial efficiency estimated using CFU method reached 87% against *S. aureus* and 85% against *E. coli* for and for materials with 10 and 20% (w/w of halloysite dry weight) of tea polyphenols.

Another widely available and widely used polysaccharide used for 3D printing for food preservation is pectin, which lately was again in focus for its inherent antibacterial properties [187]. However, reporting of antibacterial of pectin-based 3D printing inks is rare, since most of the work focuses on cast films, which are beyond the scope of this review.

A summary of the products, compositions, antibacterial efficiency, and process parameters from the papers reviewed in this section can be found in Table 6.

#### 4.5. Electrospinning

Electrospinning (ES) is a versatile technique that allows the formation of nanofiber from a polymer solution, melt or emulsion [190] by electrostatic force. First introduced by William Gilbert in the 16<sup>th</sup> century and extensively developed from the beginning of the 20<sup>th</sup> century this method has been well studied. The forma-

tion of thin fibers occurs under electrostatic force in a strong electrostatic field, see also Fig. 13. It happens in several stages as described by Reneker and Yarin [191]. Charge carriers in the polymer solution are assembled close to the surface under electrostatic force and the surface forms the so-called Taylor cone [192],  $\alpha$  in Fig. 13. Charge carriers continue to concentrate on the top of the cone, and this finally results in a jet of polymer solution pulled by the electrostatic field towards the receiving electrode [191]. While the jet is traveling towards the receiving electrode, the solvent in the solution dries and, ideally, a fully-dried fiber is deposited [191]. ES is a complex process and depends not only on the environmental effects (temperature, humidity, air flow) but also on the set parameters (voltage, distance between electrodes, material throughput, etc.) and polymer material properties, such as molecular weight [193], topology [194], charge, its concentration in the solvent as well as solvent polarity and volatility. Viscosity, surface tension, and electrical conductivity of the polymer solution are the most important properties for successful ES.

The diversity of polysaccharides in terms of chemical structure and composition, molecular weight and ionic character allows them to be desired nanofiber materials. The additional advantages of ES, such as cost-effectiveness and relatively high productivity, make ES one of the most attractive processes for the production of polysaccharide nanofibrous materials [195]. The product of ES, nanofibrous membrane has an open-pore interconnected structure [196] with a controllable pore size distribution which can provide selectivity for protection against harmful particles or bacteria and helps with better wound respiration and oxygenation [197]. Also important for other antibacterial applications, such as coatings for food preservation or orthopedic implants, the large surface of nanofiber membrane obtained due to high surface-to-volume ratio can be functionalized or coated and thus can provide prolonged release of antimicrobial agents. Additionally, ES technique allows

**Table 6**

Summary of products, compositions, antibacterial efficiency, and process parameters for 3D printing.

Products	Compositions	Antibacterial Efficiencies	Process Parameters
CS-gelatin coating on titanium alloy surface [170]	4 different compositions in deionized water with 10% (w/v) of gelatin, 3.5% (w/v) AA and 3, 5, 7, 9% (w/v) CS were used. Water and AA were poured into dry mixture of CS and gelatin and mixed for 2 h, heated up to 50 °C and mixed on magnetic plate for 12 h at 200 rpm	Disk diffusion method and OD; antibacterial efficiency of silver treated samples reached 70.39% and 97.09% against <i>E. coli</i> and <i>S. aureus</i> respectively	Pressure 0.12–0.30 MPa; printing speed 3.5 mm/s; barrel temperature 25–50 °C; platform temperature 4 °C; nozzle diameter 0.31 mm Material with 9% of CS was not printable
N,O-Carboxymethyl CS-starch ink for 3D printed wound dressing releasing mupirocin [172]	Mupirocin was added to starch-CS stock mixture with 10 mg/ml concentration. Five different ratios between starch and CS stocks were used: 100, 75, 50, 25 and 0% of CS	Disk diffusion method, <i>S. aureus</i> ; Composite material with 75% of CS reached 36.28±0.69 mm inhibition zone diameter after 72 h; inhibition zone increased in time for samples with higher starch content	Pressure 5–30 kPa; printing speed 1–3 mm/s; infill percentage 30%; cartridge 3 ml; 410 µm conical nozzle
Visible-light curable CS ink for extrusion based and VAT polymerization bio-printing [173]	Synthesized derivative of CS 1% (w/v) in solution with 1–10 mM sodium persulphate and 0.5–2 mM Ru(bpy) <sub>3</sub> was mixed to prepare the ink	Disk diffusion method; Results were not quantified; CS shows inhibition zones, that are more pronounced for <i>S. aureus</i> than for <i>E. coli</i>	Printer equipped with visible light source; printing speed 6 mm/s; room temperature light intensity 3.18 W/m <sup>2</sup> with 452 nm wavelength; 21G needle
Bacteriophage releasing 3D-plotted hydrogel for wound healing [174]	Bacteriophages extracted from local river water; $1.5 \times 10^7$ PFU/mL phage solution was mixed with 5% ALG solution (Mw=450–550 kDa) and 0.01 M phosphate buffered saline in ratio (1:8:1) to reach phage density of $1.5 \times 10^6$ PFU/mL; calcium carbonate was used for cross-linking of 3d printed structures	CFU, <i>E. coli</i> ; Bacteriophages reduced the bacterial efficiency of <i>E. coli</i> from 99.8% to 68.5%. Antibacterial effect remained between 40 and 50% during 24 h	3D plotting system; printing speed 35 mm/s; nozzle 200 µm; vertical step 0.4 mm; spacing between fibers 1mm
Alginate/Bacterial composite hydrogels with copper nanostructures [175]	4 wt% ALG solution, Cu particles synthesized using NaBH <sub>4</sub> ; bacterial CE/ALG 70/30% with 5mM of Cu crosslinked by two methods: CaCl <sub>2</sub> at 0.1M and Cu(NO <sub>3</sub> ) <sub>2</sub> ·3H <sub>2</sub> O	Disk diffusion method, <i>S. aureus</i> , <i>E. coli</i> Samples deposited on inoculated agar, inhibition zone areas were measured. An inhibition zone without halo was observed	Pressure 1 bar; printing speed 50 mm/s; barrel temperature 25 °C; 23G needle; during extrusion hydrogel was ionically cross-linked
Printable alginate-methylcellulose inks for wound dressing [176]	Sodium ALG dispersed in glycerol; methylcellulose dispersed in water at 80 °C; water-glycerol (70:30 w/w); eucalyptus essential oil dissolved in Triton X-100 (1:1 v/v), manuka honey dissolved in warm water; aloe vera added after cooling down. Different ratios of ALG to cellulose solutions were used with different amount of bioactive ingredients	Disk diffusion, CFU, <i>S. aureus</i> and <i>E. coli</i> ; All samples demonstrated inhibition zone after 24 h; samples with manuka honey showed the best antibiofilm resistance for <i>S. aureus</i> ; according to CFU sample with etheric oil has the best efficiency (>80%) compared to manuka honey (approx. 50%) and aloe vera (35–50%)	Inkredible, Cellink; printing speed 10 mm/s; cartridge 3 ml and 21G needle Samples were crosslinked in 200 mM CaCl <sub>2</sub> for 10 min
Shape-morphing and antibacterial nanocellulose (CNC) hydrogels [177]	1 and 2.5 wt% of functionalized ε-polylysine; CNC samples tested; CNC (20 wt%) and CNF (1 wt%) dispersions mixed in water, mixed using speed mixer with increasing speed, two times processed on three-roll mill, modified by adding NIPAM, photoinitiator, glucose oxidase and glucose	<i>S. aureus</i> , <i>S. arlettae</i> , <i>E. coli</i> , <i>P. fluorescens</i> ; Hydrogels were inoculated with 40 µl of bacterial suspension (OD <sub>600</sub> =0.1) in diluted 1:5 phosphate-buffered saline; incubation for 8 h at 37 °C; inoculated surface placed on agar plate; after 20–28 h assessment done visually	Direct ink writing; pressure 1.5 bar; printing speed 10 mm/s; printing temperature 10 °C; needle with 0.41 mm diameter; were cross-linked using ultraviolet light under nitrogen for 10 min, postcured for 5 min and washed in water for 5 days
CS-pigment (FeO(OH)·xH <sub>2</sub> O) composite edible ink [182]	Composite additive: Tween 80, Polyglycerol Fatty Acid Esther, soybean oil and edible bee wax mixed in mass ratio (5:3.5:1:5). Two CS with molecular weights 80 and 750 kDa with deacetylation degree of 85% were dissolved in AA solution at 2% (w/v) concentration.	Disk diffusion method; Antibacterial efficiency of high molecular weight CS is higher; for the maximal CS concentration inhibition zone diameter was 12.7±0.6 mm and 11.5±0.5 mm for <i>S. aureus</i> and <i>E. coli</i>	Screen printing; pressure 12 kg; temperature 25±0.1 °C; 50% RH; print speed 30 mm/s; squeegee angle 60°; stencil thickness 0.15 mm; coated paper 128 g/m <sup>2</sup>
CS/halloysite nanotubes/tea polyphenol nanocomposite film for food packaging [186]	5% (w/w) of CS dissolved in 2% AA aqueous solution while stirring at room temperature; 2% (w/w) HNT dispersed in distilled water for 1 h at 600 rpm; solutions mixed in different ratios (9:1, 8:2, 7:3, 6:4, 5:5 v/v) and stirred for 1 h. Tea polyphenol added at concentrations 0, 10 and 20% (w/w) of HNT dry weight, stirred for 1 h and sonicated for 1 h.	CFU, reduction of 87 and 85% for <i>S. aureus</i> and <i>E. coli</i> for materials with 10 and 20% of tea polyphenols	Pressure 4 kPa; speed 3.5 mm/s; temperature 25 °C; filling density 30%; printing nozzle 0.7 mm; layer height 0.5 mm
Anthocyanin/CS/lemongrass essential oil films by 3D printing for intelligent evaluation of pork freshness [183]	CS dissolved in glacial AA with 1.5% (v/v) concentration and stirred at 35 °C for 5 h; 15% (w/w) glycerin was added and stirred for 1 h. Essential oil was dissolved in 2% Tween-80 solution and added in 1, 2, 3, 4, 5% concentration to CS mixture, followed by 0.1 g of mulberry anthocyanin	CFU; Addition of anthocyanin reduced number of viable <i>E. coli</i> from 5.02±0.12 to 4.86±0.38 log CFU/ml and for <i>S. aureus</i> from 5.03±0.51 to 4.97±0.25 log CFU/ml; 5% of etheric oil reduced numbers to 3.64±0.19 and 1.78±0.26 log CFU/ml for <i>E. coli</i> and <i>S. aureus</i>	Pressure 40 kPa; temperature 25 °C; filling density 100%; nozzle 0.6 mm; height 0.3 mm

(continued on next page)

Table 6 (continued)

Products	Compositions	Antibacterial Efficiencies	Process Parameters
Carboxymethyl CS edible ink [184]	Inks with 6 wt% monascus pigment with different reaction times and concentration of sodium Chloroacetate were prepared. Flexographic inks contained 1, 1.5 and 2 wt% of synthesized carboxymethyl CS in water, screen printing inks - 2, 2.5 and 3 wt%	Disk diffusion method, <i>S. aureus</i> and <i>E. coli</i> ; Antibacterial effects of monascus and 1.5 wt% ink are weak; best antibacterial activity of approx. 8 mm diameter of inhibition zone was demonstrated by 2.5 wt% ink due to synergistic effect of CS and monascus CFU, <i>S. aureus</i> , <i>E. coli</i> ; Hydrogel samples were inoculated by bacterial suspension for 6 h at 37 °C; CFU on diluted survivor suspension inoculated to PCA for 24 h at 37 °C; dead/live assay under fluorescent inverted microscope	No information provided
Wound repair bandage from carboxymethyl CE/ $\epsilon$ -polylysine hydrogel [36]	Carboxymethyl CE sodium and $\epsilon$ -polylysine went through a ring-opening reaction under weakly acidic conditions with glycidyl methacrylate. Mixed in dif. Ration and dissolved in 0.05 wt% solution of 2-hydroxy-4'-(2-hydroxyethoxy)-2-methyl-propiophe	Disk diffusion method, <i>S. aureus</i> and <i>E. coli</i> ; 100 $\mu$ l of bacterial stock ( $10^6$ CFU/ml) on agar plate; filter paper submerged in pectin solution (control) and printed samples; obtained inhibition zones of around 1.5 mm attributed to copper ions	Pressure 0.06 MPa; printing speed 360 mm/min; nozzle diameter 2 mm; cross-linked under ultraviolet light source at 365 nm wavelength
Electroglated pectin hydrogels [188]	Citrus peel pectin suspension of 0.75% (w/w) concentration	Disk diffusion method, <i>S. aureus</i> and <i>E. coli</i> ; 100 $\mu$ l of bacterial stock ( $10^6$ CFU/ml) on agar plate; filter paper submerged in pectin solution (control) and printed samples; obtained inhibition zones of around 1.5 mm attributed to copper ions	Electrophoretic deposition was used as a method of 3d printing; pectin suspension was subjected to 3V under 15 min and material went through electrogelation at the anode copper plate
Gelatine methacrylate/xanthan gum wound dressing with TiO <sub>2</sub> nanoparticle and N-halamine [189]	15 wt% gelatine methacrylate solution mixed with 0, 1, 2 and 3 wt% of xanthan gum, 1 or 2 wt% of photoinitiator and N-halamine followed by titanium precursor to generate TiO <sub>2</sub> nanoparticles	CFU, disk diffusion method, bacterial biofilm method; gelatine and gum material does not have antibacterial properties; addition of TiO <sub>2</sub> NP $\phi_{75}$ N-halamine provided 100% and 96.3% sterilization rates for <i>E. coli</i> and <i>S. aureus</i> ; no inhibition zones visible due to low solubility of antibacterial components; no biofilm was detected on the samples with NP and N-halamine	Direct ink writing; pressure 0.3-0.5 MPa; printing speed 30 mm/s; needle 300 $\mu$ m diameter; crosslinked by 365 nm UV light at 10 cm for 15 min; freeze dried for 2 days; 2 wt% of xanthan gum resulted in the best print quality

combination of different materials (coaxial ES, blends, incorporated particles, etc.) that could synergistically improve antibacterial performance of the nanofiber membrane.

#### 4.5.1. Electrospun antibacterial polysaccharide coatings for medical applications

ES NF coatings from polysaccharides are often used on metal orthopedic or dental implants to decrease the possibility of biofilm formation, inflammation and costly surgical interventions. Addition of various antibacterial compounds to polysaccharides is usually required to improve their inherent bactericidal efficiency. These antibacterial properties are extremely important for medical implants and devices, where biocompatible nature of polysaccharides is an additional asset [199]. The structure of CS and ALG is similar to glycosaminoglycan which is a building block of bone and cartilage. Consequently, these materials provide bone scaffolds in combination with silica or bioactive glass [200,201]. Mechanical properties of silica nanofibers and drug release profile were improved by incorporation of CS/PEO into the system [202]. Antibiotics of the fourth generation cefepime was added into the system in order to provide efficient antibacterial properties for both Gram-positive and Gram-negative bacteria. Inhibition zones measurements demonstrated impressive results on antibiotic-loaded NF membranes (40 mm for *E. coli* and 25 mm for *S. aureus*), however, membranes without cefepime showed reduced inhibition zones (5 mm for *E. coli* and 12 mm for *S. aureus*). Very low antibacterial activity was detected against *S. epidermidis* for drug-loaded fibers. Drug release from NF membrane was continuous for 16 days, since the drug interacted with CS providing moderate release within longer time period, which is highly desirable for orthopedic applications. However, the study did not elaborate the behavior of the NF mat on the implant surface, as was done for example by Kharat et al. [203]. Here CS/PEO with natural thyme and/or henna extracts was electrospun directly on the orthopedic screw and was not subjected to cross-linking. The largest inhibition zones of  $3.9 \pm 0.3$  cm and  $5.3 \pm 0.2$  cm against *S. aureus* and *E.*

*coli* respectively were demonstrated by nanofibrous mat with thymus extract, while the implant covered by nanofibers with both plant extracts showed  $3.0 \pm 0.2$  cm and  $4.9 \pm 0.3$  cm against *S. aureus* and *E. coli*. Mechanical tests showed appropriate properties for both medical wound patches and metal implant coatings. All samples also have hemolytic index significantly lower than 5%, meaning that blood cells are not damaged by the material, and, thus NF mats are safe to be used as an implant coating. Interestingly, cell proliferation studies showed that plant extracts improve cell growth and spread on nanofibrous material, due to the presence of bioactive constituents, such as flavonoids [204,205].

ALG is a promising polysaccharide for artificial scaffolds due to its biocompatibility and biodegradability but does not possess intrinsic antibacterial properties and in some situations does not have the required optimal mechanical properties. Their improvement together with antibacterial effect can make it applicable not only for scaffolds but also for biocompatible coatings. For example, Pebdeni et al. [206] proposed to reinforce electrospun ALG/PVA NF material with Halloysite nanotubes (HNT) loaded with an antiseptic drug, cephalexin. The authors demonstrated how HNT are oriented inside of the ALG/PVA nanofibers, and that their hollow part is loaded with the drug. Antibacterial activity against the Gram-positive *S. aureus* and *S. epidermidis* was the most pronounced, as determined using disk diffusion method. As expected, samples with the highest antiseptic drug content showed the largest inhibition zones against all strains including also Gram-negative *P. aeruginosa* and *E. coli*, however, no significant difference in inhibition zone was obtained for concentrations from 5 to 10% (w/w) of HNT. Inhibition zones ranged from approx. 15 to 28 mm with maximal positive control samples of  $28.4 \pm 1.6$  mm. Due to incorporation of drug loaded HNT inside of nanofibers, drug release was continuous for 7 days.

Besides antiseptic drugs [206] and antibiotics [202], bioactive ingredients capable of increasing antibacterial activity of polysaccharide nanofiber are widely used. Among them is honey [207], which is more efficient against Gram-positive bacteria, propolis

[208] and various plant extracts [203,209]. Based on inhibition zone comparison, which should be done very carefully (see Section 3) flavonoid-enriched ES materials [203] demonstrated the largest inhibition zones. Moreover, there are indications of flavonoid efficiency and even their ability to reverse antibiotic resistance, which might be one of the reasons for efficient antimicrobial activity.

CFU method was used for evaluating antibacterial wound dressings made of cotton coated with CS/PVA nanofibers with the addition of *Agrimonia eupatoria* plant extract [210], which could exert antibacterial activity via different mechanisms such as changing the permeability of the cell membrane, inhibiting the adsorption of pathogenic bacteria to host cells, or disturbing the transmembrane transport of nutrients or energy substances [211]. The addition of 5 wt% plant extract to a solution of CS and PVA resulted in  $99.17 \pm 4.05$  and  $98.13 \pm 0.88\%$  decrease in viability of *S. aureus* and *P. aeruginosa*, respectively. Samples without plant extract also showed antibacterial activity but significantly weaker ( $64.39 \pm 10.07$  and  $61.25 \pm 4.22\%$  against *S. aureus* and *P. aeruginosa*). This was related to the intrinsic antibacterial properties of CS, which are synergistically increased by the plant extract. In contrast to other similar publications, in this work ES was performed without a needle. In such free surface ES setups, several Taylor cones are simultaneously forming on a thin layer of polymer solution. High voltages are required, however, the technique has higher productivity and avoids needle clogging.

Cellulose is another polysaccharide widely used as a basis for antibacterial wound dressings due to its surface functionality, absorbency, mechanical properties, and biocompatibility. Its poor solubility makes ES very difficult and therefore cellulose acetate (CA) is used instead. The simple step of deacetylation after ES allows obtaining cellulose nanofibers. However, the absence of inherent antibacterial properties of cellulose requires the implementation of different modification strategies (see Section 2), among which the use of silver nanoparticles (AgNP) is well-known for its efficiency.

Two different ways of silver nitrate salt reduction and their effect on antibacterial properties of cellulose nanofibrous mats were investigated by Jatoi et al. [212]. The mat originally prepared from CA and subjected to alkaline treatment in order to obtain cellulose, was coated with silver nitrate solution by dip coating. It was shown that thermal treatment resulted in smaller AgNP compared to the NP obtained by reduction using dimethylformamide (DMF). Authors proposed that smaller size and, consequently, large surface area are the reasons for higher antibacterial efficiency against *S. aureus* and *E. coli*. This was assessed using the disc diffusion method and quantified through bactericidal assay together with OD measurement, which showed 100% bactericidal properties and effectiveness in growth inhibition of tested bacteria. Often CA nanofibers are brittle and require the addition of binding polymer for a smoother ES process. Polyurethane was thus added to CA in order to assist ES process and increase the mechanical properties of the NF membranes [69]. This resulted in core-sheath fiber formation due to significantly lower molecular mass of CA compared to polyurethane and surface aggregation of CA during ES. The ES formulation was subjected to deacetylation and binding of antimicrobial (AMP) through carbohydrate-binding peptides. Antibacterial activity was characterized by MIC tests and regrowth assay using OD measurements by spectrophotometry. Materials showed lg 4 reduction against *S. aureus* for the membrane with maximal concentration of peptides and maximum lg 1 reduction for *P. aeruginosa*, which means that coatings could be more appropriate for chronic wounds treatment than to burn wounds.

Contact-killing modification of silk fibroin/CA blend was done in order to use photoactive effect against *E. coli* [213]. High bactericidal activity (99.9999% contact killing) was achieved by grafting anthraquinone-2-carboxylic acid in DMF. The esterification reaction was catalyzed in presence of N,N'-Carbonyldiimidazole. The

membrane charged with UVA radiation produces reactive oxygen species that successfully kill *E. coli* within 2 h (lg6 CFU reduction according to CFU method) and can be recharged for cycling utilization.

#### 4.5.2. Electrospun antibacterial polysaccharide coatings for food preservation and packaging

Another vast application of polysaccharide ES coatings is for food preservation and packaging [214–216]. Their biocompatibility, biodegradability, antioxidative properties and, in the case of CS inherent antibacterial properties, make these materials favorable candidates for blends with other biodegradable electrospun plastics. For example, N<sub>2</sub> plasma treated PLA films were coated by CS mixed with EDS (carbodiimide coupling agent) electrospun nanofiber without further crosslinking [199]. Something less common for the antibacterial coatings reviewed, a comparison with dip-coating into the same solution was also made. ES coating, as expected resulted in higher surface roughness but also high antioxidant activity. Unfortunately, the ES coating was not tested for antibacterial properties, but coating materials obtained by immersion after “cold” nitrogen plasma treatment showed very high percent reduction (93–100%) against both Gram-positive (*Listeria monocytogenes*) and Gram-negative (*E. coli* and *Salmonella typhimurium*) bacteria independent of CS molecular weight and deacetylation degree. Surendhiran et al. [217] used sodium ALG electrospun together with PEO using as antibacterial agent a 10% (v/v) of naturally antimicrobial marine polyphenol phlorotannin. Antibacterial testing procedure included dipping chicken meat into the broth containing *Salmonella enteritidis* for 30 min and after drying wrapping it into the ES nanofiber mat. CFU method supported by fluorescence microscopy with staining revealed a 99.9999% reduction of the population achieved within 12 h (for minimal bactericidal phlorotannin concentration).

While information on CS and ALG ES is in abundance and well covered by review papers, studies on other polysaccharides, such as carrageenan ES is quite scarce. Carrageenan is a sulfated galactan isolated primarily from marine red algae and is composed of 1,3-linked  $\beta$ -D-galactose and 1,4-linked  $\alpha$ -D-galactose. Due to the different numbers and positions of the ester sulfate groups on the repeating galactose units, carrageenan can be divided into  $\kappa$ -type (Kappa),  $\iota$ -type (iota),  $\lambda$ -type (lambda). Meanwhile, the gel strength and solubility of carrageenan are also affected by the levels of ester sulfate groups, for example,  $\kappa$ -C can form strong and rigid gel crosslinked with potassium ions while  $\iota$ -C gel is softer with the presence of calcium ion and  $\lambda$ -C does not have gelation behavior. Due to its inherent physical properties and antioxidant activity, carrageenan plays an important role as functional additive or thickening agents in the industry.

Amjadi and co-authors [218] utilized  $\kappa$ -carrageenan ( $\kappa$ -C) as reinforcement for zein ES nanofibers for food packaging systems. It was shown that both zein and  $\kappa$ -C do not possess antibacterial properties, therefore ZnO NP and rosemary oil were added as antimicrobial agents. Inhibitory zone obtained from these samples was  $18.5 \pm 1.9$  and  $14.7 \pm 1.5$  mm against *S. aureus* and *E. coli*, respectively. While in the work of Amjadi [218] antibacterial activity was caused solely by ZnO nanoparticles and rosemary oil, Abou-Okeil and co-authors [219] reported that the oxidized form of  $\kappa$ -C can have antibacterial properties. In the study,  $\kappa$ -C with different oxidation levels (with different contents of aldehyde groups) were used. Antibacterial properties of all obtained mats assessed by CFU method showed impressive results demonstrating more than 90% reduction against *S. aureus* (from 91 to 99.74%) but relatively less efficient against *E. coli* (from 66% to 88%).

A summary of the main findings on the section is presented in Table 7. Multiple applications of antibacterial electrospun coatings from polysaccharides are continuously expanded and



**Table 7**

Summary of products, compositions, antibacterial efficiency and process parameters for electrospun coatings.

Products	Compositions	Antibacterial Efficiencies	Process Parameters
CS and PEO used as a support for silica nanofibers enriched with cefepime antibiotic for orthopedic implants [202]	CS and PEO solution (0.27 g CS and 0.04 g PEO) mixed with silica solution TEOS-water-ethanol-HCl (1:3:8:0.04) in proportions 90:10, 80:20, 70:30 and 50:50. Optimal results were obtained for 30% of CS and 1% of TEOS and cefepime	Disk diffusion method; Nanofibers with ceftazidime result in 25 and 40 mm inhibition zones against <i>S. aureus</i> and <i>E. coli</i> , respectively, less effective against <i>S. epidermidis</i> ; nanofibers without antibiotic showed 5 mm and 12 mm inhibition zones against <i>E. coli</i> and <i>S. aureus</i> and no effect on <i>S. epidermidis</i> .	Capillary setup, voltage 21 kV, flow rate 0.5 mL/h, distance 11 cm; crosslinked by GA
CS/PEO/extracts of henna and/or thymus coating for orthopaedic implants [203]	2% (w/v) CS in 50% AA aqueous solution, PEO 3% (w/v) in 50% AA aqueous solution, mixed in different ratios; to optimal ratio of CS-PEO (7/3 (v/v)) 1% (v/v) of henna and/or thymus extract was added	Disk diffusion method; Nanofibrous mat with thymus extract demonstrated maximal inhibition zones of $3.9 \pm 0.3$ cm and $5.3 \pm 0.2$ cm against <i>S. aureus</i> and <i>E. coli</i> respectively	Capillary setup, voltage 21 kV, flow rate 0.3–0.5 mL/h, distance 13 cm, needle 20-gauge; done on the surface of implant
ALG-based nanofibrous mats with halloysite nanotubes loaded with cephalixin [206]	Prepared using PVA; 10 wt% of PVA in water mixed with 2% (w/v) of ALG in water together with drug loaded HNT, mixture ratio is 3:2; concentration of HNT were 2.5, 7.5 and 10 wt% of the total solution	Disk diffusion method, <i>S. aureus</i> , <i>S. epidermidis</i> , <i>E. coli</i> , <i>P. aeruginosa</i> Inhibition zones were ranging from 15 to 28 mm	Horizontal capillary setup, voltage 25–28 kV, flow rate 8–10 mL/min, 10 cm distance, 0.5 mm needle diameter; crosslinked by GA vapor
Wound dressing, cotton material coated with PVA-CS nanofibers incorporating <i>Agrimonia Eupatoria</i> L. extract [210]	Cotton fabric was preactivated with TEMPO, solution 10% (w/v) PVA and 2% (w/v) CS in water and 0.1M AA. 5 wt% of <i>Agrimonia Eupatoria</i> L. extract added	Disk diffusion method, <i>S. aureus</i> , <i>P. aeruginosa</i> ; MIC; After 24 h non coated cotton showed 25 and 27% inhibition, while PEO-CS – 64 and 61%, with the extract – 99 and 98% respectively	Free surface ES Nanospider LAB, voltage 75 kV, distance 13 cm, electrode rotation 55 Hz, duration 1 h
Cellulose nanofibers with silver nanoparticles [212]	17 wt% cellulose acetate solution in DMF:acetone (1:2), stirred for 24 h; alkaline treatment in NaOH to obtain CE; silver reduction after ES by heat treatment at 160 °C or in DMF	Disk diffusion method; <i>S. aureus</i> , <i>E. coli</i> ; Heat treated samples showed larger inhibition zones up to 347.1 mm <sup>2</sup> against <i>S. aureus</i> and 279 mm <sup>2</sup> against <i>E. coli</i> due to smaller NPs	Capillary setup, voltage 15 kV, flow rate 0.06 mm/min, distance 15 cm, temperature 25 °C, humidity 40%; coated in 200 nM AgNO <sub>3</sub> solution, dried for 2h at 40 °C before reduction
Wound dressing from cellulose membranes with AMP [69]	15% w/v of polyurethane and CA in DMF:acetone (1:2) were mixed in ratios 5:95 CA:PU and 10:90 CA:PU; deacetylation after ES by pure Na dissolved in methanol	CFU, optical; MIC and regrowth time determined spectrophotometrically. Based on regrowth rate CFU's were quantified using standard growth curve; log <sub>4</sub> reduction of <i>S. aureus</i> and max log <sub>1</sub> reduction for <i>P. aeruginosa</i>	Capillary setup; electrical bias of +9 and -2 kV; flow rate 10 µL/min, distance 15 cm, needle diameter 0.8 mm, time 120 min
Photoactive silk fibroin/cellulose acetate nanofibrous membranes [213]	Silk fibroin dialyzed and lyophilized into sponges which together with CA were dissolved in formic acid in 12% concentration.	CFU; 10 µL of <i>E. coli</i> bacterial suspension spotted on the sample surface, exposed to light and dark conditions, survivor suspension diluted and plated on agar, CFU estimate resulted in 99.9999% contact killing rate which is sustained after several light-dark cycles	Capillary setup; voltage 15 kV, flow rate 0.3 mL/h, temperature 25 °C, humidity 50%;
Coated PLA film for food preservation [199]	Functionalized PLA surface, 2% (w/v) CS in 5% AA solution with EDC; CS-EDC (30:1) by weight	CFU, Gram-positive <i>Listeria monocytogenes</i> and Gram-negative <i>E. coli</i> and <i>S. typhimurium</i> ; ES coating was not tested; dip coating showed 93–100% of reduction independently on CS molecular weight and deacetylation degree	Capillary setup, voltage 16 kV, flow rate 0.05 mL/h, distance 60 mm, time 60 min
ALG/PEO nanofibers with Phlorotannin for chicken meat preservation [217]	Sodium ALG and PEO were dissolved in concentration of 0.3 g/L in water separately; solutions were mixed in different ratios and 10% (v/v) of phlorotannin was added	CFU; 99.9999% reduction of <i>S. enteritidis</i> population was achieved within 12 h of observation (for MBC); MIC not achieved	Capillary setup, voltage 20 kV, flow rate 0.5 mL/h, distance 15 cm
Reinforced by k-carrageenan zein electrospun nanofibers with ZnO nanoparticles and rosemary essential (RE) oil for food preservation [218]	22% (w/v) zein dissolved in 80% (v/v) ethanol; 1% (w/v) κ-C dissolved in water. Solutions were mixed in different ratios. Best for ES was zein-C (90:10); 0.5 and 50 wt% of ZnO NP and RE was added. ZnO NP and oil caused fiber diameter reduction from $583 \pm 280$ to $387 \pm 169$ nm	Disk diffusion method; Nanofibers from zein and κ-C do not have antimicrobial activity; addition of ZnO NP and RE increases the inhibition zone to $18.5 \pm 1.9$ and $14.7 \pm 1.5$ mm against <i>S. aureus</i> and <i>E. coli</i> respectively. The antibacterial efficiency might be related to increased contact angle	Horizontal capillary setup, voltage 15 kV, flow rate 1.0 mL/h, 10 cm distance, 21-gauge steel needle
Hyaluronic acid (HA) with oxidized κ-carrageenan and PVA [219]	1% (w/v) solution of oxidized κ-carrageenan, 1% (w/v) solution of HA, 10% (w/v) PVA solution were mixed in different ratios	CFU; All blends showed from 91 to 99.74% reduction against <i>S. aureus</i> and from 66% to 88% against <i>E. coli</i>	Horizontal capillary setup, voltage 17.5 kV, flow rate 0.5 mL/h, 10 cm distance, 22 gauge needle

(continued on next page)

Table 7 (continued)

Products	Compositions	Antibacterial Efficiencies	Process Parameters
Two-layer ES membrane for wound healing with controlled release of ciprofloxacin and FGF-2 [225]	Hydrophilic layer: Octyl gellan gum derivative and PVA powders mixed with weight ratio (1:1) and dispersed in DI water at 4% (w/v), FGF-2 was dissolved in mixture at concentration of 25 ng per mg of polymer mix; Hydrophobic layer: PU-PCl copolymer was dissolved in DMF:THF (1:1) at 5%(w/v), ciprofloxacin hemisuccinate microparticles (2% (w/w))	CFU, <i>S. aureus</i> ; samples loaded with antibiotic showed log6 and log10 viability reduction after 24 and 48 h of incubation respectively; drug release was mostly accomplished within 48 h	Custom capillary setup; Hydrophilic layer: voltage 21-23 kV, flow rate 0.0085 ml/min, 14 cm distance, mandrel rate 70 rpm; Hydrophobic layer: voltage 10 kV, flow rate 0.01 ml/min, 20 cm distance, mandrel rate 70 rpm
Crosslinked pectin nanofibers loaded with Ag NP [226]	Apple pectin was used for dialdehyde pectin synthesis, which in water solution was mixed with PEO, Triton X-100 and DMSO in weight percentages of 9, 1, 1 and 5 respectively; electrospun samples immersed in AgNO <sub>3</sub> solution and incubated at 60 °C for 3-24 h	Optical density; <i>E. coli</i> ; sample introduced in bacterial broth with OD <sub>600</sub> of 0.01, incubated at 37 °C and measured with spectrometer every 24 h, suspension was replaced with the fresh one. Tests showed antibacterial efficiency close to 100% for over 7 days	Capillary setup, voltage 7 kV, distance 15 cm, 8-gauge steel needle; samples crosslinked in ADH solution in ethanol/water for 8 h
Degradable bone scaffold [200]	PLA/CS solution: 0.18 g of CS and 0.72 g of PLA in TFA. Bioactive glasses were deposited by dip-coating	Disk diffusion method, <i>E. coli</i> after 24h in incubation at 37°C. Only fibers coated with Cu, Ag and Ce bioglass developed inhibition zone – not related to CS	Capillary setup, 10 ml syringe with 21G needle tip, 12 kV, 8 cm distance; afterwards dried for 24 h at 80 °C.
CS-PEOEE nanofiber coating with bioactive glass for Ti alloy [201]	7 wt% of CS in mixture of AA-H <sub>2</sub> O (7:3 w/w) with addition of bioglass 15 wt% of CS, PEO weight ratio of 2/8 of CS	CFU, solution optical density tests, luminescent microscope, <i>S. epidermidis</i> ; Reduction of cell proliferation for coating with and without bioglass. Bioglass was shown to even inhibit antibacterial effect of CS	Capillary setup, voltage 27 kV, flow rate 0.1 mL/h, 30G needle, distance 10 cm, receiver rotation drum speed 120 rpm; samples were dried for 12 h at 50 °C and crosslinked by GA
Water filtration membrane of dually cross-linked ALG, coated with CS incorporating Ag NP [220]	3 wt% of PEO and 3 wt% of ALG were dissolved in deionized water separately and mixed in ratio 50:50. 0.5 wt% Triton X-100 and 5 wt% DMSO as emulsifiers were added. Ag NP containing CS were prepared separately and added with small amount of CS solution into main solution	Disk diffusion method, <i>S. aureus</i> , <i>E. coli</i> Membrane without Ag NP showed bacteriostatic affect against <i>E. coli</i> , coating with Ag NP showed antibacterial effect towards both <i>S. aureus</i> and <i>E. coli</i> with inhibition zones of 3.32±0.2 cm and 2.31±0.17 cm respectively	Capillary setup, voltage 25 kV, flow rate 0.7 mL/h, working distance 18 cm; crosslinked ionically by CaCl <sub>2</sub> and afterwards with GA vapor.

investigated, however several challenges can be emphasized. Focusing within this review primarily on antibacterial properties we, unfortunately, cannot avoid the fact that due to limited inherent antimicrobial properties of PS, bactericidal effect has to be improved by means of various additives (nanoparticles [220], plant extracts [203] or other bioactive compounds [207]). These additives interact with the ES solution, can cause changes in viscosity, electrical conductivity and surface tension and, therefore might require special settings of ES process that significantly differ from those set for non-filled/neat systems [217,218]. Additionally, cationic (CS) and anionic (ALG) polysaccharide materials have polyelectrolytic nature and, therefore, are very difficult to ES. Both materials have rigid chemical structure and intra- and intermolecular hydrogen bonds, which prevent them from forming entanglements. Some solubility issues appear as even small concentrations of added polymer result in highly viscous solution and CS does not dissolve in non-acidic medium. That is why CS and ALG are usually blended with other electrospinnable polymers, such as polylactic acid (PLA), polyethylene oxide (PEO) or polyvinyl alcohol (PVA) [221–223]. This inevitably makes the system more complicated. Another problem arising with ES of ALG and CS is related to their broad molecular weight distribution, that affects viscosity and can potentially lead to clogging of ES capillaries [224]. In this case, open surface or needless ES can be used [190,210]. As can be observed from the overview in Table 6 usually classical capillary syringe setups are utilized with relatively high voltages for such setups due to the high solution viscosity. It should be also mentioned that attachment of the coating to the substrate is practically not investigated, however some research work [199] describe measures to improve it.

#### 4.6. Layer-by-Layer Assembly

Layer-by-layer (LbL) self-assembly is a relatively simple yet versatile method for surface modification, which was first discovered

and used by Decher et al. [227]. The LbL-procedure is described in Fig. 14. A solid substrate with a charged surface is immersed in a solution containing a high concentration of polyelectrolyte. The polyelectrolyte deposits onto the surface forming a monolayer. After rinsing with deionized water, the substrate is immersed in another solution containing oppositely charged polyelectrolyte to regain its original surface charge. By repeating these two steps in a cyclic manner, alternating multilayer assemblies with desired thickness and properties can be achieved. In addition, the substrate can be either a naturally charged material, such as metal, glass, and silicon wafer, or an originally uncharged substrate modified by plasma [228], chemical grafting [229] etc. Nowadays, LbL technology has been extensively developed and allows different driving forces for depositing multilayer coatings. While the description above refers essentially to dip-coating, LbL can be applied using all other coating technologies already presented, such as spinning, spraying, dipping etc., including combinations thereof [230].

The function of the LbL-coating is determined by the composition of the different layers. Therefore, the use of suitable components is particularly important in LbL-assembly. Since many polysaccharides are charged positively or negatively, have good biocompatibility and special biological functions, such as CS [231], HA [232,233], ALG [232,234], etc., they are the desired materials for LbL. [231], HA [232,233], ALG [232,234], etc., they are the desired materials for LbL. Especially for bactericidal LbL-systems, cationic polysaccharide layers can interact with phospholipid components in the biofilms, leading to bacterial membrane deformation and protoplast lysis under osmotic stress [233]. In addition, some anionic polysaccharide layers with functional groups such as carboxyl groups can be combined with metal ions to achieve more biological properties [234].

Due to their broad applicability, LbL-assemblies can be developed through different antimicrobial strategies to meet different needs, depending on the interactions between the assembly and the antimicrobial components. Antimicrobial agents in the LbL-

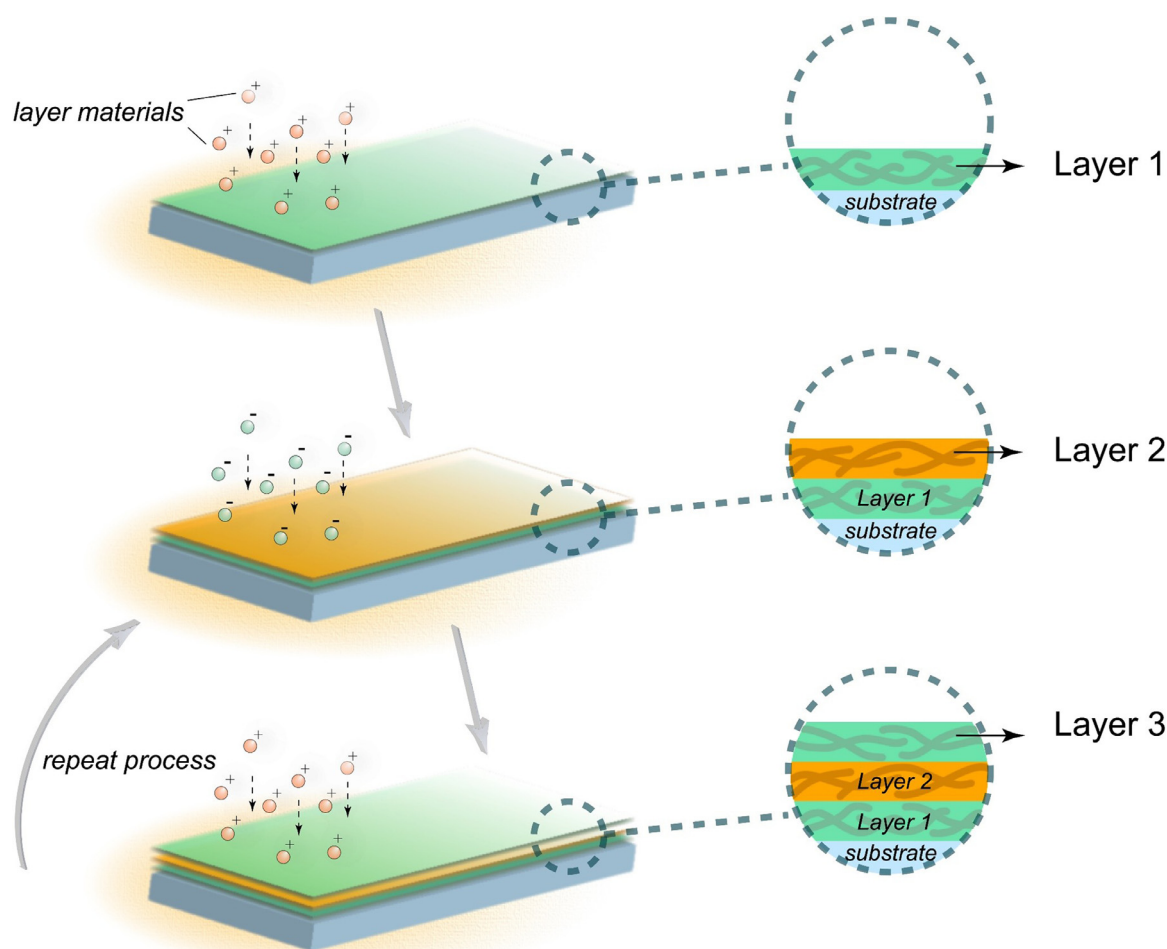


**Fig. 14.** Layer-by-layer (LbL) coating principle. The charged particles are deposited onto the oppositely charged surface/layer and form into a new layer via various methods such as spinning, spraying, dipping etc. The process can be repeated to adjust the properties of the coating depending on the applications.

films can be released into the external environment [235] or remain on the surface of the substrate for contact killing [231]. The vast majority of LbL assemblies are driven by electrostatic interactions, and thus many nanoparticles, biological macromolecules, and organic molecules can participate in the assembly [236]. Among those materials, the polysaccharides with opposite charges can be assembled through electrostatic interactions in aqueous solution via alternating deposition of polyanions and polycations. However, electrostatic interaction is not the only driving force, with other parameters such as hydrogen bonding [237], Host-Guest inclusion [235], covalent bonding [238], etc. can also be used as strategies to fabricate LbL-coatings. Nevertheless, the design and selection of driving force for the LbL-assembly needs to consider the mechanism and properties of the whole material system, therefore, not all driving forces are applicable to the fabrication of polysaccharide-based antimicrobial coatings. In the following sections, various polysaccharides for LbL assembly are discussed in the terms of interactions and properties.

In some cases, there is a need to fabricate multilayer coatings to adjust the thickness and functions, and consequently it would take more time and energy compared to the fabrication of the coating with a single layer. However, combining especially, dip-, spin- and spray-coating through LbL technology could allow for automation [239] and accelerate the film forming considerably via different forces governing the process [240], which facilitates large-scale production for the industry. Due to their substantial versatility, many studies on polysaccharide based LbL coatings tend to focus

more broadly on multifunctional properties, antibacterial among them, and we emphasize that in the sections below.

#### 4.6.1. LbL-assembly driven by electrostatic interaction for antibacterial polysaccharide coatings

As the main driven force, electrostatic interactions in multi-layer formation plays an important role because it is non-specific, with minimal steric demand, and with fairly long range [241]. LbL-assembly driven by electrostatic interactions usually requires water as solvent, therefore it is possible to incorporate with charged biological macromolecules during the formation of the LbL-films. Particularly for the charged polysaccharide solutions, due to electrostatic interactions involving all ionic species in solution, the original set of properties could be highly different. The first type of interaction exists in the attraction between polyions and oppositely charged ions while the second type of electrostatic interaction is usually referred to the repulsion between polyelectrolytes with the same charge which could lead to unusual viscosity behavior [242]. In the LbL-assembly process, the first electrostatic effect is relatively common, because when the molecular weight of the polysaccharide is high enough, the influence of the chain length on the electrostatic effect will no longer be obvious, which facilitates adjustment of film properties. In addition, numerous studies have shown that counter ions have significant effects on polysaccharide-based materials, for example, divalent counter ions favor helical transitions in gellan and carrageenan [243], thus improving the stability of LbL-films. When electrostatic complexes are formed by

polysaccharides with opposite charges, such as ALG or HA, in the presence of CS, the stability of which depends on ion concentration and pH [244].

CS is a biocompatible cationic polysaccharide that has been widely used in fabrication of LbL-films for bacteria killing. For example, to analyze the efficacy of CS as an antibacterial coating, it has been proven that a multilayered assembly consisting of CS and chlorhexidine can reach long term antibacterial properties against *S. aureus* on textile and the antibacterial activity (inhibition zone measurements) increased with the number of layers [245]. To obtain a stimuli responsive LbL-coating and enhance its antibacterial performance, CS is usually modified and combined with drugs during fabrication of the films. Kumorek et al. [246] reported a pH responsive multilayer film for biomedical application based on CS or N-(2-hydroxypropyl)-3-trimethylammonium chitosan chloride (CMCH). CMCH-terminated films prevented bacterial adhesion, especially for *E. coli*, compared to CS-terminated films. However, CS-terminated films showed higher contact killing activity against both Gram-positive and Gram-negative bacteria (70% and 45% bacterial mortality from CFU method, respectively). Grafting quaternary ammonium onto CS is also a common strategy to improve the bactericidal efficiency in LbL-assemblies. A coating composed of polyacrylic acid (PAA), quaternary ammonium salt and gentamicin sulfate and HA in the top layer as sealing agent, showed bactericidal efficiency (CFU method and live dead staining) higher than 99% in the presence of HAase (Hyaluronidase) in the top layer against *E. coli* and *S. aureus*, whereas in the absence of HAase it reached 80% at a pH of 7.4. It is worth noting that HAase alone failed to show any antibacterial activity [247].

In the case of Pectin, chosen as polyanion, Kulikouskaya et al. reported an ultrathin antibacterial coating with pectin and chitosan as polysaccharides matrix [248]. It has been found that pectin-based multilayers exhibited obvious antiadhesive characteristics due to the prevention of *E. coli* adhesion. Furthermore, pectin-silver nanocomposite shows additional bactericidal effects, making it contact killing and release-based antibacterial coatings.

Hyaluronan (HA) is a ubiquitous extracellular matrix component and present in the skin, joints and cornea [249]. HA is naturally negatively charged and can participate in LbL-assembly with other cationic polyelectrolytes. It is shown that the surface coated with HA and antibacterial agents not only can improve the effectiveness of killing the bacteria [247] but also reduce the bacterial adhesion [229,250]. For LbL applications HA is usually combined with CS. In addition, HA has biological functions that vary depending on the molecular weight [251]. Following this reasoning, Hassan et al. extracted HA from rooster comb for the LbL coating of HA having with  $M_w = 2.53 \times 10^5$  Da (value at the higher end of the typical range for HA) and CS on nylon monofilaments (NMy) [252]. CFU results showed less live bacteria for CH/HA-NMy compared to control and NMy coated with CS and HA alone against *S. aureus*. However, CS-NMy and CH/HA-NMy showed basically the same level of antibacterial improvement compared to the other formulations. We note that the content of CS and HA was not equal (4 and 8% respectively). Tripathy et al. [231] used dip-coating LbL to achieve a HA/CS bilayer on a textured silicon wafer. A controlled coating thickness of 13.7 nm was obtained by alternatively dipping the textured silicon surface in HA and CS solutions for 10 min. It was observed that the HA/CS coating on textured silicon reduced biofilm formation by 25% against *E. coli* and 38% against *S. aureus* compared to the polished silicon wafer.

Alginate (ALG) is another anionic and biocompatible polysaccharide that can degrade under physiological conditions. ALG can also be used for the preparation of polyelectrolyte solutions for LbL-assembly. Biopolymer based multilayers cannot usually resist mechanical stress under the action of lysozyme, however, by introducing ALG this limitation can be overcome. Silva et al. [232]

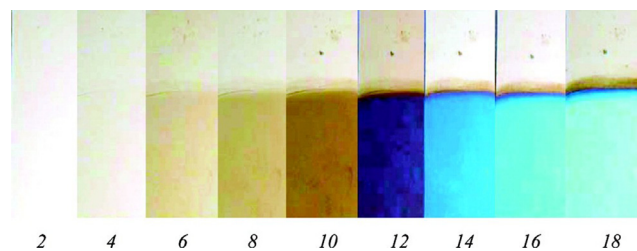


**Fig. 15.** Interference colors of films of CNFs and PEI (polyethyleneimine) as a function of the number of layers. For example, 10 refers to a combination of five bilayers [258]. Reprinted with permission from Wågberg, L.; Decher, G.; Norgren, M.; Lindström, T.; Ankerfors, M.; Axnäs, K., The Build-up of Polyelectrolyte Multilayers of Microfibrillated Cellulose and Cationic Polyelectrolytes. *Langmuir* 2008, 24, 784-795. Copyright 2008 American Chemical Society.

fabricated a LbL-coating based on ALG and other polysaccharides loaded with diclofenac sodium salt to achieve sustainable release from soft contact lens. The coating was biocompatible and exhibited antifouling properties and some antibacterial properties against *P. aeruginosa* and *S. aureus*, more significantly against the latter, as determined from optical density (OD) measurements. It is noted, however, that the antibacterial effect was attributed to the top layer of HA [232]. For preventing infection and promoting mineralization, Jialong et al. created a composite ALG coating on a porous titanium surface via LbL assembly followed by the *in-situ* reduction of silver nanoparticles induced by dopamine [253]. Through the methods of disk diffusion, OD measurements, CFU and live-dead staining, the coating showed antibacterial properties against *S. mutans* and *S. aureus*.

Carrageenan biopolymers are widely utilized in the food packaging, but they have also found utility in the fields of antibacterial applications and wound healing [254]. Jessie et al. proposed a method to embed Nisin as component into multilayer films made of carrageenan and chitosan via LbL assembly [255]. In comparison to control films, CFU data showed that the Nisin-containing films were able to eliminate over 90% and 99% of planktonic and biofilm cells from *S. aureus* and methicillin-resistant *S. aureus* strains, respectively.

Moreover, as mentioned in Section 2.2.2, cellulose can be widely used as coating material for antibacterial applications with chemical modification or combined with other components giving additional antibacterial activities. The same strategies can be also applied to the LbL assembly. Specifically, over the last decade, nanocellulose, has gained particular attraction in advanced materials formed by LbL since charged surface groups on nanocellulose can provide good colloidal stability in aqueous media, leading to well-defined structures and high efficiency of LbL assembly [256], see Fig. 15. Combined with oppositely charged compositions such as polyelectrolytes, nanoparticles or even nanocellulose, strong and ductile coatings can be created on different types of 2D and 3D surfaces [68]. Furthermore, the influence of cellulose charge in LbL technique on antibiofouling and antibacterial properties has also been investigated. It has been suggested that in the assembly of cationic polyvinylamine (PVAm)/anionic cellulose nanofibril/PVAm, high cationic surface potential on the LbL-treated surfaces caused by high surface charge of the cellulose can adsorb and disrupt the cell membrane of *E. coli* via high interaction force  $\sim 50$  nN between bacteria membrane and surface [67] (optical density (OD) with spectrophotometry (LIVE/DEAD BacLight Viability Kit). With modification of natural cellulose, negatively-charged carboxymethyl cellulose and positively-charged  $\epsilon$ -poly(L-lysine) were alternately deposited on a 2D paper surface and reached up to over 99% antibacterial reduction (shaking flask method, typical for textiles, followed by CFU method on agar plates) for 4.5 bilayers against *E. coli* and *S. aureus* without being toxic to animal cells [257].



Polyanion gum arabic is an edible tree gum exudate used mainly in food, cosmetic and pharmaceutical industries [259]. In recent years, gum arabic has also been used for LbL-film fabrication via electrostatic interaction. Zhang et al. reported multilayer polysaccharide composite films incorporated with dopamine chemistry for coating of an orthopedic implants [260]. Gum arabic was introduced to improve the biocompatibility for clinical applications. The results showed that with the increase of the number of composite layers, the antibacterial properties of the coatings were significantly enhanced, and the coating was also endowed with long-term antibacterial effects (live/dead staining; results, however, were not quantitatively discussed).

#### 4.6.2. LbL-assembly driven by Host-Guest Inclusion for antibacterial polysaccharide coatings

Host-Guest inclusion is usually developed with the use of solvents, since most macrocyclic hosts are solid at room temperature, while guest molecules are either solid or liquid [261]. A Host-Guest complex forms when the host molecule meets the guest molecule, and this behavior occurs in a solution containing both host and guest molecules. Considering that the number of solute molecules is much smaller than that of solvent molecules (in this case, the host and guest molecules are solute molecules) solvent molecules keep the host molecules at a distance from the guest molecules, resulting in reduced opportunities for complex formation and increased opportunities for complex dissociation [261]. Therefore, Host-Guest inclusion is not the main strategy for LbL-assembly but can be combined with electrostatic interaction to realize the multifunctionality of composite films.

$\beta$ -cyclodextrin ( $\beta$ -CD) as a special polysaccharide or oligosaccharide, is a cylindrical host molecule with seven glucose subunits linked by  $\alpha$ -(1, 4) glycosidic bonds [262]. The hydrophobic cavity of  $\beta$ -CD allows the formation of host-guest inclusion complexes with various substrates in aqueous media [262]. In addition, since the dynamic nature of supramolecular interaction, it is found that the LbL-coating based on cyclodextrin can be endowed with self-healing properties [263]. To achieve an enhanced disinfection effect, Hongyun et al. [264] obtained a self-healing and antibacterial spin-coated LbL coating consisting of  $\beta$ -CD and  $\text{MoS}_2$ . They demonstrated that the coating self-healed immediately after scratching, and after UV light irradiation, the antibacterial effect of the coating was shown based on visual exclusion region inspection against *E. coli* from disk diffusion tests. Moreover, the  $\beta$ -CD based LbL-coating loaded with drugs can be further used as functional carriers to control the release of antibacterial agents [235]. Antibacterial activity against Gram-positive bacteria has not been reported.

#### 4.6.3. LbL-assembly driven by covalent bonding for antibacterial polysaccharide coatings

In order to improve the durability and rigidity of the LbL-coatings, covalent bonds can be introduced into LbL-multilayers directly, which also leads to multifunctionality and structural diversity of the films. One of the mostly used material to create covalent bonds in LbL-assembly is dopamine, which is widespread in the adhesion proteins of mussels [265]. In general, there are three reasons for the use of dopamine or its derivatives in LbL assembly. First, the catechol groups on dopamine provide strong adhesion between layers, which broadens the applications of LbL-assemblies. Second, when metallic ions are immobilized in LbL-films, the dopamine can contribute to the reduction of metal ions into nanoparticles providing antibacterial properties. Third, the reaction of dopamine with specific functional groups on polymers is mild and can be used to construct LbL-multilayers at room temperature [266].

Based on dopamine chemistry and chitosan quaternary ammonium salt, Wu et al. fabricated a dynamic surface that could respond to the variation of pH in environment [267]. Under acidic conditions, the multilayer films were endowed with bactericidal effects, examined based on area ratios of stained live/dead bacteria (LIVE/DEAD BacLight Viability Kit) for *S. aureus* and *E. coli*. Importantly, when the pH was shifted to neutral, dead bacteria could be expelled to regenerate the biocidal surface. Furthermore, it was found that the dopamine-modified polysaccharide coating through LbL-assembly can be also deposited on different types of substrates.

A summary of the main findings regarding LbL strategies for fabricating antibacterial coatings can be found in Table 8.

### 5. From polysaccharides to antibacterial coatings: trends, roadmap, opportunities and challenges

Polysaccharides present significant potential for antibacterial coating applications combining a broad range of bactericidal strategies and coating technologies. This has been substantiated by a significant number of publications dedicated to the subject, with a broad range of potential applications, see Fig. 16. As expected, CS has been most investigated. Cellulose feature prominently as the second-most popular polysaccharide, however, this is likely due to its availability making it a very attractive for developing into antibacterial coatings. ALG and HA have also been considerably investigated, albeit mainly as part of other polysaccharide formulations. All major polysaccharides used in antibacterial coatings refer to layer-by-layer (LbL) assembly as fabrication method. This is a testament to both the versatility of the LbL technique but also to the suitability of polysaccharides for LbL. For CS, dip coating and ES constitute the second most significant fabrication techniques, while ES and spin coating feature also significantly for ALG and HA.

From the point of view of developing novel material formulations with enhanced bactericidal effect based on polysaccharides, choosing an appropriate coating method may seem like a daunting task. A direct comparison between the different coating technologies in terms of antibacterial performance is hindered by the lack of a clear standard in testing antimicrobial properties (see Section 3). However, what is clear is that the choice of fabrication technology can in-itself be an enabler of antibacterial properties through the obtained material structure, e.g. surface morphology [268] and that the scalability and versatility of the fabrication method is a decisive factor for practical applications.

#### 5.1. Considerations for selecting a coating technology

We identify three major factors that need to be considered when aiming to transform a material formulation into an antibacterial coating. (i) The first factor depends on the attainable material structures through the respective fabrication method that may bring forth the best in the formulation. (ii) Another major factor is intrinsic to the material formulation through its rheological properties and may be a limiting factor in choosing an appropriate technique. (iii) Finally, when pursuing a specific biomedical application, scalability is another major aspect that is best considered early in the research. An additional important factor that is not discussed in this publication is related to regulatory challenges [269]. A comparative summary considering processing and material parameters, structural benefits and limitations, and scalability of the methods reviewed in this publication can be found in Fig. 17.

(i) As structural enablers, coating methods vary significantly from easy to use readily scalable dip coating that can yield relatively smooth surfaces on a variety of substrates, to more challenging 3D printing and electrospinning techniques that are capable of delivering controlled porous hierarchical structures [225]. Porous

**Table 8**

Summary of Layer-by-Layer fabrication strategies for antibacterial applications.

Assembly mechanism	Composition	Bacteria tested	Findings
Electrostatic Interaction [245]	CS, chlorhexidine.	Disk diffusion method; <i>S. aureus</i> .	Long-term antibacterial properties.
Electrostatic Interaction [246]	CS, HA, PEI.	CFU; <i>S. aureus</i> , <i>E. coli</i> .	Bacterial anti-adhesion; Strong contact killing activity; Controlled release of therapeutics.
Electrostatic Interaction [247]	Modified-CS, HA, PAA.	CFU; <i>S. aureus</i> , <i>E. coli</i> .	Controlled drug delivery; Promising antibacterial performance.
Electrostatic Interaction [252]	CS, HA.	CFU; <i>S. aureus</i> , <i>E. coli</i> .	Enhanced bactericidal performance; Controlled release behavior.
Electrostatic Interaction [231]	CS, HA.	Fluorescence microscopy; <i>S. aureus</i> , <i>E. coli</i> .	Enhanced antibacterial efficacy.
Electrostatic Interaction [232]	ALG, CS, HA.	OD method; <i>S. aureus</i> , <i>P. aeruginosa</i> .	Antifouling capability; Biocompatible and antibacterial properties.
Electrostatic Interaction [67]	Cellulose nanofibril, PVAm	OD method; <i>E. coli</i> .	Enhanced antibacterial efficacy.
Electrostatic Interaction [257]	Carboxymethyl cellulose, $\epsilon$ -poly(L-lysine).	CFU; <i>S. aureus</i> , <i>E. coli</i> .	Enhanced antibacterial efficacy.
Electrostatic Interaction [260]	Gum Arabic, $\epsilon$ -polylysine.	Fluorescence microscopy; <i>S. aureus</i> , <i>E. coli</i> .	Enhanced and Long-term antibacterial properties.
Electrostatic Interaction [248]	CS, pectin, silver nanoparticles.	CFU; <i>S. aureus</i> , <i>E. coli</i> .	Both antiadhesive and bactericidal effects.
Electrostatic Interaction [253]	ALG, poly(L-lysine), silver nanoparticles.	disk diffusion, OD measurement, CFU and fluorescence microscopy; <i>S. mutans</i> , <i>S. aureus</i> .	prevent bacterial adhesion and colonization; good cytocompatibility.
Electrostatic Interaction [255]	CS, Carrageenan, nisin.	CFU; <i>S. aureus</i> .	High bactericidal efficiency
Electrostatic Interaction; Host-Guest Inclusion [264]	$\beta$ -CD, modified PAA, PEI, MoS <sub>2</sub> .	Disk diffusion method and CFU; <i>E. coli</i> .	Self-healing; High bactericidal efficiency.
Electrostatic Interaction; Covalent Bonding [267]	Modified-CS, modified-PAA.	Fluorescence microscopy; <i>S. aureus</i> , <i>E. coli</i> .	High bactericidal efficiency

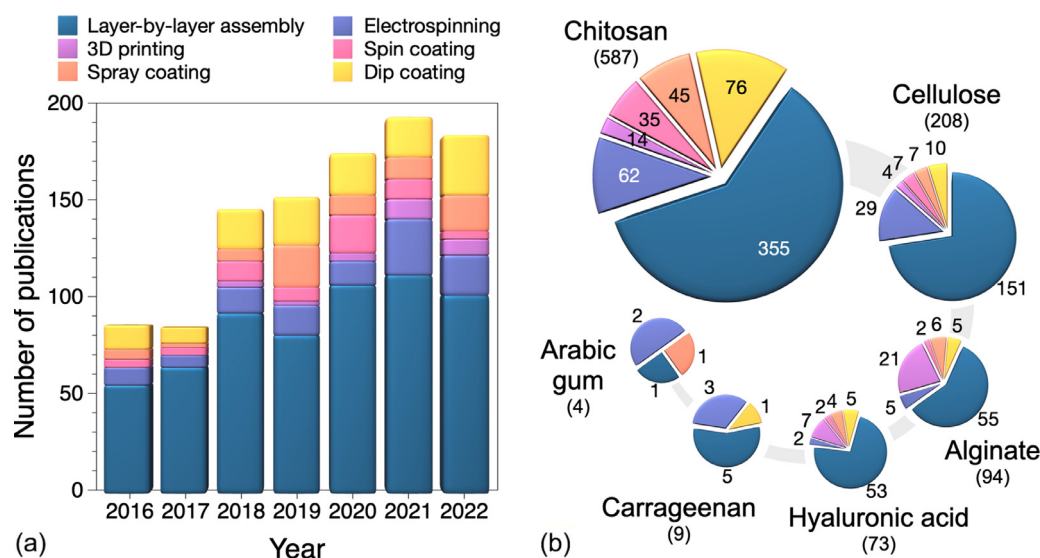


**Fig. 16.** (a) Number of publications regarding antibacterial coatings based on CS, cellulose, ALG, HA, carrageenan and arabic gum per year since 2016 for each coating technology reviewed. Search terms used: antibacterial AND <polysaccharide name> AND coatings (Web of Science). (b) Number of publications regarding antibacterial coatings for the main types of polysaccharides for antibacterial applications and the coating technologies used.

structures are especially important for cases where the bone or tissue scaffolds require biomimetic surfaces for better cell proliferation and attachment. We also note that the surface roughness can be influenced by the presence of particulate additives especially in the presence of large agglomerates [130], even if the coating technology used is expected to produce smooth surfaces. In addition, special consideration needs to be given to post-processing requirements to alter or preserve the coating surfaces. This could include smoothening electrospun or 3D printed surfaces, if that is an application requirement, or preserving a 3D printed structure through crosslinking. In the latter case, special attention has to be given

to the cross-linking of the printed materials. Cross-linking can be performed after printing, during printing using a light source or by submersion into an ionic bath. This also increases the mechanical properties of the coating, which is not the strongest side of pure polysaccharides. In addition to cross-linking, mechanical properties are usually improved by the addition of various fillers or by blending with different polysaccharides or synthetic polymers. Flexible films for the wearable electronics also turn towards hydrogel coatings or specific additives, such as dopamine [270].

(ii) Virtually all types of polysaccharide antibacterial formulations for antibacterial coatings are rheologically-complex, typically

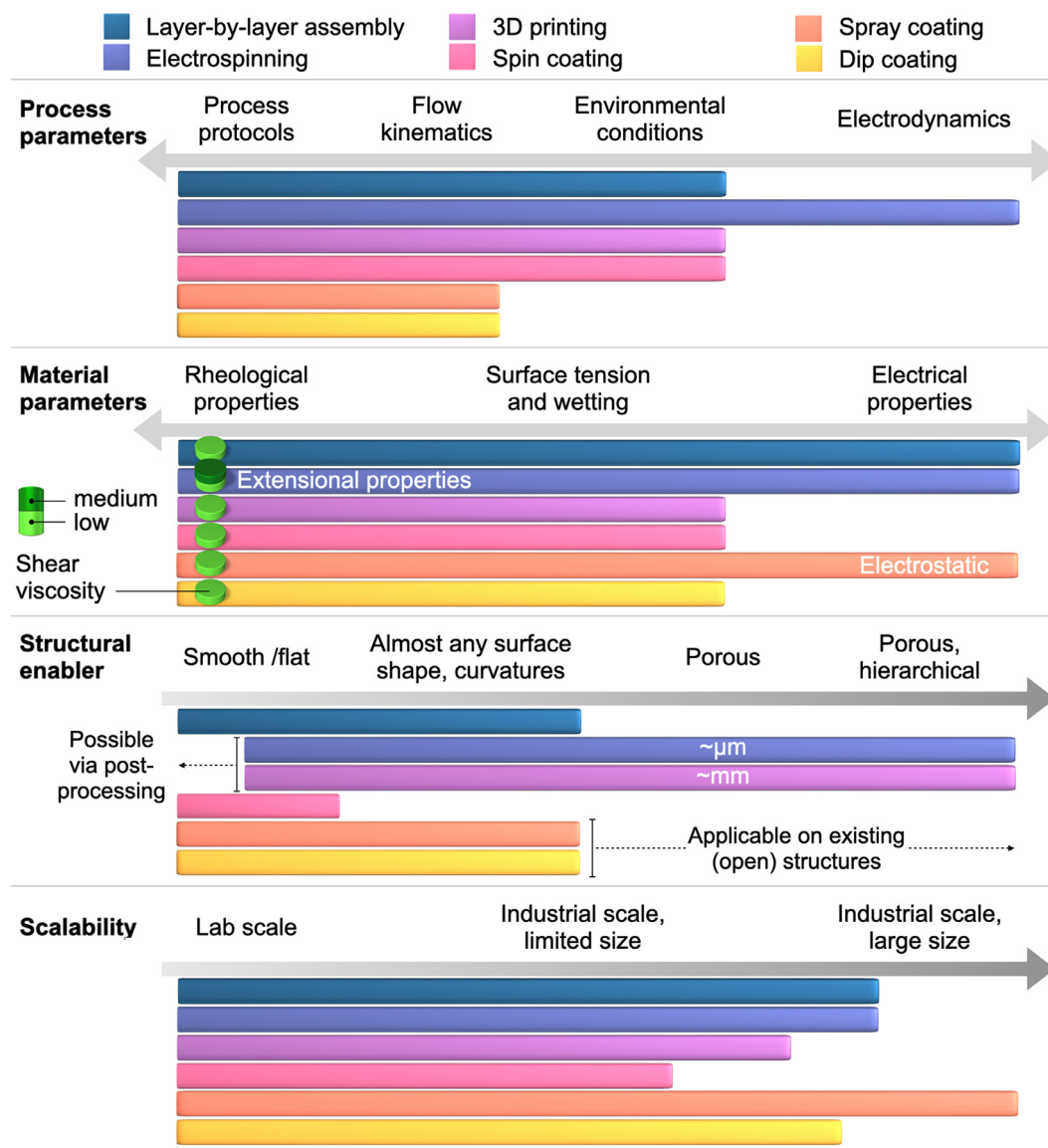


**Fig. 17.** Comparative summary of key processing and material parameters together with structural and scalability aspects for the coating methods considered in this review. Process protocols refer to the succession and timing of events, such as the dip time and evaporation time in dip coating. Flow dynamics includes all geometrical parameters of a flow domain, flow input parameters such as flow rates, and the resulting velocity and stress distributions. Electrodynamics refers to cases that involve charge transport.

showing a combination of shear thinning, thixotropy and yield stress, depending on the formulation [271–274]. Especially their thixotropic behavior and yield stress can be of advantage or detrimental for certain fabrication methods. If substantial extensional deformations are present in the process, e.g. electrospinning and 3D printing, then those would have to be taken into account with the note that characterization of extensional properties is far more challenging than shear properties. Surprisingly, however, rheological properties are often not reported, which is the case for example of most spin coated antibacterial formulations reported in this review.

Since the inherent antibacterial properties of pristine polysaccharides are relatively limited, see Section 2.2.1, polysaccharide-based formulations need to be augmented by the addition of antimicrobial agents. This can be both an enabler for the use of a certain technique or a limiting factor excluding the use of certain techniques. For example, the addition of nanoparticles and surface modifications of polysaccharides typically increase the solution viscosity and induce thixotropy and a yield stress in the formulation. Up to moderate viscosities this could be advantageous for e.g. 3D

printing and dip coating but be detrimental to e.g. spin and spray coating. Adding rheology modifiers to make a formulation suitable for a certain process, if those modifiers / additives have no antibacterial role could lead to undesirable effects. Such is the case for example for spin coating where traces of solvents added to reduce viscosity could be found in the coatings [139]. In addition, very high viscosities especially complemented by high volume fractions of agglomerated nanoparticles can cause clogging of the printing nozzle in 3D printing or spinneret in ES. Another underreported aspect of the physical properties of importance for scalability are the adhesion properties to the substrate. This could prove a challenge when trying to reproduce results, especially for upscaling. This is of utmost importance since as polysaccharides can be obtained from various natural sources and there is an inherent variability associated to them.

## 5.2. Challenges and opportunities

We identify the following challenges for future advances in antibacterial coating technologies:

- Despite multiple sources agreeing on the issue, it remains a challenge to compare the antibacterial performance of polysaccharides coatings. Thus, trends of potential importance for technological transfer may still be unknown.
- Critical material properties are in general underreported; this coupled with the inherent variability in polysaccharides sources can make the technological transfer from principle to a biomedical application a challenge. It is easy within a lab environment to call a surface a coating compared to considering the full technological implications of upscaling.
- It is an enormous challenge to analyze all available data, considering e.g. the source material physico-chemical properties, specific mechanisms to kill bacteria, the coating process and procedures, antibacterial testing methods etc. in a detailed systematic way. In this respect, there could be trends, correlations and/or causal relationships that may not be evident, but they could be revealed on the basis of this review through e.g. artificial neural networks or machine learning techniques.

At the same time, the state of the art in antibacterial coating technologies offers a solid platform for future progress in the field:

- The potential for multifunctional properties in polysaccharide coatings has yet to be fully explored. Here in particular, the addition of nanoparticles, such as 2D nanomaterials, has the potential to further increase the range of envisioned uses of polysaccharide based antibacterial coatings [275], particularly considering the novel 2D material heterostructures currently being developed.
- The individual coating technologies present a template that could be further explored for tailored multilayer hierarchical structures as antibacterial coatings. An example could be combining micron-sized porous electrospun surfaces with millimeter sized 3D printed pores. Such combinations could be essential e.g. with respect to the development of controlled release strategies necessary to optimize therapeutic effects.

To conclude, significant progress has been made on converting polysaccharides from promising antibacterial materials into antibacterial coatings. The developments have covered a broad range of the most commonly used coating techniques, with various potential for scalability. Perspectives for further technological advances lie both in terms of further enhancing the properties of polysaccharides and structures thereof as coatings as well as developing market-ready polysaccharide-based coatings for specific applications. In the case of the latter, further key aspects that may be keeping such technologies from being adopted at industrial scale may still emerge.

### Declaration of Competing Interest

The authors declare that they have no known competing financial interests or personal relationships that could have appeared to influence the work reported in this paper.

### Acknowledgements

HR, RK and IM are grateful for the financial support of the PEST-BIN project that has received funding from the European Union's Horizon 2020 research and innovation programme under the Marie Skłodowska-Curie grant agreement No 955626. AA, SP, RK IM and ML are grateful for the financial support of the Strategic Innovation Program SIO Grafen through grant 2020-00792. SIO Grafen is a joint venture by Vinnova, the Swedish Energy Agency and Formas. VG and RK are grateful for the financial support of the 2D-TECH Vinnova Competence Centre at Chalmers. SP is grateful for the financial support of Vetenskapsrådet (2020-04096). IM is grateful

for the financial support of NordForsk and NNF20CC0035580. RK is grateful for the financial support of the Wallenberg Wood Science Centre (WWSC). The authors are grateful to Prof. Tiina Nypelö for proof-reading the parts dedicated to the chemical structure of polysaccharides.

### References

- [1] S. Szabo, B. Feier, D. Capatina, M. Tertis, C. Cristea, A. Popa, An overview of healthcare associated infections and their detection methods caused by pathogen bacteria in Romania and Europe, *J. Clin. Med* 11 (11) (2022).
- [2] K.M. Busl, Healthcare-associated infections in the neurocritical care unit, *Curr. Neurol. Neurosci. Rep.* 19 (10) (2019) 76.
- [3] J. Gray, Infection control: beyond the horizon, *J. Hosp. Infect.* 89 (4) (2015) 237–240.
- [4] J. O'Neill, Tackling Drug-Resistant Infections Globally: Final Report and Recommendations, Government of the United Kingdom, 2016.
- [5] P. Singh, S. Pandit, C. Jers, A.S. Joshi, J. Garnæs, I. Mijakovic, Silver nanoparticles produced from *Cedecea* sp. exhibit antibiofilm activity and remarkable stability, *Sci. Rep.* 11 (1) (2021) 12619.
- [6] P. Singh, S. Pandit, J. Garnæs, S. Tunjic, V.R. Mokkapati, A. Sultan, A. Thygesen, A. Mackevica, R.V. Mateiu, A.E. Daugaard, A. Baun, I. Mijakovic, Green synthesis of gold and silver nanoparticles from *Cannabis sativa* (industrial hemp) and their capacity for biofilm inhibition, *Int. J. Nanomed.* 13 (2018) 3571–3591.
- [7] V.P. Chakka, T. Zhou, Carboxymethylation of polysaccharides: Synthesis and bioactivities, *Int. J. Biol. Macromol.* 165 (Pt B) (2020) 2425–2431.
- [8] Z. Wang, P. Chen, N. Tao, H. Zhang, R. Li, X. Zhan, F. Wang, Y. Shen, Anticancer activity of polysaccharides produced from glycerol and crude glycerol by an endophytic fungus *Chaetomium globosum* CGMCC 6882 on human lung cancer A549 cells, *Biomolecules* 8 (4) (2018).
- [9] A. Mahdhi, N. Leban, I. Chakroun, S. Bayar, K. Mahdouani, H. Majdoub, B. Kouidhi, Use of extracellular polysaccharides, secreted by *Lactobacillus plantarum* and *Bacillus* spp., as reducing indole production agents to control biofilm formation and efflux pumps inhibitor in *Escherichia coli*, *Microb. Pathog.* 125 (2018) 448–453.
- [10] J. Vunduk, W.A.A.Q.I. Wan-Mohtar, S.A. Mohamad, N.H. Abd Halim, A.Z. Mohd Dzomir, Ž. Žizak, A. Klaus, Polysaccharides of *Pleurotus flabellatus* strain Mynuk produced by submerged fermentation as a promising novel tool against adhesion and biofilm formation of foodborne pathogens, *LWT* 112 (2019).
- [11] D. Rubini, P.V. Varthan, S. Jayasankari, B.N. Vedahari, P. Nithyanand, Suppressing the phenotypic virulence factors of Uropathogenic *Escherichia coli* using marine polysaccharide, *Microb. Pathog.* 141 (2020) 103973.
- [12] Y. Kim, S. Oh, S.H. Kim, Released exopolysaccharide (r-EPS) produced from probiotic bacteria reduce biofilm formation of enterohemorrhagic *Escherichia coli* O157:H7, *Biochem. Biophys. Res. Commun.* 379 (2) (2009) 324–329.
- [13] B. Zhao, Q. Tian, Y. Bagheri, M. You, Lipid-Oligonucleotide Conjugates for Simple and Efficient Cell Membrane Engineering and Bioanalysis, *Curr. Opin. Biomed. Eng.* 13 (2020) 76–83.
- [14] M. Liu, Y. Liu, M.J. Cao, G.M. Liu, Q. Chen, L. Sun, H. Chen, Antibacterial activity and mechanisms of depolymerized fucoidans isolated from *Laminaria japonica*, *Carbohydr. Polym.* 172 (2017) 294–305.
- [15] J. Tantala, K. Thumanu, C. Rachtanapun, An assessment of antibacterial mode of action of chitosan on *Listeria innocua* cells using real-time HATR-FTIR spectroscopy, *Int. J. Biol. Macromol.* 135 (2019) 386–393.
- [16] J. Vishwakarma, S.L. Vavilala, Evaluating the antibacterial and antibiofilm potential of sulphated polysaccharides extracted from green alga *Chlamydomonas reinhardtii*, *J. Appl. Microbiol.* 127 (4) (2019) 1004–1017.
- [17] G.A. Junter, P. Thebault, L. Lebrun, Polysaccharide-based antibiofilm surfaces, *Acta Biomater.* 30 (2016) 13–25.
- [18] G. Crini, Recent developments in polysaccharide-based materials used as adsorbents in wastewater treatment, *Prog. Polym. Sci.* 30 (1) (2005) 38–70.
- [19] H.J. Flint, E.A. Bayer, M.T. Rincon, R. Lamed, B.A. White, Polysaccharide utilization by gut bacteria: potential for new insights from genomic analysis, *Nat. Rev. Microbiol.* 6 (2) (2008) 121–131.
- [20] M. Rinaudo, Chitin and chitosan: Properties and applications, *Prog. Polym. Sci.* 31 (7) (2006) 603–632.
- [21] S.-C. Park, J.-W. Nah, Y. Park, pH-dependent mode of antibacterial actions of low molecular weight water-soluble chitosan (LMWSC) against various pathogens, *Macromol. Res.* 19 (8) (2011) 853–860.
- [22] Z. Deng, T. Wang, X. Chen, Y. Liu, Applications of chitosan-based biomaterials: a focus on dependent antimicrobial properties, *Mar. Life Sci. Technol.* 2 (4) (2020) 398–413.
- [23] X.-f. Li, X.-q. Feng, S. Yang, G.-q. Fu, T.-p. Wang, Z.-x. Su, Chitosan kills *Escherichia coli* through damage to be of cell membrane mechanism, *Carbohydr. Polym.* 79 (3) (2010) 493–499.
- [24] F. Zamboni, C.K. Wong, M.N. Collins, Hyaluronic acid association with bacterial, fungal and viral infections: Can hyaluronic acid be used as an antimicrobial polymer for biomedical and pharmaceutical applications? *Bioact. Mater.* 19 (2023) 458–473.
- [25] G.A. Carlson, J.L. Dragoo, B. Samimi, D.A. Bruckner, G.W. Bernard, M. Hedrick, P. Benham, Bacteriostatic properties of biomaterials against common or-



- thopaedic pathogens, *Biochem. Biophys. Res. Commun.* 321 (2) (2004) 472–478.
- [26] Y. Xia, V. Adibnia, C. Shan, R. Huang, W. Qi, Z. He, G. Xie, M. Olszewski, G. De Crescenzo, K. Matyjaszewski, X. Banquy, R. Su, Synergy between zwitterionic polymers and hyaluronic acid enhances antifouling performance, *Langmuir* 35 (48) (2019) 15535–15542.
- [27] O. Zaitseva, A. Khudyakov, M. Sergushkina, O. Solomina, T. Polezhaeva, Pectins as a universal medicine, *Fitoterapia* 146 (2020) 104676.
- [28] M.B. Aga, A.H. Dar, G.A. Nayik, P.S. Panesar, F. Allai, S.A. Khan, R. Shams, J.F. Kennedy, A. Altaf, Recent insights into carrageenan-based bio-nanocomposite polymers in food applications: a review, *Int. J. Biol. Macromol.* 192 (2021) 197–209.
- [29] R. Yegappan, V. Selvaprithiviraj, S. Amirthalingam, R. Jayakumar, Carrageenan based hydrogels for drug delivery, tissue engineering and wound healing, *Carbohydr. Polym.* 198 (2018) 385–400.
- [30] M.N.F. Norrrahim, N.M. Nurazzi, M.A. Jenol, M.A.A. Farid, N. Janudin, F.A. Ujang, T.A.T. Yasim-Anuar, S.U.F. Syed Najmuddin, R.A. Ilyas, Emerging development of nanocellulose as an antimicrobial material: an overview, *Mater. Adv.* 2 (11) (2021) 3538–3551.
- [31] Y. Lu, X. Zhao, S. Fang, Characterization, antimicrobial properties and coatings application of gellan gum oxidized with hydrogen peroxide, *Foods* 8 (1) (2019) 31.
- [32] A.H. Bacelar, J. Silva-Correia, J.M. Oliveira, R.L. Reis, Recent progress in gellan gum hydrogels provided by functionalization strategies, *J. Mater. Chem. B* 4 (37) (2016) 6164–6174.
- [33] Polysaccharides I, 1 ed., Springer, Berlin, Heidelberg, 2005.
- [34] A. Tiwari, Polysaccharides: Development, Properties and Applications: Development, Properties and Applications, Nova Science Publishers, Incorporated, Hauppauge, United States, 2010.
- [35] S. Dumitriu, Polysaccharides. Structural Diversity and Functional Versatility, 2 ed., 2004.
- [36] X. Wang, J. Qi, W. Zhang, Y. Pu, R. Yang, P. Wang, S. Liu, X. Tan, B. Chi, 3D-printed antioxidant antibacterial carboxymethyl cellulose/epsilon-polylysine hydrogel promoted skin wound repair, *Int. J. Biol. Macromol.* 187 (2021) 91–104.
- [37] R. Roy, M. Tiwari, G. Donelli, V. Tiwari, Strategies for combating bacterial biofilms: a focus on anti-biofilm agents and their mechanisms of action, *Virulence* 9 (1) (2018) 522–554.
- [38] K.K. Jefferson, What drives bacteria to produce a biofilm? *FEMS Microbiol. Lett.* 236 (2) (2004) 163–173.
- [39] R.A. Burne, Oral streptococci... Products of their environment, *J. Dent. Res.* 77 (3) (1998) 445–452.
- [40] Z. Khatoun, C.D. McTiernan, E.J. Suuronen, T.F. Mah, E.I. Alarcon, Bacterial biofilm formation on implantable devices and approaches to its treatment and prevention, *Heliyon* 4 (12) (2018) e01067.
- [41] M.H. Muhammad, A.L. Idris, X. Fan, Y. Guo, Y. Yu, X. Jin, J. Qiu, X. Guan, T. Huang, Beyond risk: bacterial biofilms and their regulating approaches, *Front. Microbiol.* 11 (2020) 928.
- [42] C. Zhao, L. Zhou, M. Chiao, W. Yang, Antibacterial hydrogel coating: Strategies in surface chemistry, *Adv. Colloid Interface Sci.* 285 (2020) 102280.
- [43] J. Palmer, S. Flint, J. Brooks, Bacterial cell attachment, the beginning of a biofilm, *J. Ind. Microbiol. Biotechnol.* 34 (9) (2007) 577–588.
- [44] M. Choi, L. Xiangde, J. Park, D. Choi, J. Heo, M. Chang, C. Lee, J. Hong, Superhydrophilic coatings with intricate nanostructure based on biotic materials for antifogging and antibiofouling applications, *Chem. Eng. J.* 309 (2017) 463–470.
- [45] H.W. Chien, H.Y. Lin, C.Y. Tsai, T.Y. Chen, W.N. Chen, Superhydrophilic coating with antibacterial and oil-repellent properties via naio4-triggered polydopamine/sulfobetaine methacrylate polymerization, *Polymers* 12 (9) (2020).
- [46] Y. Chen, Y. Ding, J. Zheng, A polymer nanocomposite coating with enhanced hydrophilicity, antibacterial and antibiofouling properties: Role of polymerizable emulsifier/anionic ligand, *Chem. Eng. J.* 379 (2020).
- [47] S. Park, H.H. Kim, S.B. Yang, J.H. Moon, H.W. Ahn, J. Hong, A polysaccharide-based antibacterial coating with improved durability for clear overlay appliances, *ACS Appl. Mater. Interfaces* 10 (21) (2018) 17714–17721.
- [48] S. Park, J. Park, J. Heo, S.-E. Lee, J.-W. Shin, M. Chang, J. Hong, Polysaccharide-based superhydrophilic coatings with antibacterial and anti-inflammatory agent-delivering capabilities for ophthalmic applications, *J. Ind. Eng. Chem.* 68 (2018) 229–237.
- [49] W. Barthlott, C. Neinhuis, Purity of the sacred lotus, or escape from contamination in biological surfaces, *Planta* 202 (1) (1997) 1–8.
- [50] X. Gao, L. Jiang, Water-repellent legs of water striders, *Nature* 432 (7013) (2004) 36–36.
- [51] M. Ghasemlou, P.H. Le, F. Daver, B.J. Murdoch, E.P. Ivanova, B. Adhikari, Robust and eco-friendly superhydrophobic starch nanohybrid materials with engineered lotus leaf mimetic multiscale hierarchical structures, *ACS Appl. Mater. Interfaces* 13 (30) (2021) 36558–36573.
- [52] M. Maayan, K.A. Mani, N. Yaakov, M. Natan, G. Jacobi, A. Atkins, E. Zelinger, E. Fallik, E. Banin, G. Mechrez, Fluorine-free superhydrophobic coating with antibiofilm properties based on pickering emulsion templating, *ACS Appl. Mater. Interfaces* 13 (31) (2021) 37693–37703.
- [53] Z. Wei, S. Teng, Y. Fu, Q. Zhou, W. Yang, Micro/nano-structured electrospun membranes with superhydrophobic and photodynamic antibacterial performances, *Prog. Org. Coat.* 164 (2022).
- [54] Q. Zeng, C. Zheng, K. Han, W. Wu, H. Qi, K. Wang, P. Sahu, R. Dong, T. Lu, A biomimetic superhydrophobic and anti-blood adhesion coating, *Prog. Org. Coat.* 140 (2020).
- [55] M. Hermansson, The DLVO theory in microbial adhesion, *Colloids Surf. B* 14 (1–4) (1999) 105–119.
- [56] A.T. Poortinga, R. Bos, W. Norde, H.J. Busscher, Electric double layer interactions in bacterial adhesion to surfaces, *Surf. Sci. Rep.* 47 (1) (2002) 1–32.
- [57] Y.E. Collins, G. Stotzky, Heavy metals alter the electrokinetic properties of bacteria, yeasts, and clay minerals, *Appl. Environ. Microbiol.* 58 (5) (1992) 1592–1600.
- [58] A.C. Plette, W.H. van Riemsdijk, M.F. Benedetti, A. van der Wal, pH dependent charging behavior of isolated cell walls of a gram-positive soil bacterium, *J. Colloid Interface Sci.* 173 (2) (1995) 354–363.
- [59] D. Alkekha, A. Shukla, Influence of poly-L-lysine molecular weight on antibacterial efficacy in polymer multilayer films, *J. Biomed. Mater. Res. Part A* 107 (6) (2019) 1324–1339.
- [60] S. Pandit, K. Gaska, V.R.S.S. Mokkapati, E. Celauro, A. Derouiche, S. Forsberg, M. Svensson, R. Kádár, I. Mijakovic, Precontrolled alignment of graphite nanoplatelets in polymeric composites prevents bacterial attachment, *Small* 16 (5) (2020).
- [61] N.M. Milovic, J. Wang, K. Lewis, A.M. Klibanov, Immobilized N-alkylated polyethylenimine avidly kills bacteria by rupturing cell membranes with no resistance developed, *Biotechnol. Bioeng.* 90 (6) (2005) 715–722.
- [62] R. Kaur, S. Liu, Antibacterial surface design – contact kill, *Prog. Surf. Sci.* 91 (3) (2016) 136–153.
- [63] L.G.S. Garcia, G.M. de Melo Guedes, X. Fonseca, W.A. Pereira-Neto, D. Castelo-Branco, J.J.C. Sidrim, R. de Aguiar Cordeiro, M.F.G. Rocha, R.S. Vieira, R.S.N. Brillhante, Antifungal activity of different molecular weight chitosans against planktonic cells and biofilm of *Sporothrix brasiliensis*, *Int. J. Biol. Macromol.* 143 (2020) 341–348.
- [64] Z. Wang, Q. Yang, X. Wang, R. Li, H. Qiao, P. Ma, Q. Sun, H. Zhang, Antibacterial activity of xanthan-oligosaccharide against *Staphylococcus aureus* via targeting biofilm and cell membrane, *Int. J. Biol. Macromol.* 153 (2020) 539–544.
- [65] M. Bračić, O. Šauperl, S. Strnad, I. Kosalec, O. Plohl, L.F. Zemljčić, Surface modification of silicone with colloidal polysaccharides formulations for the development of antimicrobial urethral catheters, *Appl. Surf. Sci.* 463 (2019) 889–899.
- [66] X. Zhang, W. Zhu, J. Guo, J. Song, H. Xiao, Impacts of degree of substitution of quaternary cellulose on the strength improvement of fiber networks, *Int. J. Biol. Macromol.* 181 (2021) 41–44.
- [67] C. Chen, T. Petterson, J. Illergård, M. Ek, L. Wågberg, Influence of cellulose charge on bacteria adhesion and viability to PVAm/CNF/PVAm-modified cellulose model surfaces, *Biomacromolecules* 20 (5) (2019) 2075–2083.
- [68] M. Ghanadpour, B. Wicklein, F. Carosio, L. Wågberg, All-natural and highly flame-resistant freeze-cast foams based on phosphorylated cellulose nanofibrils, *Nanoscale* 10 (8) (2018) 4085–4095.
- [69] R. Weishaupt, J.N. Zund, L. Heuberger, F. Zuber, G. Faccio, F. Robotti, A. Ferrari, G. Fortunato, Q. Ren, K. Maniura-Weber, A.G. Guex, Antibacterial, cytocompatible, sustainably sourced: cellulose membranes with bifunctional peptides for advanced wound dressings, *Adv. Healthc. Mater.* 9 (7) (2020) e1901850.
- [70] S. Wang, Y. Li, R. Zhao, T. Jin, L. Zhang, X. Li, Chitosan surface modified electrospun poly(epsilon-caprolactone)/carbon nanotube composite fibers with enhanced mechanical, cell proliferation and antibacterial properties, *Int. J. Biol. Macromol.* 104 (Pt A) (2017) 708–715.
- [71] F. Xie, X. Bian, Y. Lu, T. Xia, D. Xu, Y. Wang, J. Cai, Versatile antibacterial surface with amphiphilic quaternized chitin-based derivatives for catheter associated infection prevention, *Carbohydr. Polym.* 275 (2022) 118683.
- [72] J.B. Paris, D. Seyer, T. Jouenne, P. Thebault, Various methods to combine hyaluronic acid and antimicrobial peptides coatings and evaluation of their antibacterial behaviour, *Int. J. Biol. Macromol.* 139 (2019) 468–474.
- [73] M. Garay-Sarmiento, L. Witzdam, M. Vorobii, C. Simons, N. Herrmann, A. de los Santos Pereira, E. Heine, I. El-Awaad, R. Lütticken, F. Jakob, U. Schwaneberg, C. Rodriguez-Emmenegger, Kill&Repel coatings: the marriage of antifouling and bactericidal properties to mitigate and treat wound infections, *Adv. Funct. Mater.* 32 (9) (2021).
- [74] B. Wang, Q. Lin, T. Jin, C. Shen, J. Tang, Y. Han, H. Chen, Surface modification of intraocular lenses with hyaluronic acid and lysozyme for the prevention of endophthalmitis and posterior capsule opacification, *RSC Adv.* 5 (5) (2015) 3597–3604.
- [75] A. Mogrovejo-Valdivia, O. Rahmouni, N. Tabary, M. Maton, C. Neut, B. Martel, N. Blanchemain, In vitro evaluation of drug release and antibacterial activity of a silver-loaded wound dressing coated with a multilayer system, *Int. J. Pharm.* 556 (2019) 301–310.
- [76] M.A. Akhtar, K. Ilyas, I. Dlouhy, F. Siska, A.R. Boccaccini, Electrophoretic deposition of copper(II)-chitosan complexes for antibacterial coatings, *Int. J. Mol. Sci.* 21 (7) (2020).
- [77] H.A. Mansouri-Tehrani, M. Keyhanfar, M. Behbahani, G. Dini, Synthesis and characterization of algae-coated selenium nanoparticles as a novel antibacterial agent against *Vibrio harveyi*, a *Penaeus vannamei* pathogen, *Aquaculture* 534 (2021).
- [78] K.H. Le, M.D.-B. Nguyen, L.D. Tran, H.P. Nguyen Thi, C.V. Tran, K.V. Tran, H.P. Nguyen Thi, N. Dinh Thi, Y.S. Yoon, D.D. Nguyen, D.D. La, A novel antimicrobial ZnO nanoparticles-added polysaccharide edible coating for the preservation of postharvest avocado under ambient conditions, *Prog. Org. Coat.* 158 (2021).

- [79] S. Mallakpour, V. Ramezanzade, Green fabrication of chitosan/tragacanth gum bionanocomposite films having TiO<sub>2</sub>@Ag hybrid for bioactivity and antibacterial applications, *Int. J. Biol. Macromol.* 162 (2020) 512–522.
- [80] H. Deng, J. Sun, Z. Yu, Z. Guo, C. Xu, Low-intensity near-infrared light-triggered spatiotemporal antibiotics release and hyperthermia by natural polysaccharide-based hybrid hydrogel for synergistic wound disinfection, *Mater. Sci. Eng. C* 118 (2021) 111530.
- [81] S. Pacelli, P. Paolicelli, M. Avitabile, G. Varani, L. Di Muzio, S. Cesa, J. Tirillò, C. Bartuli, M. Nardoni, S. Petralito, A. Adrover, M.A. Casadei, Design of a tunable nanocomposite double network hydrogel based on gellan gum for drug delivery applications, *Eur. Polym. J.* 104 (2018) 184–193.
- [82] L. Hua, H. Qian, T. Lei, Y. Zhang, P. Lei, Y. Hu, 3D-printed porous tantalum coated with antitubercular drugs achieving antibacterial properties and good biocompatibility, *Macromol. Biosci.* 22 (1) (2022) 2100338.
- [83] J. Pulit-Prociak, A. Staron, P. Staron, A. Chmielowiec-Korzeniowska, A. Drabik, L. Tymczyna, M. Banach, Preparation and of PVA-based compositions with embedded silver, copper and zinc oxide nanoparticles and assessment of their antibacterial properties, *J. Nanobiotechnol.* 18 (1) (2020) 148.
- [84] S. Mallakpour, N. Mohammadi, Development of sodium alginate-pectin/TiO<sub>2</sub> nanocomposites: antibacterial and bioactivity investigations, *Carbohydr. Polym.* 285 (2022).
- [85] Z. Ma, J. Liu, Y. Liu, X. Zheng, K. Tang, Green synthesis of silver nanoparticles using soluble soybean polysaccharide and their application in antibacterial coatings, *Int. J. Biol. Macromol.* 166 (2021) 567–577.
- [86] J. Liu, Z. Ma, Y. Liu, X. Zheng, Y. Pei, K. Tang, Soluble soybean polysaccharide films containing in-situ generated silver nanoparticles for antibacterial food packaging applications, *Food Packag. Shelf Life* 31 (2022).
- [87] T. Chaiwarit, W. Ruksiriwanich, K. Jantanasakulwong, P. Jantrawut, Use of orange oil loaded pectin films as antibacterial material for food packaging, *Polymers* (2018).
- [88] S.L. Aktug, S. Durdu, S. Kalkan, K. Cavusoglu, M. Usta, In vitro biological and antimicrobial properties of chitosan-based bioceramic coatings on zirconium, *Sci. Rep.* 11 (1) (2021) 15104.
- [89] D. Li, P. Liu, F. Hao, Y. Lv, W. Xiong, C. Yan, Y. Wu, H.A. Luo, Preparation and application of silver/chitosan-sepiolite materials with antimicrobial activities and low cytotoxicity, *Int. J. Biol. Macromol.* 210 (2022) 337–349.
- [90] E. Matuschek, D.F. Brown, G. Kahlmeter, Development of the EUCAST disk diffusion antimicrobial susceptibility testing method and its implementation in routine microbiology laboratories, *Clin. Microbiol. Infect.* 20 (4) (2014) 0255–0266.
- [91] M. Benkova, O. Soukup, J. Marek, Antimicrobial susceptibility testing: currently used methods and devices and the near future in clinical practice, *J. Appl. Microbiol.* 129 (4) (2020) 806–822.
- [92] R. Temmerman, K. Goethals, A. Garmyn, G. Vanantwerpen, M. Vanrobaeys, F. Haesebrouck, G. Antonissen, M. Devreese, Agreement of quantitative and qualitative antimicrobial susceptibility testing methodologies: the case of enrofloxacin and avian pathogenic *Escherichia coli*, *Front Microbiol* 11 (2020) 570975.
- [93] J.T. Seil, T.J. Webster, Antimicrobial applications of nanotechnology: methods and literature, *Int. J. Nanomed.* 7 (2012) 2767–2781.
- [94] A. Masri, D.M. Brown, D.G.E. Smith, V. Stone, H.J. Johnston, Comparison of in vitro approaches to assess the antibacterial effects of nanomaterials, *J. Funct. Biomater* 13 (4) (2022).
- [95] X. Zhang, X. Hou, L. Ma, Y. Shi, D. Zhang, K. Qu, Analytical methods for assessing antimicrobial activity of nanomaterials in complex media: advances, challenges, and perspectives, *J. Nanobiotechnol.* 21 (1) (2023) 97.
- [96] I. Wiegand, K. Hilpert, R.E. Hancock, Agar and broth dilution methods to determine the minimal inhibitory concentration (MIC) of antimicrobial substances, *Nat. Protoc.* 3 (2) (2008) 163–175.
- [97] S. Pandit, S. Rahimi, A. Derouiche, A. Boulaoued, I. Mijakovic, Sustained release of usnic acid from graphene coatings ensures long term antibiofilm protection, *Sci. Rep.* 11 (1) (2021) 9956.
- [98] N. Wang, S. Pandit, L. Ye, M. Edwards, V.R.S.S. Mokkapati, M. Murugesan, V. Kuzmenko, C. Zhao, F. Westerlund, I. Mijakovic, J. Liu, Efficient surface modification of carbon nanotubes for fabricating high performance CNT based hybrid nanostructures, *Carbon* 111 (2017) 402–410.
- [99] M. Balouiri, M. Sadiki, S.K. Ilnsouda, Methods for in vitro evaluating antimicrobial activity: a review, *J. Pharm. Anal.* 6 (2) (2016) 71–79.
- [100] V.O. Fasiku, C.A. Omolo, N. Devnarain, U.H. Ibrahim, S. Rambharose, M. Faya, C. Mocktar, S.D. Singh, T. Govender, Chitosan-based hydrogel for the dual delivery of antimicrobial agents against bacterial methicillin-resistant *Staphylococcus aureus* biofilm-infected wounds, *ACS Omega* 6 (34) (2021) 21994–22010.
- [101] S. Pandit, V. Ravikumar, A.M. Abdel-Haleem, A. Derouiche, V.R.S.S. Mokkapati, C. Sihlbom, K. Mineta, T. Gojibori, X. Gao, F. Westerlund, I. Mijakovic, Low concentrations of vitamin C reduce the synthesis of extracellular polymers and destabilize bacterial biofilms, *Front Microbiol* 8 (2017).
- [102] S. Pandit, J.N. Cai, J.E. Jung, J.G. Jeon, Effect of 1-minute fluoride treatment on potential virulence and viability of a cariogenic biofilm, *Caries Res.* 49 (4) (2015) 449–457.
- [103] Ö. Acet, E. Dikici, B.Ö. Acet, M. Odabaşı, I. Mijakovic, S. Pandit, Inhibition of bacterial adhesion by epigallocatechin gallate attached polymeric membranes, *Colloids Surf. B* 221 (2023) 113024.
- [104] S. Pandit, Z. Cao, V.R.S.S. Mokkapati, E. Celauro, A. Yurgens, M. Lovmar, F. Westerlund, J. Sun, I. Mijakovic, Vertically aligned graphene coating is bactericidal and prevents the formation of bacterial biofilms, *Adv. Materials Interfaces* 5 (7) (2018) 1701331.
- [105] S. Pandit, K. Gaska, V. Mokkapati, E. Celauro, A. Derouiche, S. Forsberg, M. Svensson, R. Kádár, I. Mijakovic, Precontrolled alignment of graphite nanoplatelets in polymeric composites prevents bacterial attachment, *Small* 16 (5) (2020) e1904756.
- [106] S. Helgadóttir, S. Pandit, V.R.S.S. Mokkapati, F. Westerlund, P. Apell, I. Mijakovic, Vitamin C pretreatment enhances the antibacterial effect of cold atmospheric plasma, *Front. Cell Infect. Microbiol.* 7 (2017).
- [107] S. Pandit, J.N. Cai, J.E. Jung, Y.S. Lee, J.G. Jeon, Effect of brief cetylpyridinium chloride treatments during early and mature cariogenic biofilm formation, *Oral Dis.* 21 (5) (2015) 565–571.
- [108] A.P. Mathew, K. Oksman, Processing of bionanocomposites: solution casting, in: *Handbook of Green Materials*, World Scientific, 2013, pp. 35–52.
- [109] J. Jovanović, J. Čirković, A. Radojković, D. Mutavdžić, G. Tanasijević, K. Joksimović, G. Bakić, G. Branković, Z. Branković, Chitosan and pectin-based films and coatings with active components for application in antimicrobial food packaging, *Prog. Org. Coat.* 158 (2021) 106349.
- [110] A. Kraskouski, K. Hileuskaya, A. Ladutska, V. Kabanava, A. Liubimau, G. Novik, T.T.Y. Nhi, V. Agabekov, Multifunctional biocompatible films based on pectin-Ag nanocomposites and PVA: design, characterization and antimicrobial potential, *J. Appl. Polym. Sci.* 139 (42) (2022) e53023.
- [111] J.R.V. Matheus, T.B.d.B. Nogueira, A.P.A. Pereira, T.R. Correia, A.M.F. de Sousa, G.M. Pastore, F.M. Pelissari, R.F. Miyahira, A.E.C. Fai, Antibacterial films made with persimmon (*Diospyros kaki* L.), pectin, and glycerol: an experimental design approach, *J. Food Sci.* 86 (10) (2021) 4539–4553.
- [112] P. Chen, F. Xie, T. McNally, Understanding the effects of montmorillonite and sepiolite on the properties of solution-cast chitosan and chitosan/silk peptide composite films, *Polym. Int.* 70 (5) (2021) 527–535.
- [113] P. Zimet, Á.W. Mombrú, D. Mombrú, A. Castro, J.P. Villanueva, H. Pardo, C. Rufo, Physico-chemical and antilisterial properties of nisin-incorporated chitosan/carboxymethyl chitosan films, *Carbohydr. Polym.* 219 (2019) 334–343.
- [114] D. Lončarević, Ž. Čupić, The perspective of using nanocatalysts in the environmental requirements and energy needs of industry, *Ind. Appl. Nanomater.* (2019) 91–122.
- [115] I.A. Neacșu, A.I. Nicoră, O.R. Vasile, B.S. Vasile, Inorganic micro- and nanostructured implants for tissue engineering, *Nanobiomater. Hard Tissue Eng.* (2016) 271–295.
- [116] C.J. Brinker, in: *Dip Coating, Chemical Solution Deposition of Functional Oxide Thin Films*, Springer, 2013, pp. 233–261.
- [117] J. Puetz, M. Aegerter, Dip coating technique. V: Sol-gel technologies for glass producers and users, in: *MA Aegerter (Ed.), M. MENNIG, Springer Science & Business Media*, New York, 2004.
- [118] S.L. Banerjee, P. Potluri, N.K. Singha, Antimicrobial cotton fibre coated with UV cured colloidal natural rubber latex: a sustainable material, *Colloids Surf. A* 566 (2019) 176–187.
- [119] D.d.S. Biron, V.d. Santos, M. Zeni, C.P. Bergmann, Copper-impregnated ceramic membranes and their anti-microbial effect against *Escherichia coli*, *Desalin. Water Treat.* 111 (2018) 48–56.
- [120] S. Kumari, H.R. Tiyyagura, Y.B. Pottathara, K.K. Sadasivuni, D. Ponnamm, T.E. Douglas, A.G. Skirtach, M. Mohan, Surface functionalization of chitosan as a coating material for orthopaedic applications: a comprehensive review, *Carbohydr. Polym.* 255 (2021) 117487.
- [121] J. Kurowiak, A. Kaczmarek-Pawelska, A.G. Mackiewicz, R. Bedzinski, Analysis of the degradation process of alginate-based hydrogels in artificial urine for use as a bioresorbable material in the treatment of urethral injuries, *Processes* 8 (3) (2020) 304.
- [122] M. Nasir, R. Sugatri, D. Agustini, Surface modification of PVDF copolymer nanofiber by chitosan/Ag (NP)/nanosilica composite, in: *International Conference on Nanotechnologies and Biomedical Engineering*, Springer, 2019, pp. 225–230.
- [123] Q. Li, S. Wang, X. Jin, C. Huang, Z. Xiang, The application of polysaccharides and their derivatives in pigment, barrier, and functional paper coatings, *Polymers* (2020).
- [124] R. Nawaz, S.T.R. Naqvi, B. Fatima, N. Zulfiqar, M.U. Farooq, D. Hussain, A. Javed, A. Rasul, L. Jafri, S. Majeed, Cost-effective fabrication, antibacterial application and cell viability studies of modified nonwoven cotton fabric, *Sci. Rep.* 12 (1) (2022) 1–12.
- [125] Z. Wang, F. Yan, H. Pei, K. Yan, Z. Cui, B. He, K. Fang, J. Li, Environmentally-friendly halloysite nanotubes@ chitosan/polyvinyl alcohol/non-woven fabric hybrid membranes with a uniform hierarchical porous structure for air filtration, *J. Membr. Sci.* 594 (2020) 117445.
- [126] J. Jung, G.M. Raghavendra, D. Kim, J. Seo, Improving properties of Hanji by coating chitosan-silver nanoparticle solution, *Int. J. Biol. Macromol.* 93 (2016) 933–939.
- [127] N. Hongsririphan, S. Sanga, Antibacterial food packaging sheets prepared by coating chitosan on corona-treated extruded poly (lactic acid)/poly (butylene succinate) blends, *J. Plast. Film Sheeting* 34 (2) (2018) 160–178.
- [128] Y. Yuan, H. Wang, Y. Fu, C. Chang, J. Wu, Sodium alginate/gum arabic/glycerol multicomponent edible films loaded with natamycin: Study on physicochemical, antibacterial, and sweet potatoes preservation properties, *Int. J. Biol. Macromol.* 213 (2022) 1068–1077.
- [129] E. Sanchis, C. Ghidelli, C.C. Sheth, M. Mateos, L. Palou, M.B. Perez-Gago, Integration of antimicrobial pectin-based edible coating and active modified at-

- mosphere packaging to preserve the quality and microbial safety of fresh-cut persimmon (*Diospyros kaki* Thunb. cv. Rojo Brillante), *J. Sci. Food Agric.* 97 (1) (2017) 252–260.
- [130] K. Yang, K. Kim, E.A. Lee, S.S. Liu, S. Kabli, S.A. Alsudir, S. Albrahim, A. Zhou, T.G. Park, H. Lee, Robust low friction antibiotic coating of urethral catheters using a catechol-functionalized polymeric hydrogel film, *Front. Mater.* 6 (2019) 274.
- [131] B. Li, X. Xia, M. Guo, Y. Jiang, Y. Li, Z. Zhang, S. Liu, H. Li, C. Liang, H. Wang, Biological and antibacterial properties of the micro-nanostructured hydroxyapatite/chitosan coating on titanium, *Sci. Rep.* 9 (1) (2019) 1–10.
- [132] G. Liu, J. Xiang, Q. Xia, K. Li, T. Lan, L. Yu, Superhydrophobic cotton gauze with durably antibacterial activity as skin wound dressing, *Cellulose* 26 (2) (2019) 1383–1397.
- [133] K. Brindhadevi, B.H. Elesaw, A. Elfasakhany, I.A. Badruddin, S. Kamangar, Wound dressings coated with silver nanoparticles and essential oil of *Labdanum*, *Appl. Nanosci.* 13 (2) (2021) 1345–1354.
- [134] A.K. Paras, *Anti-Wetting Polymeric Coatings*.
- [135] A. Kumar, D. Nanda, in: *Methods and fabrication Techniques of Superhydrophobic Surfaces, Superhydrophobic Polymer Coatings*, Elsevier, 2019, pp. 43–75.
- [136] J.X. Zhang, K. Hoshino, Fundamentals of nano/microfabrication and scale effect, in: J.X. Zhang, K. Hoshino (Eds.), *Molecular Sensors and Nanodevices*, 2019, pp. 43–111.
- [137] L. Scriven, in: *Physics and Applications of Dip Coating and Spin Coating*, MRS Online Proceedings Library (OPL), 1988, p. 121.
- [138] J.Le Roux, D. Paul, Preparation of composite membranes by a spin coating process, *J. Membr. Sci.* 74 (3) (1992) 233–252.
- [139] B. Yilbas, A. Al-Sharafi, H. Ali, Self-Cleaning of Surfaces and Water Droplet Mobility, Elsevier, 2019.
- [140] N.-T. Nguyen, in: Chapter 4—Fabrication technologies, *Micro and Nano Technologies*, William Andrew Publishing, Oxford, 2012, pp. 113–161.
- [141] Y. Duan, Y. Wu, R. Yan, M. Lin, S. Sun, H. Ma, Chitosan-sodium alginate-based coatings for self-strengthening anticorrosion and antibacterial protection of titanium substrate in artificial saliva, *Int. J. Biol. Macromol.* 184 (2021) 109–117.
- [142] Y.-J. Kuo, C.-H. Chen, P. Dash, Y.-C. Lin, C.-W. Hsu, S.-J. Shih, R.-J. Chung, Angiogenesis, osseointegration, and antibacterial applications of polyelectrolyte multilayer coatings incorporated with silver/strontium containing mesoporous bioactive glass on 316L stainless steel, *Front. Bioeng. Biotechnol.* 10 (2022) 818137.
- [143] N. Vakili, A. Asefnejad, Titanium coating: introducing an antibacterial and bioactive chitosan-alginate film on titanium by spin coating, *Biomed. Eng.* 65 (5) (2020) 621–630.
- [144] V. Zarghami, M. Ghorbani, K.P. Bagheri, M.A. Shokrgozar, Melittin antimicrobial peptide thin layer on bone implant chitosan-antibiotic coatings and their bactericidal properties, *Mater. Chem. Phys.* 263 (2021) 124432.
- [145] W.-Z. Yu, Y. Zhang, X. Liu, Y. Xiang, Z. Li, S. Wu, Synergistic antibacterial activity of multi components in lysozyme/chitosan/silver/hydroxyapatite hybrid coating, *Mater. Des.* 139 (2018) 351–362.
- [146] L. Ren, Y. Zhao, L. Yang, W. Cao, H. Wang, X. Lian, X. Gao, B. Niu, W. Li, Preparation and characterization of the catechol functionalized chitosan-Ag NPs deposited onto titanium surface, *Surf. Coat. Technol.* 420 (2021) 127319.
- [147] S. Kim, J.M. Moon, J.S. Choi, W.K. Cho, S.M. Kang, Mussel-inspired approach to constructing robust multilayered alginate films for antibacterial applications, *Adv. Funct. Mater.* 26 (23) (2016) 4099–4105.
- [148] M. Ashok, S. Deepika, P. Sowndharya, K. Muthukumar, Cotton candy driven chitosan and gelatin coated poly (styrene-co-acrylonitrile) microfibers for anti-microbial wound dressing applications, *Mater. Res. Express* 6 (12) (2019) 125339.
- [149] M. Korica, L.F. Zemljic, M. Bračić, R. Kargl, S. Spirk, D. Reishofer, K. Mihajlovski, M. Kostić, Novel protein-repellent and antimicrobial polysaccharide multilayer thin films, *Holzforchung* 73 (1) (2019) 93–103.
- [150] J. Shojaeiari, D.S. Bajwa, N.M. Stark, T.M. Bergholz, A.L. Kraft, Spin coating method improved the performance characteristics of films obtained from poly(lactic acid) and cellulose nanocrystals, *Sustain. Mater. Technol.* 26 (2020) e00212.
- [151] A. Mishra, N. Bhatt, A. Bajpai, Nanostructured superhydrophobic coatings for solar panel applications, in: *Nanomaterials-Based Coatings*, Elsevier, 2019, pp. 397–424.
- [152] F. Mandoj, S. Nardis, C. Di Natale, R. Paolesse, Porphyrinoid Thin Films for Chemical Sensing, 2018.
- [153] A. Boudrioua, M. Chakaroun, A. Fischer, Organic light-emitting diodes, in: A. Boudrioua, M. Chakaroun, A. Fischer (Eds.), *Organic Lasers*, 2017, pp. 49–93.
- [154] F. Aziz, A.F. Ismail, Spray coating methods for polymer solar cells fabrication: a review, *Mater. Sci. Semicond. Process.* 39 (2015) 416–425.
- [155] R. Yu, M. Tian, L. Qu, S. Zhu, J. Ran, R. Liu, Fast and simple fabrication of SiO<sub>2</sub>/poly (vinylidene fluoride) coated cotton fabrics with asymmetric wettability via a facile spray-coating route, *Text. Res. J.* 89 (6) (2019) 1013–1026.
- [156] A. Halahlah, V. Piironen, K.S. Mikkonen, T.M. Ho, Polysaccharides as wall materials in spray-dried microencapsulation of bioactive compounds: Physico-chemical properties and characterization, *Crit. Rev. Food Sci. Nutr.* (2022) 1–33.
- [157] S. Cho, S. Ko, Y. Jeong, S.M. Kang, J.S. Choi, W.K. Cho, Coordination-driven antifouling spray coating using a sulfated polysaccharide Fucoidan, *Prog. Org. Coat.* 169 (2022) 106916.
- [158] P. Ekabutr, P. Chuysinuan, S. Suksamrarn, W. Sukhumsirichart, P. Hongmaene, P. Supaphol, Development of antibacterial melt-blown polypropylene filters coated with mangosteen extracts for medical face mask applications, *Polym. Bull.* 76 (4) (2019) 1985–2004.
- [159] R.A. Ilyas, H.A. Aisyah, A.H. Nordin, N. Ngadi, M.Y.M. Zuhri, M.R.M. Asyraf, S.M. Sapuan, E.S. Zainudin, S. Sharma, H. Abrol, Natural-fiber-reinforced chitosan, chitosan blends and their nanocomposites for various advanced applications, *Polymers* 14 (5) (2022) 874.
- [160] R. Shanmugam, V. Mayakrishnan, R. Kesavan, K. Shanmugam, S. Veeramani, R. Ilangoan, Mechanical, barrier, adhesion and antibacterial properties of pullulan/graphene bio nanocomposite coating on spray coated nanocellulose film for food packaging applications, *J. Polym. Environ.* 30 (5) (2022) 1749–1757.
- [161] N. Velkova, L.F. Zemljic, B. Saake, S. Strnad, Adsorption of cationized xylylans onto polyethylene terephthalate fabrics for antimicrobial medical textiles, *Text. Res. J.* 89 (4) (2019) 473–486.
- [162] S.T. Gedarawatte, J.T. Ravensdale, M.L. Johns, A. Azizi, H. Al-Salami, G.A. Dykes, R. Coorey, Effectiveness of gelatine and chitosan spray coating for extending shelf life of vacuum-packaged beef, *Int. J. Food Sci. Technol.* 56 (8) (2021) 4026–4037.
- [163] J. Jovanović, J. Čirković, A. Radojković, D. Mutavdžić, G. Tanasijević, K. Joksimović, G. Bakić, G. Branković, Z. Branković, Chitosan and pectin-based films and coatings with active components for application in antimicrobial food packaging, *Prog. Org. Coat.* 158 (2021).
- [164] D. Mitra, M. Li, R. Wang, Z. Tang, E.-T. Kang, K.G. Neoh, Scalable aqueous-based process for coating polymer and metal substrates with stable quaternized chitosan antibacterial coatings, *Ind. Eng. Chem. Res.* 55 (36) (2016) 9603–9613.
- [165] P. Tyagi, R. Mathew, C. Opperman, H. Jameel, R. Gonzalez, L. Lucia, M. Hubbe, L. Pal, High-strength antibacterial chitosan-cellulose nanocrystal composite tissue paper, *Langmuir* 35 (1) (2018) 104–112.
- [166] D. Banerjee, S. Bose, Effects of aloe vera gel extract in doped hydroxyapatite-coated titanium implants on in vivo and in vitro biological properties, *ACS Appl. Bio Mater.* 2 (8) (2019) 3194–3202.
- [167] R. Jia, W. Tian, H. Bai, J. Zhang, S. Wang, J. Zhang, Sunlight-driven wearable and robust antibacterial coatings with water-soluble cellulose-based photosensitizers, *Adv. Healthc. Mater.* 8 (5) (2019) 1801591.
- [168] A. Blaesus, D.F.D. Campos, H. Fischer, 3D bioprinting of cell-laden hydrogels for advanced tissue engineering, *Curr. Opin. Biomed. Eng.* 2 (2017) 58–66.
- [169] R.R. McCarthy, M.W. Ullah, P. Booth, E. Pei, G. Yang, The use of bacterial polysaccharides in bioprinting, *Biotechnol. Adv.* 37 (8) (2019) 107448.
- [170] X. Wu, S. Liu, K. Chen, F. Wang, C. Feng, L. Xu, D. Zhang, 3D printed chitosan-gelatin hydrogel coating on titanium alloy surface as biological fixation interface of artificial joint prosthesis, *Int. J. Biol. Macromol.* 182 (2021) 669–679.
- [171] S. Wu, H. Dong, Q. Li, G. Wang, X. Cao, High strength, biocompatible hydrogels with designable shapes and special hollow-formed character using chitosan and gelatin, *Carbohydr. Polym.* 168 (2017) 147–152.
- [172] E. Naseri, C. Cartmell, M. Saab, R.G. Kerr, A. Ahmadi, Development of N, O-carboxymethyl chitosan-starch biomaterial inks for 3D printed wound dressing applications, *Macromol. Biosci.* 21 (12) (2021) 2100368.
- [173] M. Hidaka, M. Kojima, M. Nakahata, S. Sakai, Visible light-curable chitosan ink for extrusion-based and vat polymerization-based 3D bioprintings, *Polymers* 13 (9) (2021) 1382.
- [174] H.-Y. Shen, Z.-H. Liu, J.-S. Hong, M.-S. Wu, S.-J. Shiue, H.-Y. Lin, Controlled-release of free bacteriophage nanoparticles from 3D-plotted hydrogel fibrous structure as potential antibacterial wound dressing, *J. Controlled Release* 331 (2021) 154–163.
- [175] E. Gutierrez, P.A. Burdiles, F. Quero, P. Palma, F. Olate-Moya, H. Palza, 3D Printing of antimicrobial alginate/bacterial-cellulose composite hydrogels by incorporating copper nanostructures, *ACS Biomater. Sci. Eng.* 5 (11) (2019) 6290–6299.
- [176] C. Karavasili, K. Tsongas, I.I. Andreadis, E.G. Andriotis, E.T. Papachristou, R.M. Papi, D. Tzetzis, D.G. Fatouros, Physico-mechanical and finite element analysis evaluation of 3D printable alginate-methylcellulose inks for wound healing applications, *Carbohydr. Polym.* 247 (2020) 116666.
- [177] O. Fourmann, M.K. Hausmann, A. Neels, M. Schubert, G. Nyström, T. Zimmermann, G. Siqueira, 3D printing of shape-morphing and antibacterial anisotropic nanocellulose hydrogels, *Carbohydr. Polym.* 259 (2021) 117716.
- [178] A. Jafari, M. Farahani, M. Sedighi, N. Rabiee, H. Savoji, Carrageenans for tissue engineering and regenerative medicine applications: a review, *Carbohydr. Polym.* (2021) 119045.
- [179] R. Zhang, B. Yu, Y. Tian, L. Pang, T. Xu, H. Cong, Y. Shen, Diversified antibacterial modification and latest applications of polysaccharide-based hydrogels for wound healthcare, *Appl. Mater. Today* 26 (2022) 101396.
- [180] Y. Liang, Y. Liang, H. Zhang, B. Guo, Antibacterial biomaterials for skin wound dressing, *Asian J. Pharm. Sci.* 17 (3) (2022) 353–384.
- [181] T. Hughes, S. Azim, Z. Ahmad, Inhibition of *Escherichia coli* ATP synthase by dietary ginger phenolics, *Int. J. Biol. Macromol.* 182 (2021) 2130–2143.
- [182] H. Wang, T. Guo, Y. Zhang, Q. Zhang, H. Li, Rheological properties, antimicrobial activity and screen-printing performance of chitosan-pigment (FeO (OH)·xH<sub>2</sub>O) composite edible ink, *Prog. Org. Coat.* 111 (2017) 75–82.
- [183] S. Li, Y. Jiang, Y. Zhou, R. Li, Y. Jiang, M.A. Hossen, J. Dai, W. Qin, Y. Liu, Facile fabrication of sandwich-like anthocyanin/chitosan/lemongrass essential oil films via 3D printing for intelligent evaluation of pork freshness, *Food Chem.* 370 (2022) 131082.



- [184] F. Ding, B. Hu, S. Lan, H. Wang, Flexographic and screen printing of carboxymethyl chitosan based edible inks for food packaging applications, *Food Packag. Shelf Life* 26 (2020) 100559.
- [185] N. Caro, E. Medina, M. Díaz-Dosque, L. López, L. Abugoch, C. Tapia, Novel active packaging based on films of chitosan and chitosan/quinoa protein printed with chitosan-tripolyphosphate-thymol nanoparticles via thermal ink-jet printing, *Food Hydrocoll.* 52 (2016) 520–532.
- [186] Y. Wang, S. Yi, R. Lu, D.E. Sameen, S. Ahmed, J. Dai, W. Qin, S. Li, Y. Liu, Preparation, characterization, and 3D printing verification of chitosan/halloysite nanotubes/tea polyphenol nanocomposite films, *Int. J. Biol. Macromol.* 166 (2021) 32–44.
- [187] R. Ciriminna, A. Fidalgo, F. Meneguzzo, A. Presentato, A. Scurria, D. Nuzzo, R. Alduina, L.M. Ilharco, M. Pagliaro, Pectin: A Long-Neglected Broad-Spectrum Antibacterial, *ChemMedChem* 15 (23) (2020) 2228–2235.
- [188] Z. Yang, S. Yu, H. Chen, X. Guo, P. Cai, H. Meng, One-step electrogelation of pectin hydrogels as a simpler alternative for antibacterial 3D printing, *Colloids Surf. A* 654 (2022).
- [189] Z. Yang, X. Ren, Y. Liu, Multifunctional 3D printed porous GelMA/xanthan gum based dressing with biofilm control and wound healing activity, *Mater. Sci. Eng. C* 131 (2021) 112493.
- [190] C. Zhang, F. Feng, H. Zhang, Emulsion electrospinning: Fundamentals, food applications and prospects, *Trends Food Sci. Technol.* 80 (2018) 175–186.
- [191] D.H. Reneker, A.L. Yarin, Electrospinning jets and polymer nanofibers, *Polymer* 49 (10) (2008) 2387–2425.
- [192] G.I. Taylor, Disintegration of water drops in an electric field, *Proc. R. Soc. Lond. Ser. A* 280 (1382) (1964) 383–397.
- [193] F. Yu, A. Budyka, V. Kirichenko, Electrospinning of Micro-and Nanofibers: Fundamentals and Applications in Separation and Filtration Processes, Begell House Inc publ, NY, 2007.
- [194] K. Riaz, J. Kübel, M. Abbasi, K. Bachtin, S. Indris, H. Ehrenberg, R. Kádár, M. Wilhelm, Polystyrene comb architectures as model systems for the optimized solution electrospinning of branched polymers, *Polymer* 104 (2016) 240–250.
- [195] K.Y. Lee, L. Jeong, Y.O. Kang, S.J. Lee, W.H. Park, Electrospinning of polysaccharides for regenerative medicine, *Adv. Drug. Deliv. Rev.* 61 (12) (2009) 1020–1032.
- [196] D. Ahirwal, A. Hébraud, R. Kádár, M. Wilhelm, G. Schlatter, From self-assembly of electrospun nanofibers to 3D cm thick hierarchical foams, *Eur. Phys. J. E* 9 (11) (2013) 3164–3172.
- [197] H. Adeli, M.T. Khorasani, M. Parvazinia, Wound dressing based on electrospun PVA/chitosan/starch nanofibrous mats: fabrication, antibacterial and cytocompatibility evaluation and in vitro healing assay, *Int. J. Biol. Macromol.* 122 (2019) 238–254.
- [198] A. Aulova, M. Bek, L. Kossovich, I. Emri, Needleless Electrospinning of PA6 Fibers: The Effect of Solution Concentration and Electrospinning Voltage on Fiber Diameter 66 (7–8) (2020) 10 2020.
- [199] E. Stoleru, R.P. Dumitriu, B.S. Munteanu, T. Zaharescu, E.E. Tănase, A. Mitelut, G.-L. Aliliese, C. Vasile, Novel procedure to enhance PLA surface properties by chitosan irreversible immobilization, *Appl. Surf. Sci.* 367 (2016) 407–417.
- [200] Y.-f. Goh, M. Akram, A. Alshemary, R. Hussain, Antibacterial polylactic acid/chitosan nanofibers decorated with bioactive glass, *Appl. Surf. Sci.* 387 (2016) 1–7.
- [201] F. Boschetto, H. Ngoc Doan, P. Phong Vo, M. Zanocco, W. Zhu, W. Sakai, T. Adachi, E. Ohgiani, N. Tsutsumi, O. Mazda, Antibacterial and osteoconductive effects of chitosan/polyethylene oxide (PEO)/bioactive glass nanofibers for orthopedic applications, *Appl. Sci.* 10 (7) (2020) 2360.
- [202] A.B. Pebdeni, M. Sadri, S.B. Pebdeni, Synthesis of chitosan/peo/silica nanofiber coating for controlled release of cefepime from implants, *RSC Adv.* 6 (29) (2016) 24418–24429.
- [203] Z. Kharat, M. Sadri, M. Kabiri, Herbal extract loaded chitosan/PEO nanocomposites as antibacterial coatings of orthopaedic implants, *Fibers Polym.* 22 (4) (2021) 989–999.
- [204] A. Biharee, A. Sharma, A. Kumar, V. Jaitak, Antimicrobial flavonoids as a potential substitute for overcoming antimicrobial resistance, *Fitoterapia* 146 (2020) 104720.
- [205] H.X. Xu, S.F. Lee, Activity of plant flavonoids against antibiotic-resistant bacteria, *Phytother. Res.* 15 (1) (2001) 39–43.
- [206] R.T. De Silva, R.K. Dissanayake, M.P.G. Mantilaka, W.S.L. Wijesinghe, S.S. Kaleel, T.N. Premachandra, L. Weerasinghe, G.A. Amaratunga, K.N. de Silva, Drug-loaded halloysite nanotube-reinforced electrospun alginate-based nanofibrous scaffolds with sustained antimicrobial protection, *ACS Appl. Mater. Interfaces* 10 (40) (2018) 33913–33922.
- [207] Y. Tang, X. Lan, C. Liang, Z. Zhong, R. Xie, Y. Zhou, X. Miao, H. Wang, W. Wang, Honey loaded alginate/PVA nanofibrous membrane as potential bioactive wound dressing, *Carbohydr. Polym.* 219 (2019) 113–120.
- [208] K. Khoshnevisan, H. Maleki, H. Samadian, M. Doostan, M.R. Khorramzadeh, Antibacterial and antioxidant assessment of cellulose acetate/polycaprolactone nanofibrous mats impregnated with propolis, *Int. J. Biol. Macromol.* 140 (2019) 1260–1268.
- [209] Y. Liu, X. Chen, Y. Gao, Y. Liu, D. Yu, P. Liu, Electrospun core-sheath nanofibers with variable shell thickness for modifying curcumin release to achieve a better antibacterial performance, *Biomolecules* 12 (8) (2022).
- [210] C. Mouro, C.P. Dunne, I.C. Gouveia, Designing new antibacterial wound dressings: development of a dual layer cotton material coated with poly (vinyl alcohol) \_chitosan nanofibers incorporating Agrimonia eupatoria L. extract, *Molecules* 26 (1) (2020) 83.
- [211] Y. Zhou, X. Chen, T. Chen, X. Chen, A review of the antibacterial activity and mechanisms of plant polysaccharides, *Trends Food Sci. Technol.* 123 (2022) 264–280.
- [212] A.W. Jatoti, I.S. Kim, Q.Q. Ni, A comparative study on synthesis of AgNPs on cellulose nanofibers by thermal treatment and DMF for antibacterial activities, *Mater. Sci. Eng. C* 98 (2019) 1179–1195.
- [213] S. Yi, Y. Wu, Y. Zhang, Y. Zou, F. Dai, Y. Si, Antibacterial activity of photoactive silk fibroin/cellulose acetate blend nanofibrous membranes against *Escherichia coli*, *ACS Sustain. Chem. Eng.* 8 (45) (2020) 16775–16780.
- [214] H. Cui, M. Bai, M.M. Rashed, L. Lin, The antibacterial activity of clove oil/chitosan nanoparticles embedded gelatin nanofibers against *Escherichia coli* O157: H7 biofilms on cucumber, *Int. J. Food Microbiol.* 266 (2018) 69–78.
- [215] L. Lin, J. Wu, C. Li, X. Chen, H. Cui, Fabrication of a dual-response intelligent antibacterial nanofiber and its application in beef preservation, *LWT* 154 (2022) 112606.
- [216] S. Lu, J. Tao, X. Liu, Z. Wen, Baicalin-liposomes loaded polyvinyl alcohol-chitosan electrospinning nanofibrous films: characterization, antibacterial properties and preservation effects on mushrooms, *Food Chem.* 371 (2022) 131372.
- [217] D. Surendhiran, H. Cui, L. Lin, Encapsulation of Phlorotannin in Alginate/PEO blended nanofibers to preserve chicken meat from *Salmonella* contaminations, *Food Packag. Shelf Life* 21 (2019) 100346.
- [218] S. Amjadi, H. Almasi, M. Ghorbani, S. Ramazani, Reinforced ZnONPs/rosemary essential oil-incorporated zein electrospun nanofibers by  $\kappa$ -carrageenan, *Carbohydr. Polym.* 232 (2020) 115800.
- [219] A. Abou-Okeil, H. Fahmy, M.M. Fouda, A. Aly, H. Ibrahim, Hyaluronic acid/oxidized  $\kappa$ -carrageenan electrospun nanofibers synthesis and antibacterial properties, *J. Bionanosci.* 11 (3) (2021) 687–695.
- [220] T.C. Mokheba, A.S. Luyt, Development of multifunctional nano/ultrafiltration membrane based on a chitosan thin film on alginate electrospun nanofibers, *J. Cleaner Prod.* 156 (2017) 470–479.
- [221] M.Z. Elsalbe, H.F. Naguib, R.E. Morsi, Chitosan based nanofibers, review, *Mater. Sci. Eng. C* 32 (7) (2012) 1711–1726.
- [222] T.C. Mokheba, M.J. Mochane, A. Mtibe, M.J. John, E.R. Sadiku, J.S. Sefadi, Electrospun alginate nanofibers toward various applications: a review, *Materials* 13 (4) (2020) 934.
- [223] E. Antaby, K. Klinkhammer, L. Sabantina, Electrospinning of chitosan for antibacterial applications—current trends, *Appl. Sci.* 11 (24) (2021) 11937.
- [224] K.A. Kumar, E.N. Zare, R. Torres-Mendieta, S. Wacławek, P. Makvandi, M. Černík, V.V. Padil, R.S. Varma, Electrospun fibers based on botanical, seaweed, microbial, and animal sourced biomacromolecules and their multidimensional applications, *Int. J. Biol. Macromol.* 171 (2021) 130–149.
- [225] S. Federico, G. Pitarresi, F.S. Palumbo, C. Fiorica, V. Catania, D. Schillaci, G. Giannone, An asymmetric electrospun membrane for the controlled release of ciprofloxacin and FGF-2: Evaluation of antimicrobial and chemoattractant properties, *Mater. Sci. Eng. C* 123 (2021) 112001.
- [226] K. Li, S. Cui, J. Hu, Y. Zhou, Y. Liu, Crosslinked pectin nanofibers with well-dispersed Ag nanoparticles: preparation and characterization, *Carbohydr. Polym.* 199 (2018) 68–74.
- [227] G. Decher, J.D. Hong, J. Schmitt, Buildup of ultrathin multilayer films by a self-assembly process: III. Consecutively alternating adsorption of anionic and cationic polyelectrolytes on charged surfaces, *Thin. Solid. Films* 210–211 (1992) 831–835.
- [228] R. Liu, J. Dai, L. Ma, J. Chen, X. Shi, Y. Du, Z. Li, H. Deng, Low-temperature plasma treatment-assisted layer-by-layer self-assembly for the modification of nanofibrous mats, *J. Colloid Interface Sci.* 540 (2019) 535–543.
- [229] L. Pérez-Álvarez, L. Ruiz-Rubio, I. Azua, V. Benito, A. Bilbao, J.L. Vilas-Vilela, Development of multiactive antibacterial multilayers of hyaluronic acid and chitosan onto poly(ethylene terephthalate), *Eur. Polym. J.* 112 (2019) 31–37.
- [230] J.J. Richardson, M. Bjornmalm, F. Caruso, Multilayer assembly, Technology-driven layer-by-layer assembly of nanofilms, *Science* 348 (6233) (2015) aaa2491.
- [231] A. Tripathy, S. Pahal, R.J. Mudakavi, A.M. Raichur, M.M. Varma, P. Sen, Impact of bioinspired nanotopography on the antibacterial and antibiofilm efficacy of chitosan, *Biomacromolecules* 19 (4) (2018) 1340–1346.
- [232] D. Silva, H.C. de Sousa, M.H. Gil, L.F. Santos, G.M. Moutinho, M. Salema-Oom, C. Alvarez-Lorenzo, A.P. Serro, B. Saramago, Diclofenac sustained release from sterilised soft contact lens materials using an optimised layer-by-layer coating, *Int. J. Pharm.* 585 (2020) 119506.
- [233] J. Lin, X. Chen, C. Chen, J. Hu, C. Zhou, X. Cai, W. Wang, C. Zheng, P. Zhang, J. Cheng, Z. Guo, H. Liu, Durably antibacterial and bacterially antiadhesive cotton fabrics coated by cationic fluorinated polymers, *ACS Appl. Mater. Interfaces* 10 (7) (2018) 6124–6136.
- [234] H. Kindi, M. Menzel, A. Heilmann, C.E.H. Schmelzer, M. Herzberg, B. Fuhrmann, G. Gallego-Ferrer, T. Groth, Effect of metal ions on the physical properties of multilayers from hyaluronan and chitosan, and the adhesion, growth and adipogenic differentiation of multipotent mouse fibroblasts, *Eur. Phys. J. E* 17 (36) (2021) 8394–8410.
- [235] H. Xuan, Y. Zhu, J. Ren, W. Dai, L. Ge, Self-healing, antibacterial, and dual cross-linked multilayer films for microcapsule-based controllable drug release applications, *Appl. Surf. Sci.* 476 (2019) 182–188.
- [236] S. Guo, X. Zhu, X.J. Loh, Controlling cell adhesion using layer-by-layer approaches for biomedical applications, *Mater. Sci. Eng. C* 70 (Pt 2) (2017) 1163–1175.



- [237] N. Yang, R. Yuan, D. You, Q. Zhang, R. Yang, J. Wang, Q. Cheng, L. Ge, Dual fire-alarm LBL safeguarding coatings with flame-retardant, EMI shielding and antibacterial properties, *Colloids Surf. A* 643 (2022).
- [238] T.-D. Zhang, X. Deng, Y.-F. Wang, X.-T. Wang, X. Zhang, L.-L. Chen, X. Cao, Y.-Z. Zhang, C.-Y. Zhang, X. Zheng, D.-C. Yin, Layer-by-layer coating of polyvinylamine and dopamine-modified hyaluronic acid inhibits the growth of bacteria and tumor cell lines on the surface of materials, *Appl. Surf. Sci.* 530 (2020).
- [239] S. Vozar, Y.-C. Poh, T. Serbowicz, M. Bachner, P. Podsiadlo, M. Qin, E. Verploegen, N. Kotov, A.J. Hart, Automated spin-assisted layer-by-layer assembly of nanocomposites, *Rev. Sci. Instrum.* 80 (2) (2009) 023903.
- [240] J. Cho, K. Char, J.D. Hong, K.B. Lee, Fabrication of highly ordered multilayer films using a spin self-assembly method, *Adv. Mater.* 13 (14) (2001) 1076–1078.
- [241] G. Decher, Fuzzy nanoassemblies: toward layered polymeric multicomposites, *Science* 277 (5330) (1997) 1232–1237.
- [242] R. Geremia, M. Rinaudo, Biosynthesis, structure, and physical properties of some bacterial polysaccharides, *Polysaccharides* 15 (2005) 411–430.
- [243] E. Miyoshi, T. Takaya, K. Nishinari, Gel–sol transition in gellan gum solutions. II. DSC studies on the effects of salts, *Food Hydrocoll.* 8 (6) (1994) 529–542.
- [244] M. Rinaudo, Non-covalent interactions in polysaccharide systems, *Macromol. Biosci.* 6 (8) (2006) 590–610.
- [245] F. Aubert-Viard, A. Mogrovejo-Valdivia, N. Tabary, M. Maton, F. Chai, C. Neut, B. Martel, N. Blanchemain, Evaluation of antibacterial textile covered by layer-by-layer coating and loaded with chlorhexidine for wound dressing application, *Mater. Sci. Eng. C* 100 (2019) 554–563.
- [246] M. Kumorek, I.M. Minisy, T. Krunclova, M. Vorsilakova, K. Venclikova, E.M. Chanova, O. Janouskova, D. Kubies, pH-responsive and antibacterial properties of self-assembled multilayer films based on chitosan and tannic acid, *Mater. Sci. Eng. C* 109 (2020) 110493.
- [247] P. Ayaz, B. Xu, X. Zhang, J. Wang, D. Yu, J. Wu, A pH and hyaluronidase dual-responsive multilayer-based drug delivery system for resisting bacterial infection, *Appl. Surf. Sci.* 527 (2020).
- [248] V. Kulikouskaya, T. Zhdanko, K. Hileuskaya, A. Kraskouski, A. Zhura, H. Skorohod, V. Butkevich, K. Pal, S. Tratsyak, V. Agabekov, Physicochemical aspects of design of ultrathin films based on chitosan, pectin, and their silver nanocomposites with antiadhesive and bactericidal potential, *J. Biomed. Mater. Res. Part A* 110 (1) (2022) 217–228.
- [249] C.G. Boeriu, J. Springer, F.K. Kooy, L.A.M. van den Broek, G. Eggink, Production methods for hyaluronan, *Int. J. Carbohydr. Chem.* 2013 (2013) 1–14.
- [250] Y. Yu, Q. Ran, X. Shen, H. Zheng, K. Cai, Enzyme responsive titanium substrates with antibacterial property and osteo/angiogenic differentiation potentials, *Colloids Surf. B* 185 (2020) 110592.
- [251] T. Kojima, T. Nagata, H. Kudo, W.G. Müller-Lierheim, G.-B. van Setten, M. Dogru, K. Tsubota, The effects of high molecular weight hyaluronic acid eye drop application in environmental dry eye stress model mice, *Int. J. Mol. Sci.* 21 (10) (2020) 3516.
- [252] H. Mohammadi, F. Alihosseini, S.A. Hosseini, Improving physical and biological properties of nylon monofilament as suture by Chitosan/Hyaluronic acid, *Int. J. Biol. Macromol.* 164 (2020) 3394–3402.
- [253] C. Guo, W. Cui, X. Wang, X. Lu, L. Zhang, X. Li, W. Li, W. Zhang, J. Chen, Poly-L-lysine/sodium alginate coating loading nanosilver for improving the antibacterial effect and inducing mineralization of dental implants, *ACS Omega* 5 (18) (2020) 10562–10571.
- [254] K.M. Zepón, M.S. Marques, M.M. da Silva Paula, F.D.P. Morisso, L.A. Kanis, Facile, green and scalable method to produce carrageenan-based hydrogel containing in situ synthesized AgNPs for application as wound dressing, *Int. J. Biol. Macromol.* 113 (2018) 51–58.
- [255] J.L. Webber, R. Namivandi-Zangeneh, S. Drozdek, K.A. Wilk, C. Boyer, E.H.H. Wong, B.H. Bradshaw-Hajek, M. Krasowska, D.A. Beattie, Incorporation and antimicrobial activity of nisin Z within carrageenan/chitosan multilayers, *Sci. Rep.* 11 (1) (2021) 1690.
- [256] L. Wågberg, J. Erlandsson, The use of layer-by-layer self-assembly and nanocellulose to prepare advanced functional materials, *Adv. Mater.* 33 (28) (2021) 2001474.
- [257] H. Li, R. Cui, L. Peng, S. Cai, P. Li, T. Lan, Preparation of antibacterial cellulose paper using layer-by-layer assembly for cooked beef preservation at ambient temperature, *Polymers* (2018).
- [258] L. Wågberg, G. Decher, M. Norgren, T. Lindström, M. Ankerfors, K. Axnäs, The build-up of polyelectrolyte multilayers of microfibrillated cellulose and cationic polyelectrolytes, *Langmuir* 24 (3) (2008) 784–795.
- [259] S.A. Khalid, A. Musa, A. Saeed, N. Elkhair Ali Ali, E.A. Abugroun, G. Mohamed, E.I. Elmima, S.Y. Alkarib, E. Gbir Agib, G.O. Phillips, A.O. Phillips, Gum Arabic in renal disease (GARDS Study): clinical evidence of dietary supplementation impact on progression of renal dysfunction, *J. Funct. Foods* 82 (2021).
- [260] Y. Zhang, F. Wang, Q. Huang, A.B. Patil, J. Hu, L. Fan, Y. Yang, H. Duan, X. Dong, C. Lin, Layer-by-layer immobilizing of polydopamine-assisted epsilon-polylysine and gum Arabic on titanium: Tailoring of antibacterial and osteogenic properties, *Mater. Sci. Eng. C* 110 (2020) 110690.
- [261] S. Ohtani, K. Kato, S. Fa, T. Ogoshi, Host–Guest chemistry based on solid-state pillar[n]arenes, *Coord. Chem. Rev.* (2022).
- [262] A. Hashidzume, Y. Takashima, H. Yamaguchi, A. Harada, 1,12 - Cyclodextrin, in: J.L. Atwood (Ed.), *Comprehensive Supramolecular Chemistry II*, Elsevier, Oxford, 2017, pp. 269–316.
- [263] T. Wan, D. Chen, Preparation of  $\beta$ -cyclodextrin reinforced waterborne polyurethane nanocomposites with excellent mechanical and self-healing property, *Compos. Sci. Technol.* 168 (2018) 55–62.
- [264] H. Xuan, W. Dai, Y. Zhu, J. Ren, J. Zhang, L. Ge, Self-Healing, antibacterial and sensing nanoparticle coating and its excellent optical applications, *Sens. Actuat. B* 257 (2018) 1110–1117.
- [265] L. Yang, H. Wu, Y. Liu, Q. Xia, Y. Yang, N. Chen, M. Yang, R. Luo, G. Liu, Y. Wang, A robust mussel-inspired zwitterionic coating on biodegradable poly(L-lactide) stent with enhanced anticoagulant, anti-inflammatory, and anti-hyperplasia properties, *Chem. Eng. J.* 427 (2022).
- [266] Z. Yang, Y. Yang, L. Zhang, K. Xiong, X. Li, F. Zhang, J. Wang, X. Zhao, N. Huang, Mussel-inspired catalytic selenocystamine-dopamine coatings for long-term generation of therapeutic gas on cardiovascular stents, *Biomaterials* 178 (2018) 1–10.
- [267] J. Wu, S. Zhao, S. Xu, X. Pang, G. Cai, J. Wang, Acidity-triggered charge-reversible multilayers for construction of adaptive surfaces with switchable bactericidal and bacteria-repelling functions, *J. Mater. Chem. B* 6 (45) (2018) 7462–7470.
- [268] C. Chen, A. Enrico, T. Pettersson, M. Ek, A. Herland, F. Niklaus, G. Stemme, L. Wågberg, Bactericidal surfaces prepared by femtosecond laser patterning and layer-by-layer polyelectrolyte coating, *J. Colloid Interface Sci.* 575 (2020) 286–297.
- [269] M. Kazemzadeh-Narbat, H. Cheng, R. Chabok, M.M. Alvarez, C. de la Fuente-Nunez, K.S. Phillips, A. Khademhosseini, Strategies for antimicrobial peptide coatings on medical devices: a review and regulatory science perspective, *Crit. Rev. Biotechnol.* 41 (1) (2021) 94–120.
- [270] J. Szewczyk, D. Aguilar-Ferrer, E. Coy, Polydopamine films: Electrochemical growth and sensing applications, *Eur. Polym. J.* 174 (2022).
- [271] N.M. Gasbarro, M.J. Solomon, Yield stress and rheology of a self-associating chitosan solution, *Rheol. Acta* 58 (11) (2019) 729–739.
- [272] A. Martínez-Ruvalcaba, E. Chornet, D. Rodrigue, Dynamic Rheological Properties of Concentrated Chitosan Solutions 14 (3) (2004) 140–147.
- [273] D.A. Gibbs, E.W. Merrill, K.A. Smith, E.A. Balazs, Rheology of hyaluronic acid, *Biopolymers* 6 (6) (1968) 777–791.
- [274] M. Fazilati, S. Ingelsten, S. Wojno, T. Nypelö, R. Kádár, Thixotropy of cellulose nanocrystal suspensions, *J. Rheol.* 65 (2021) 1035–1052.
- [275] S. Pandit, K. Gaska, R. Kádár, I. Mijakovic, Graphene-based antimicrobial biomedical surfaces, *ChemPhysChem* 22 (3) (2021) 250–263.